THE ASSESSMENT OF THE BACTERICIDAL EFFECT OF GREEN SYNTHESIZED SILVER NANOPARTICLES AGAINST A PANEL OF INFECTIOUS MICROORGANISMS

MMOLA MOKONE

A mini-thesis submitted in partial fulfilment of the requirements for the degree of Magister Scientiae in Nanoscience, Department of Biotechnology,
University of the Western Cape

Supervisor: Prof D. R. Beukes
Co-supervisors: Dr. E. M. Antunes & Prof M. Meyer

March 2016

Declaration

I declare that this thesis *"The assessment of the bactericidal effect of green synthesized silver nanoparticles against a panel of infectious microorganisms"* is a presentation of my original research work and it has not been submitted for any degree or examination in any other university. Wherever contributions of others are involved, every effort is made to indicate this clearly, with due reference to the literature and acknowledgement of collaborative research and discussions.

The work was done under the guidance of Professor Denzil R. Beukes, at the University of the Western Cape, South Africa.

Mokone Mmola ……

In my capacity as supervisor of the candidate's thesis, I certify that the above statements are true to the best of my knowledge.

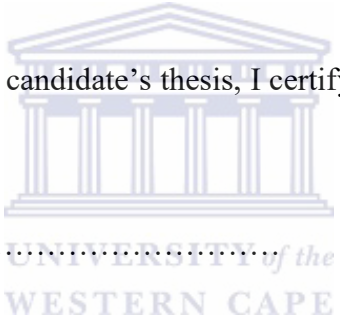

Prof. Denzil R. Beukes ……

Date:

Acknowledgements

- Mom I really am overwhelmed with gratitude for all the support you have shown me throughout my career. I can never thank you enough. May God bless you abundantly with days of your life so that you may witness the success of your son. I can never express my ecstasy enough Ma. I really appreciate your support and patience throughout the course of my career.
- To my beloved supervisors Prof Beukes and Dr. Antunes, I send a heartfelt Thank you. What have I done to deserve such passionate and determined supervisors? It has been a tough academic journey but I can almost swallow my words because you have demystified it. It would have never been easy without your guidance. Your warm benevolence and welcoming attitudes are priceless. You have treated me as one of your own, and for that I say BIG THANK YOU!
- I would also like to thank Prof Meyer who has been of imperative help to me. My research project wouldn't be complete if I had not been provided with facilities for tissue culturing. I thank you for allowing me to use your TC lab Prof!
- I would like thank Dr Marilize le Roes-Hill from the Cape Peninsula University of Technology (CPUT) for allowing me space in her microbiology lab so that I can perform antimicrobial assays. It wouldn't have been possible without your help Dr.
- Nicole Sibuyi, the sweetest lady I have ever met. I thank you so much for the help; for taking me step by step with tissue culturing. Your patience is amazing. You made me comfortable around you and that had helped me greatly because I always knew where to go when I needed help. Although I was pestering you, it was worth it. Thank you my friend.
- To tissue culture lab mates, Thank you for your support.
- How can I ever forget my adorable MBDR lab mates? You guys are the best. Working with you has been a very sensational experience. Thank you for being there when I needed help.
- This would have never been feasible, let alone being to this end if it were not for Nanoscience platform. For that I really want to say thank you to this platform for making my research programme a success.

- To the University of the Western Cape, thank you for providing facilities to enable smooth progress of my research project.
- Lastly, I would very much like to thank God for being there for me. Always guiding me in His own way, giving me strength when I was weak. I really exalt you my Lord. There is no one like You!

Abstract

The emergence of multiple drug resistant microorganisms poses a major threat to human life. These microorganisms have made the currently used antibiotics ineffective and therefore continue to thrive. Therefore, there is a need for development of new, broad-secptrum antibiotics which is effective against almost every infectious microorganism. These antibiotics should ensure high effectiveness against the infectious pathogens while it is less detrimental to human health. Thus the search is channelled in nanoscience and nanotechnology in order to develop antibiotics that can kill infectious microorganisms effectively and hindering the development of drug resistance by these microorganisms.

Nanoscience is the study of properties of a material when reduced to it smallest size (below 100 nm). It is a newly developing field of science which includes chemistry, physics and biology and has made it easy to synthesise nanomaterials for applications in many sectors of life including in medicine. The synthesis of nanoparticles can be achieved by physical and chemical methods. However, these methods are energy and capital intensive. Additionally, chemical method of synthesis uses chemicals that may be toxic which restrict the use of resultant nanoparticles in medicine. Therefore, there is a need for the use of eco-friendly methods of nanoparticle synthesis.

The synthesis of silver and gold nanoparticles in this study was carried out by a green synthesis method, at room temperature, using an aqueous extract from the endemic brown alga *Sargassum incisifolium*. For comparison, commercially available brown algal fucoidans were also used to synthesise these nanoparticle, in addition to conventional methods of synthesis. The formation of nanoparticles was followed by the use of UV-Vis spectrophotometry. The characterization of the nanoparticles was done by TEM, XRD, DLZ and FT-IR.

The rate of nanoparticle formation varied with specific reducing agent used. The faster reaction rate was recorded with *S. incisifolium* aqueous extracts pretreated with organic solvents while extracts obtained without this pretreatment produced slightly slower reaction rates. However, the commercially available fucoidans were less effective and required elevated temperatures for

nanoparticle formation. Sodium borohydride reduction of silver nitrate was faster than the biological methods while the reduction of auric chloride by the *S. incisifolium* extracts and sodium citrate proceeded at similar rates.

The nanoparticles synthesised with the help of the untreated aqueous extract were bigger than those synthesised from pre-treated extracts with both giving irregular shaped of nanoparticles. Also the nanoparticles formed from commercially available fucoidans were not of the same size, with bigger sizes recorded with *Macrocystis* fucoidan and smaller sizes with *Fucus* fucoidan. The shapes of nanoparticles from these fucoidans were spherical. From the conventional method, the nanoparticle sizes were smaller compared to the green synthesised nanoparticles and were predominantly spherical.

The silver nanoparticles synthesised from the *Sargassum* aqueous extracts showed excellent antimicrobial activity against five pathogenic microorganisms including *A. baumannii, K. pneumoniae, E. faecalis, S. aureus, and C. albicans.* The gold nanoparticles were much less effective.

To adequately assess the antimicrobial activities of the nanoparticles, it is or paramount importance to also asses their cytotoxicity activity. Three cell lines were used in this study namely, MCF-7, HT-29 and MCF-12a. The silver nanoparticles were found to be toxic to HT-29 and MCF-7 cell lines, exhibiting sligtly less toxicity against MCF-12a cells. The gold nanoparticles showed lower toxicity but a similar trend was observed.

Keywords:

Green synthesis, fucoidans, *Sargassum incisifolium*, antibacterial activity, cytotoxicity

CONTENTS

LIST OF FIGURES

LIST OF TABLES

List of Abbreviations:

AgNPs	Silver nanoparticles
AuNPs	Gold nanoparticles
L-AC	Aqueous extract *with* prior organic extraction (without being freeze dried)
L-AR	Aqueous extract *without* prior organic extraction (without being freeze dried)
AE	Aqueous extract which is inclusive of L-AC, L-AR, AC and AR.
AC	Freeze-dried aqueous extract with prior organic extraction
AR	Freeze-dried aqueous extraction without prior organic extraction
L-AC-AgNP	Silver nanoparticles synthesised using 10 ml of liquid aqueous extract with prior organic extraction
L-AR-AgNP	Silver nanoparticles synthesised using 10 ml of liquid aqueous extract without prior organic extraction
AC-AgNP	Silver nanoparticles synthesised using freeze-dried aqueous extracts with prior organic extraction
AR-AgNP	Silver nanoparticles synthesised using freeze-dried aqueous extract without prior organic extraction
L-AC-AuNP	Gold nanoparticles synthesised using aqueous extract with prior organic extraction
L-AR-AuNP	Gold nanoparticles synthesised using aqueous extract without prior organic extraction
AC-AuNP	Gold nanoparticles synthesised using freeze-dried aqueous with prior organic extraction
AR-AuNP	Gold nanoparticles synthesised using freeze-dried aqueous extract without prior organic extraction
Mp	*Macrocystis pyrifera* Fucoidan
Fv	*Fucus vesiculosus* Fucoidan
Mp-AgNP	Silver nanoparticles synthesised using fucoidan from *Macrocystis pyrifera*
Fv-AgNP	Silver nanoparticles synthesised using fucoidan from *Fucus vesiculosus*
SB-AgNP	Silver nanoparticles synthesised using sodium borohydride
SC-AuNP	Gold nanoparticles synthesised using sodium citrate

SC	Sodium citrate
SB	Sodium borohydride
SPR	Surface plasmon resonance
NPs	Nanoparticles
TEM	Transmission electron microscope
MRSA	Methicillin resistant *Staphylococcus aureus*
Ag^{+}	Silver ion
Ag^{0}	Silver atom
UV	Ultraviolet light
IUPAC	International Union of Pure and Applied Chemistry
DPHC	Diphlorethohydroxycarmalol
SEM	Scanning electron microscope
UV-Vis	Ultraviolet visible
FT-IR	Fourier transform infrared
IR	Infrared
ATR	Attenuated total reflectance
AFM	Atomic force microscope
XRD	X-ray diffractometry
$NaBH_4$	Sodium borohydride
Up	*Undaria pinatifida* fucoidan
NMR	Nuclear magnetic resonance
HSQC	Heteronuclear single quantum coherence
ATR	Attenuated total reflectance
FWHM	Full width at half maximum
EDX	Energy dispersive X-ray
DLS	Dynamic light scattering
PdI	Polydispersity index
d_H	Hydrodynamic radius
FCC	Face-centered-cubic
MIC	Minimum inhibition concentration
ATCC	American type culture collection

EGF	Epidermal growth factor
IC_{50}	Concentration at which 50 % of test sample is inhibited (Half maximal inhibitory concentration)

CHAPTER 1

1. GENERAL INTRODUCTION

1.1. What is nanotechnology?

Nanoscience is the study of small materials ranging in size from 1-100 nm (Sepeur, 2008; Song & Kim, 2009; Vaidyanathan *et al*., 2009). The manipulation and application of these nanomaterials is called nanotechnology (Buzea *et al.*, 2007; Vaidyanathan *et al.*, 2009). Nanoscience is a newly developing, multidisciplinary field of science, involving physics, chemistry and biology (Joshi *et al.*, 2008). Nanoscience and nanotechnology have made it easy for the scientist to synthesise nanomaterials of controllable sizes, while the exceptional characteristics of nanomaterials, as compared to the bulk materials, have led to intensive research in the field of nanoscience. These novel characteristics include remarkable mechanical, electrical, conductance, magnetic and optical properties (Sironmani & Daniel, 2011). These properties enable nanomaterials to have wide applications in many sectors including catalysis, drug delivery, diagnostics, transport, energy, cosmetics and the development of new drugs (Ramteke *et al.*, 2012; Rickerby & Morrison, 2007). Most materials change their characteristics at the nanoscale, e.g., gold changes colour to red or purple, while silver changes colour to yellow or yellow-brown. These characteristics result, in part, from the increase in surface area of the material as the size decreases, as well as the quantum confinement effects that dominate at the nano-level (Le *et al.*, 2010). The flexibility of the properties associated with nanoparticles of a particular size and shape has drawn a great deal of interest for use in medical field, and in telecommunication, and transportation (Asharani *et al.*, 2009; Bhumkar *et al*., 2007; Ramesh *et al.*, 2014; Rickerby & Morrison, 2007; Yang *et al.*, 2009).

1.2. The potential of nanotechnology in the development of new antibiotics/drugs

The emergence of multiple drug resistant microorganisms poses a global threat to public health (Rai *et al.*, 2009). Inappropriate use of antibiotics enables microorganisms to develop mutations that are resistant to antibiotics. As a result, those diseases which have been cured easily in the past have now become a major health threat due to the development of resistance. In addition, treatment of diseases caused by drug resistant pathogens are costly and result in long periods of hospitalization, as well as increased morbidity and mortality (Bhatt *et al.*, 2015; Huh & Kwon,

2011; Sousa *et al.*, 2011). For this reason, a cost-effective, broad spectrum treatment (i.e., the antibiotics that can act against a wide range of microbial infections) is sought. Thus, extensive research in nanotechnology for the development of an effective treatment against drug resistant bacteria is an important area of research (Morones *et al.*, 2005).

Silver has long been known to effectively kill almost all microorganisms (Kim *et al.*, 2007). For this reason, silver nanoparticles (AgNPs) have captured the attention of a number of scientists and this has led to intensive research on AgNPs (as opposed to bulk silver) because of their wide range of applications in many sectors of life and industry including chemical, biological and physical sectors (Sun & Xia, 2002; Kim *et al.*, 2006). AgNPs have distinctive properties such as good conductivity, chemical stability, catalytic, anti-fungal, anti-bacterial and anti-inflammatory activity (Sironmani & Daniel, 2011).

Silver nanoparticles are one of the most widely used nanoparticles in commercial products as they are well-known for their anti-microbial activity and have therefore been used in cosmetics, wound dressings as well as in hospital equipment to avoid infections (Chen & Schluesener, 2008).

With the increase in interest in the application of nanoparticles, there is a need to develop green and environmentally friendly synthetic methods for nanoparticles. In recent years, the use of plant extracts and natural products in the synthesis of nanoparticles has received increasing attention (Kannan *et al*., 2013; Mollick *et al*., 2015; Salem *et al.*, 2014; Song & Kim, 2009; Zargar *et al*, 2011). In this study we will focus our attention on the use of aqueous extracts of the seaweed *Sargassum incissifolium*, an endemic South African species (Stegenga *et al*., 1997), in the green synthesis of silver and gold nanoparticles (AgNPs and AuNPs respectively). To the best of the author's knowledge, *S. incisifolium* has never been reported for use in the synthesis of AgNPs and AuNPs, thus this study reports on the synthesis of AgNPs and AuNPs using aqueous extracts from *S. incisifolium* sp. This study will also give an insight into which of these two metallic nanoparticles (AgNP and AuNP) is a better antimicrobial agent. However, the focus is primarily on AgNPs.

1.3. Aims, objectives and hypothesis of the study

The aim of this study is to synthesise AgNPs using an aqueous extract of the brown marine alga *Sargassum incisifolium* and assess their antimicrobial activty.

The objectives are as follows:

1. To synthesise silver and gold nanoparticles using a range of reducing agents including an aqueous extract of *S. incisifolium.*
2. To test the "green" and conventionally synthesized silver and gold nanoparticles against a panel of infectious microorganisms.
3. To assess the selectivity and cytotoxicity of the AgNPs and AuNPs against MCF-7, HT-29 and MCF12a cell lines.

Hypotheses:

- Fucoidan (a polysaccharide), found in aqueous extracts of brown algae, including *S. incissifolium* may be involved in the bioreduction of silver nitrate to form nanoparticles.
- Silver nanoparticles synthesised from the seaweed aqueous extract is capable of selectively killing microorganisms effectively.

1.4. Research questions

- Does the aqueous seaweed extract effectively reduce silver ions to Ag^0?
- Which molecules in the seaweed extract likely stabilise the silver nanoparticles?
- Will the "green" synthesized silver nanoparticles selectively kill microorganisms effectively?

1.5. Thesis outline

Chapter 1 provides a brief introduction to nanotechnology and ends with the research aims and objectives.

Chapter 2 gives an overview of nanoscience and nanotechnology, different types of nanomaterials available, the characteristics of nanoparticles, synthetic methods employed for nanoparticles, characterisation techniques and the reason for choosing silver nanoparticles for this study.

Chapter 3 includes the synthetic methods, together with the results obtained from the characterisation of the nanoparticles.

Chapter 4 presents the biological assessment (cytotoxicity and antimicrobial tests) carried out in this study.

Chapter 5 presents the conclusions and future perspectives.

CHAPTER 2
2. LITERATURE REVIEW

2.1. Nanoscience and nanotechnology

Nanoscience is the study of materials at their smallest size (1-100 nm) (Handford *et al.*, 2015). Materials at nanoscale are usually measured in nanometres. Manipulation of these materials (termed nanoparticles) for a variety of applications is called nanotechnology (Adams and Barbante, 2013; Supraja *et al.*, 2013).

Materials at the nanoscale level develop characteristics that are different from the characteristics observed in their bulk form, *i.e.* they gain exceptional, novel characteristics at the nanoscale (Liu *et al.*, 2014; Ahn-Tuan *et al.*, 2010). The remarkable properties associated with nanoscale materials have led to a great deal of research in the field of nanotechnology. The unique properties have enabled nanoparticles to have a wide range of applications in a variety of fields such as healthcare, transport, energy, water remediation and including information and communication technologies (Rickerby & Morrison, 2007; Das *et al.*, 2012). The extraordinary properties observed with nanoparticles include optical, magnetic and electrical properties and they depend on the size and shape of the nanoparticles together with their interaction with stabilizers and surrounding media, and the synthetic method employed (Ahn-Tuan *et al.*, 2010). Additionally, the traditional laws of physics can no longer explain the behaviour of nanoparticles at this scale, and the focus is therefore based on the laws of quantum physics. The reason for the shift in focus from the traditional laws of physics to the quantum laws of physics is that the processes that occur at the nanoscale are based on the quantum confinement effects (Daniel & Astruc, 2004). Furthermore, the fact that most biological processes take place at the nanoscale, has further enlightened scientists, enabling them to develop processes that can improve their work in medicine, imaging, computing, printing, chemical catalysis and materials synthesis. Nanotechnology enables scientists to mimic natural processes by using the material's unique physical, chemical, mechanical and optical properties (Pedersen, 2006). Moreover, nanoparticles may develop unique properties such as a vastly increased surface area, which causes changes in cohesive forces, new chemical forms (*e.g*, carbon can bond in different ways to form different

new materials such as graphite, diamond, fullerenes and carbon nanotubes), chemical reactivity and quantum size effects.

2.2. Quantum effects

The properties of a material in its actual (bulk) size and smaller sized particles of the same bulk material that can be viewed under a regular optical microscope differ slightly, but an excessive difference is seen when the same material is reduced to a size in the nanometre range. At this size, optical microscopes can no longer be used to view the material and electron microscopes have to be employed since electrons have a much shorter wavelength, *e.g.*, scanning electron microscopes and transmission electron microscopes. The quantum effects begin to appear at the nanoscale level, where they control the behaviour and properties of the nanoparticles (Aitken *et al.*, 2006), such as melting point, fluorescence, electrical conductivity, magnetic permeability and the chemical reactivity which changes as the size of the material changes. Thus, the properties of the material become size-dependent at the nanometre range (scale 1-100 nm). The colour of bulk gold, for example, is yellow. When gold is reduced in size to nanometre scale, its colour changes from yellow to red or purple (Bhattacharya & Mukherjee, 2008). This occurs due to the confinement of electron at the nanometre scale which makes it difficult for electrons to move freely and thus gold nanoparticles react differently upon interaction with light as opposed to the bulk form. Unique to metallic nanoparticles like sliver nanoparticles (AgNPs) and gold nanoparticles (AuNPs), is the physical phenomenon known as surface plasmon resonace (SPR). Upon irradiation with electromagnetic radiation, there is a coherent oscillation of conduction band electrons thereby inducing SPR. The SPR band appears at around 400 nm for spherical AgNPs (Figure 2.1) and at around 520 nm for AuNPs (Figure 2.2) (Gherbawy *et al.*, 2013; Huang & El-Sayed, 2010; Jones *et al.*, 2011). Due to their size and optical properties, gold nanoparticles can selectively accumulate in tumours. Once present in the tumour, gold nanoparticles are capable of providing precise imaging and targeted laser destruction without harming healthy cells.

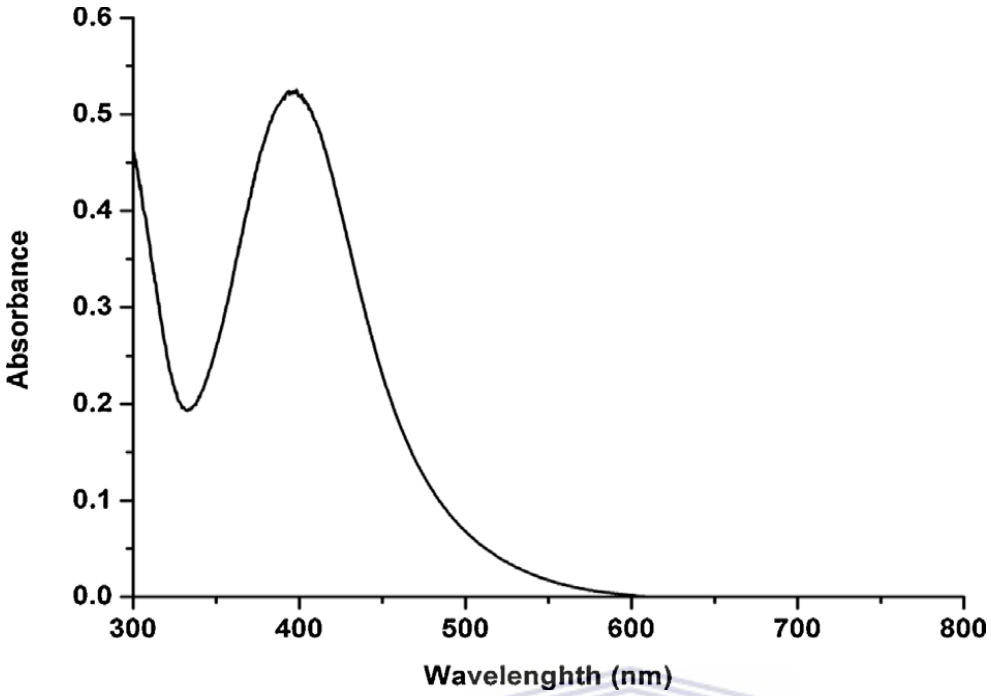

Figure 2.1 UV-Vis absorption spectrum illustrating the SPR band in AgNPs (Guo *et al*., 2015)

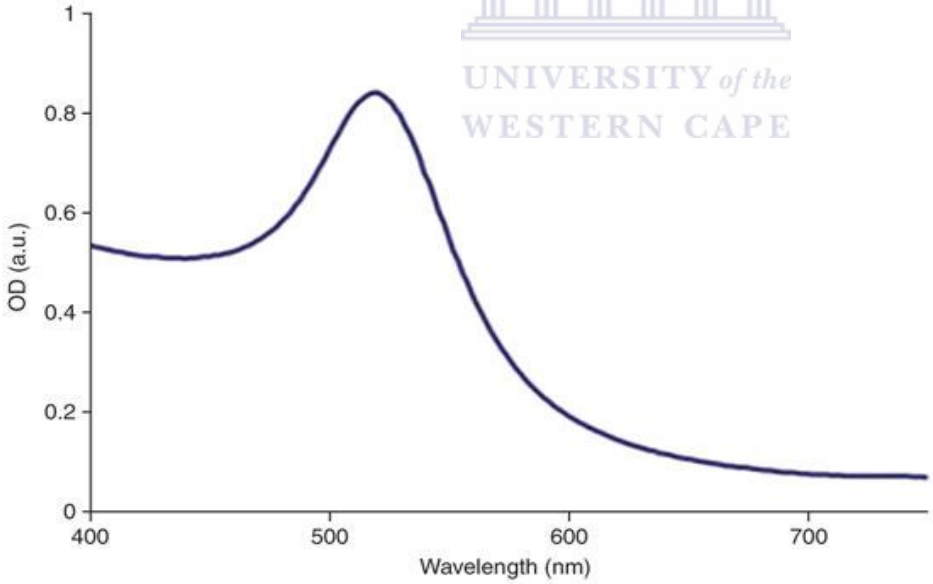

Figure 2.2 UV-Vis absorption spectrum illustrating the SPR band in AuNPs (Kumar *et al*., 2008)

2.3. Nanoparticles and their applications

Nanoparticles have been synthesized from several noble metals including gold, silver, platinum and palladium. Although the noble metal nanoparticles (NPs) are used mostly in medical and pharmaceutical products, NPs are present in shampoos, soaps, detergents, shoes, cosmetic products, and toothpaste (Ramesh *et al.*, 2014). Gold nanoparticles have found application in medicine, diagnostics for various diseases and drug delivery (Bhumkar *et al.*, 2007). Silver nanoparticles have obtained applications in technology, biological labelling and several other biomedical applications (Asharani *et al.*, 2009). Platinum nanoparticles are well-known for their application in catalysis (Narayan & El-Sayed, 2004) and biomedical applications when combined with other nanoparticles to form biosensors (Yang *et al.*, 2006). Also applied in catalysis are the nanoparticles synthesized from palladium, where they have play a role in electrocatalysis, sensing and plasmonic wave guiding (Kora and Rastogi, 2015). Other types of nanoparticles include, but are not limited to, carbon nanotubes, fullerenes, quantum dots/nanocrystals, dendrimers, nanopowders, nanocomposites, nanoalloys, nanowires and metal oxides.

2.4. Green nanotechnology

The research focus in nanotechnology has recently been channelled into developing "greener" methods for the synthesis of nanoparticles as it is more beneficial in terms of cost- and energy-effectiveness and environmental friendliness (Sun *et al.*, 2014). The chemical method of nanoparticle synthesis involves chemicals that can be dangerous when disposed of in the environment (Mollick *et al*, 2015) and the chemical synthesis of nanoparticles is additionally capital intensive (Akhtar *et al*., 2013). Furthermore, with the traditional methods employed for the chemical synthesis of nanoparticles, for example, the synthesis of silver nanoparticles with sodium borohydride or sodium citrate, still require stabilizing agents like sodium dodecyl sulphate, polyvinyl pyrrolidone, and trisodium citrate as capping agents in order to prevent nanoparticle aggregation (Ghorbani *et al.*, 2011). For these reasons, microorganisms and plant extracts have recently been used for the synthesis of nanoparticles (Binupriya *et al.*, 2010b).

The green synthesis of nanoparticles involves synthesizing nanoparticles intracellularly and extracellularly (Vithiya & Sen, 2011). Intracellular synthesis involves the synthesis of nanoparticles using microorganisms, where these microorganisms absorb the metals and use their

cellular machinery to convert them into nanoparticles. Several microorganisms have been reported to have the capability of synthesising nanoparticles intracellularly. These include bacteria (Klaus *et al.*, 1999; Sharma *et al.*, 2007), fungi and plants (Prabhu & Poulose, 2012). However, the use of microorganisms to synthesise nanoparticles has a number of limiting factors such as the need for multi-step processes such as the isolation of microbes and the maintenance of these microbes is expensive (Shankar *et al.*, 2004). To eliminate these steps, the more "green", less time-consuming and more cost-effective method is sought.Green methods also involve the use of plant extracts that are used to synthesize these nanoparticles extracellularly (Akhtar *et al.*, 2013). The rate of nanoparticle synthesis using plant extracts has been found to be faster compared to intracellular nanoparticle synthesis (Iravani & Zolfaghari, 2013). Silver nanoparticles have been synthesized using terrestrial plant extracts obtained from lemongrass, neem, tamarind, geranium, and *Aloe vera* to name a few (Akhtar *et al.*, 2013). It is believed that the bioreduction of nanoparticles using plant extracts is due to the presence of phytochemicals such as polyphenols, flavones, organic acids and quinones (Prathna *et al.*, 2010; Kumar *et al.*, 2012). Shankar *et al.* (2003) proposed that proteins from the geranium plant play a role in the formation of nanoparticles. Flavonoids and terpenoids from neem leaves, reducing sugars such as aldoses, aldehydes/ketones from lemongrass and polyols are also thought to play role in the formation of nanoparticles (Akhtar *et al.*, 2013). Nanoparticles synthesised using these plants are found to be mostly polydisperse and they are composed of different shapes, as can be seen in Figure 2.3. Similarly, marine algae have also been used to synthesise nanoparticles, especially gold and silver nanoparticles, details of which will follow in Section 2.9.

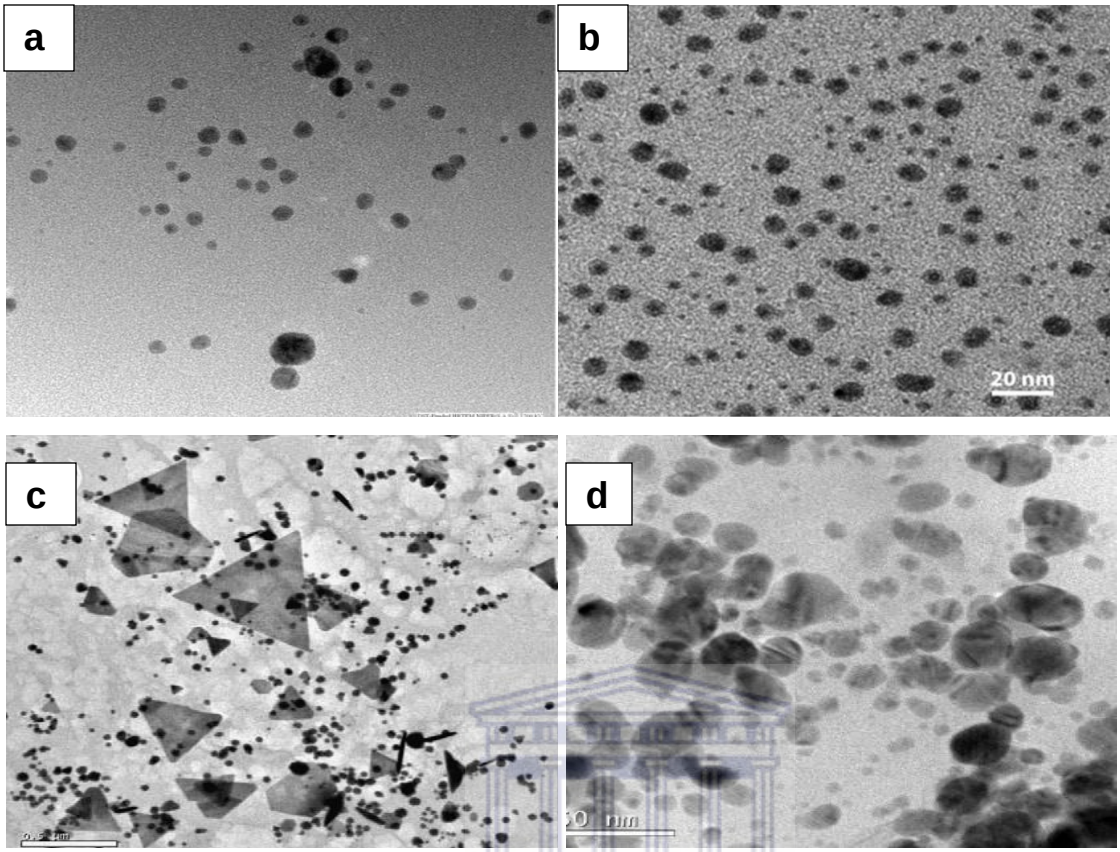

Figure 2.3 TEM images depicting the different sizes and shapes of nanoparticles synthesised from different biological systems: a) AgNPs synthesised from *Saccharomyces boulardii* (Kaler *et al.*, 2013), b) AgNPs synthesised from *Abelmschus esculentus* (Mollick *et al.*, 2015), c) AuNPs synthesised from a mushroom extract (Philip, 2009), and d) AgNPs synthesised from Marine macroalga, *Padina tetrastromatica* (Princy & Gopinath, 2013).

2.5. Multidrug resistance

The emergence of multiple drug resistant microorganisms poses a global threat to public health (Rai *et al.*, 2009). Resistant microorganisms, which can be bacteria, fungi, viruses and parasites, are unresponsive to drugs used against them such as antibiotics, antifungals, antivirals and antimalarials. Those antimicrobial drugs which were effective against the infections become ineffective, while the microorganisms thrive (WHO, 2015). As a result, these increasing drug resistant infections have led to an increased mortality rate, morbidity and cost due to prolonged hospitalization and treatment (Lara *et al.*, 2010).

The first discovery of drugs to treat antibacterial infections dates back to 1928 when penicillin was used (Derderian, 2007). An approximate scale of the amount of antibiotics produced

annually is 100 000 tons globally (Nikaido, 2009). Nevertheless, other bacteria have developed into antibiotic resistant strains (Temime *et al*, 2003). The current pressing issue is the emergence of gram negative infectious microorganisms that are resistant to almost every kind of antibiotic available (Levin *et al.*, 1999; Nikaido, 2009).

Staphylococcus aureus is one of the bacteria that have developed antibiotic (methicillin) resistant (MRSA) strains. MRSA together with *Pseudomonas aeruginosa* and *Acinetobacter baumanii* are the major pathogens responsible for infections acquired in hospitals because they are resistant also to disinfectants (Levin *et al.*, 1999).

2.6. Silver nanoparticles

Silver is well known for its bactericidal activity against almost all microorganisms, and consequently silver-based medical products have been used to prevent and treat bacterial infections (Sironmani & Daniel, 2011; Pavaghadhi *et al.*, 2014).

There are quite a number of studies that have used plant extracts for the synthesis of AgNPs. For example, Shankar *et al.* (2003) synthesized silver nanoparticles using plant extracts from geranium leaves. The size of silver nanoparticles ranged from 16-40 nm and the rate of nanoparticle formation was quite rapid with a reaction time of 60 min, where 90% of silver ions were reduced after 9 hours. This proves that the use of plant extracts to synthesize nanoparticles is less time consuming (Akhtar *et al.*, 2013) as compared to intracellular methods which take 24 to 120 hours to complete the reaction (Shankar *et al.*, 2003). Moreover, Chadran *et al.* (2006) conducted a study where silver nanoparticles were synthesized using an *Aloe vera* extract, while Arokiyaraj *et al.*, (2013) reported on the synthesis of AgNPs using aqueous floral leaf extracts from *Nelumbo nucifera*. Other green synthesis studies conducted on AgNPs using plant extracts, include those by Leela & Vivekanandan (2008) who compared the potential capabilities of different extracts from *Helianthus annus* (sunflower), *Basella alba* (spinach), *Oryza sativa* (rice), *Saccharum officinarum* (sugarcane), *Sorghum bicolar* (sorghum), *and Zea mays* (maize), where *H. annus* exhibited exceptional Ag^{+} to Ag(0) reducing capabilities. Furthermore, Gnanojobitha *et al.* (2013) used extracts from the fruit of *Vitis vinifera* to synthesise AgNPs and evaluated them for antimicrobial efficacy. Another group reported on the synthesis of AgNPs using tea leaf

extract (Begum *et al.*, 2009). Although quite a number of studies have reported on the synthesis of AgNPs with plant extracts, the number of studies which synthesized AgNPs for further application is far less compared to those which focused only on nanoparticle formation. Experimental details such as concentrations used and conditions employed are sketchy. Furthermore, there has been extensive AgNP synthesis using terrestrial plants, but more work still needs to be done in terms of exploring the reducing capabilities of marine plants such as seaweeds (Kannan *et al.* 2013).

Although they are the most commonly used nanoparticles, it is worth mentioning that silver nanoparticles can pose a major problem to the environment through their route of release into the environment during production, usage and disposal. This then leads to their accumulation, transformation and degradation in the atmosphere, water and soil spheres and in organisms (Benn *et al.*, 2008; Wiesner *et al*., 2006). The toxicity associated with silver nanoparticles raises concern since their use in commercial products entails contact with the human body (Banerjee & Narendhirakannan, 2011). Silver nanoparticles may be released to the environment *via* their routes of synthesis as well as through washing machines, or through the disposal of material containing silver nanoparticles (Benn *et al.*, 2008; Wiesner *et al.*, 2006). Silver can be hazardous if disposed in water, especially to microorganisms (Borm & Berube, 2008; Liu *et al.*, 2010). There is, therefore, still a need to study AgNP toxicity as health and safety information regarding this topic is scant especially since silver nanoparticles are also toxic to the human body (Rai *et al.*, 2009).

2.7. Gold nanoparticles

Gold nanoparticles are known for their application in catalysis, nonlinear optics, nanoelectronics, gene expression, and disease diagnosis (Wu *et al.*, 2015). Most medical applications for AuNPs fall under drug delivery, tissue/tumour imaging, photothermal therapy and immunochromatographic identification of pathogens in clinical specimens (Rajathi *et al.*, 2012). AuNPs assume their role in medicine due to their advantageous properties such as being biocompatible and their ability to deliver therapeutic substances to target areas.

Studies have also been conducted on gold nanoparticle synthesis using plant extracts. These include but are not limited to studies by Tripathy *et al*. (2012) who used the leaf extract of *Fiscus benghalensis*, Yu and colleagues, (2016) who employed *Citrus maxima* extracts to synthesise AuNP, and Sathishkumar *et al*, (2016) who synthesised AuNPs from *Couroupita guianensis* (Aubl.). Moreover, Elia *et al.* (2014) synthesised AuNPs from the leaf extracts of different plants namely: *Salvia afficinalis* (common sage), *Lippia citriodosa* (lemon verbena), *Perlagonium graveolens* (rose geranium), and *Punica granatum* (pomegranate).

As is the case with AgNPs, not much has been reported on the synthesis of AuNP using marine algae. These studies include the synthesis of AuNPs from a brown seaweed, *Stoechospermum marginatum* (Kützing) where the NPs were tested for antibacterial activity against a panel of infectious microorganisms. Senapati *et al.* (2012), synthesised AuNPs intracellularly using the alga *Tetraselmis kochinensis*. Furthermore, AuNPs have also been synthesised from marine alga, *Sargassum wightii* (Singaravelu *et al.*, 2007). Detailed summery of the use of marine algae, seaweeds in particular, for the synthesis of gold nanoparticles is shown in Table 2.1.

Table 2.1 Summery of studies that have used marine seaweeds for synthesis of gold nanoparticles

Organism	Species	Name of Species	NP type	Size (nm)	Biological activity	Author and year
Marine algae	Green seaweed	*Tetraselmis kochinensis*	AuNP	18	-	Senepati *et al*, 2012
Marine algae	Brown seaweed	*Sargassum wightii*	AuNP	5-15	-	Singaravelu *et al*, 2007
Marine algae	Brown seaweed	*Stoechospermum marginatum* (Kützing)	AuNP	18.7-93.7	Antibacterial	Rajathi *et al*, 2012
Marine algae	Green seaweed	*Prasiola crispa*	AuNP	5-25	-	Sharma *et al*, 2014
Marine algae	Brown seaweed	*Sargassum swatzii*	AuNP	20-60	Cytotoxicity	Dhas *et al*, 2014
Marine algae	Red seaweed	*Galaxaura elongata*	AuNP	3.85-77.13	Antibacterial	Abdel-Raouf *et al*, 2013
Marine algae	Brown seaweed	*Sargassum myriocystum*	AuNP	10-23	-	Dhas *et al*, 2012

Even though there are studies that have reported on the bactericidal activity of AuNPs (Cui *et al.*, 2012; Senapati *et al.*, 2012), there is still more to be done in order to explore antibacterial activities of green synthesised gold nanoparticles. Also, since they are made from noble metals, AuNPs are good candidates to be compared to AgNPs (alsois much known for its bactericidal activity).

2.8. Factors influencing synthesis of metal nanoparticles using plant extracts

The size of metallic nanoparticles has been found to decrease with an increase in pH (Armendariz *et al.,* 2004). Temperature also influences the formation of the nanoparticles by increasing the rate of formation with an increase in temperature (Muralidharan *et al.,* 2011; Gericke & Pinches, 2006). Incubation or contact time also plays a role in the formation of nanoparticles. The contact time is the time it takes for nanoparticles to form completely (Akhtar

et al., 2013). In their work, Carrillo-Lopez *et al.* (2014) showed that sharpness of the UV absorption peaks in the spectra increased as the contact time was increased when using a *Chenopodium* leaf extract to synthesise AuNPs. Isaac *et al.* (2013) also had the same observation when they synthesized AgNPs and AuNPs using *Averrhoa bilimbi* fruit extract.

2.9. Seaweed extracts in the bioreduction of metal salts to forms nanoparticles

There are a few studies that described the synthesis of AgNPs using seaweed extracts. Seaweeds are known for their high metal uptake capacity, low cost and macroscopic structures (Kannan *et al.*, 2013), and seaweeds have long been used as medicine in some parts of the world because they contain anti-oxidants that act against degenerative diseases. In addition, seaweeds have also been found to have anti-bacterial and anti-fungal activities (Gamal, 2010**)**. There is little information to support the biosynthesis of metallic nanoparticles using marine algae. In one study, AgNPs were synthesised using green seaweed, *Codium capitatum* P.C. Silva (Chlorophyceae) (Kannan *et al.* 2013). Red seaweeds, *Gelidiella acerosa* for example, have also been used to synthesise AgNPs for use as antifungal agents (Vivek *et al.*, 2011). Marine brown algae are known to possess polysaccharides that are not found in terrestrial plants. These polysaccharides were coined "fucoidans" for the first time they were isolated from brown seaweeds (Senthilkumar & Kim, 2014) and it is still currently called fucoidan according to IUPAC rules. Other names for this polysaccharide include fucan, fucosan, or sulfated fucan (Li *et al.*, 2008). For convenience, this polysaccharide will be referred to as fucoidan in this study. It is believed that fucoidan plays a role in the synthesis of nanoparticles due to their sulfonated side chains (Tengdelius *et al.*, 2015). For this reason, fucoidans were used as a control in the synthesis of the nanoparticles in this research. Figure 2.4 shows the Pankter average structure (Figure 2.4a) of fucoidans and the typical structures associated with fucoidans isolated from *Fucus vesiculosus* (Figure 2.4b). Fucoidans comprise mainly fucose and sulphate moieties. Fucoidans obtained from other different species have also been found to have a complex chemical composition. In addition to the fucose and sulphate moieties, these fucoidans may be composed of other monosaccharides (mannose, galactose, glucose, and xylose), uronic acids, acetyl groups and proteins (Li *et al.*, 2008). Fucoidan is made up of a backbone that consists of fucose residues linked in α (1-3) fashion. Sulphate groups are substituted on the C-4 position and

some fucose moieties are attached to C-4 as well, thus forming branched points with a single fucose for every 2-3 fucose residues in the polymer chain (Figure 2.4).

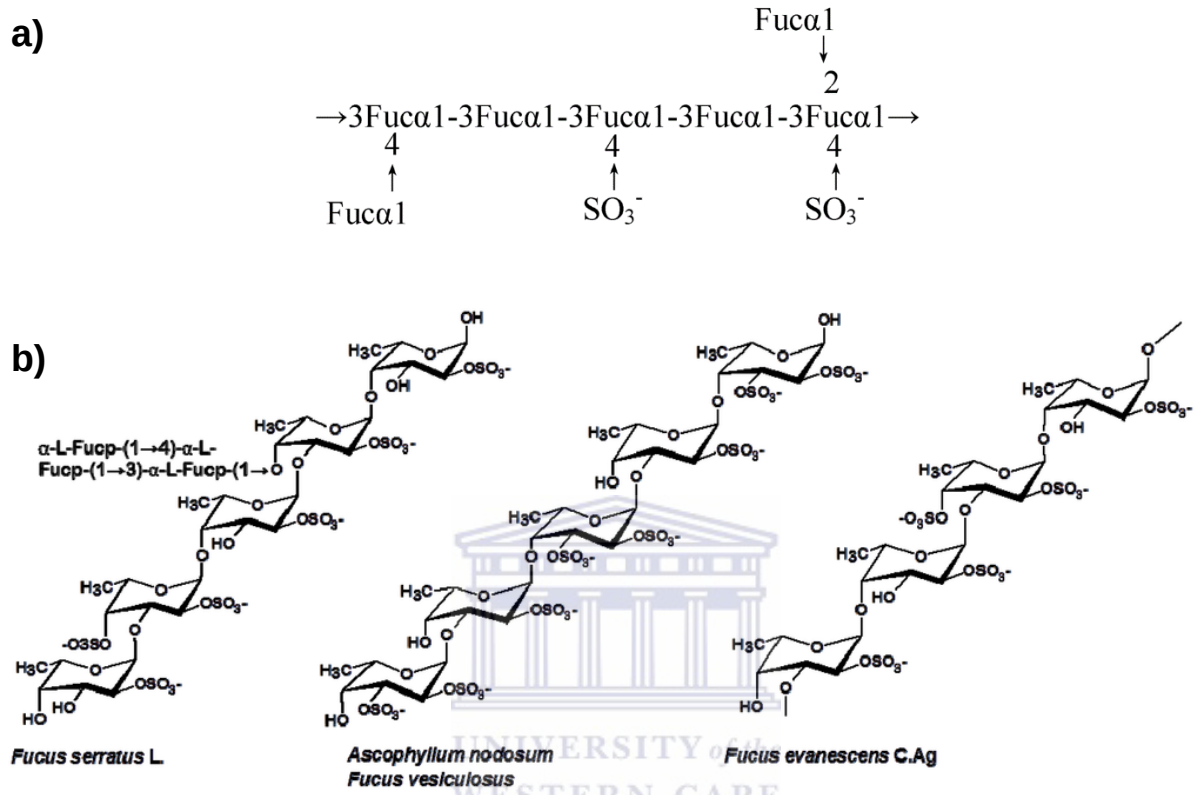

Figure 2.4 Structural illustration of the fucoidans obtained from brown marine algae. a) Pankter average fucoidan structure (Pankter, 1993); b) Typical structure of *F. veliculosus* (Ale *et al.*, 2011).

In addition to the fucoidans found in brown algae, a number of complex phlorotannins (Figure 2.5) have also been isolated from marine brown algae. These compounds have displayed potent antioxidant activities (Barbosa et al., *2014*) and may therefore be very useful in the reduction of metals salts to nanoparticles.

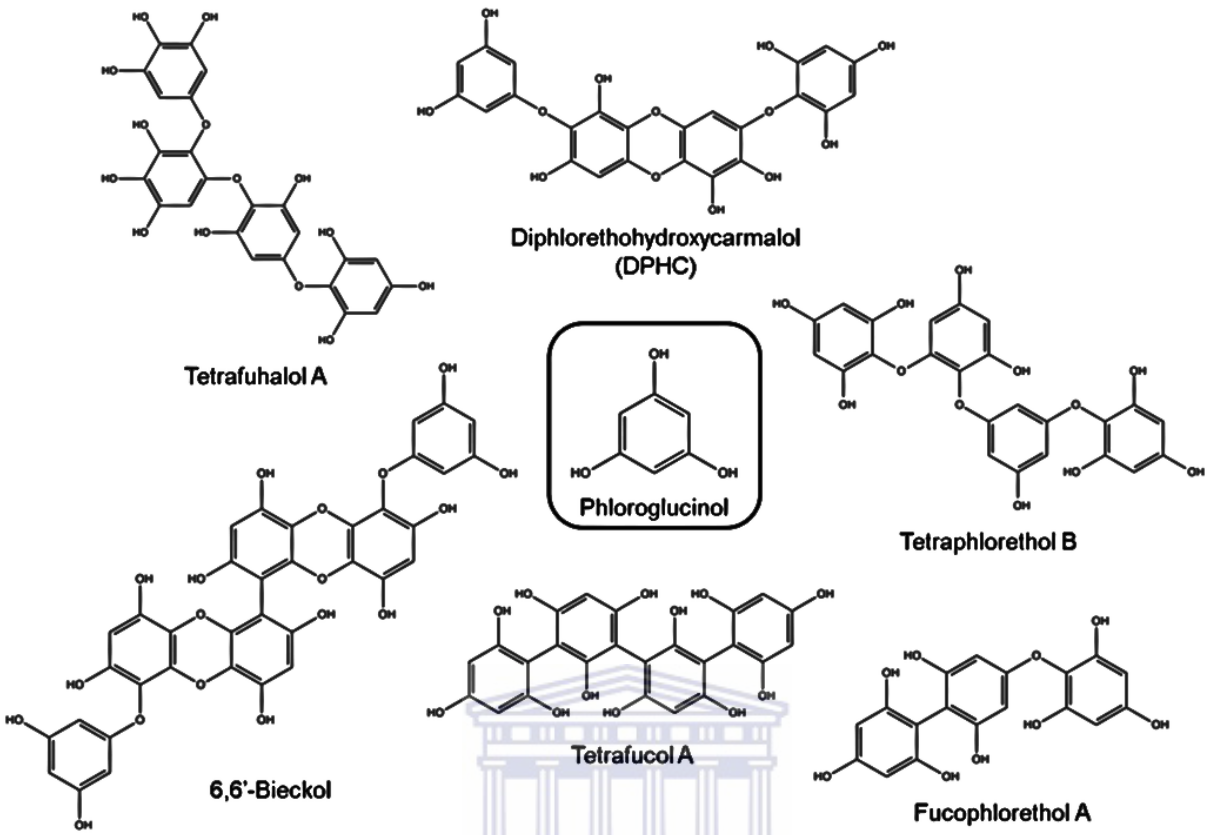

Figure 2.5 Selected phlorotannins reported from brown algae (Barbosa *et al.*, 2014).

This study reports the synthesis of AgNPs using marine brown alga, *S. incisifolium*. To the best of the author's knowledge, *S. incisifolium* has never been reported for use in the synthesis of AgNPs. However, several small molecules have previously been isolated and reported from this species (Afolayan *et al.*, 2008). These molecules include sargahydroquinoic acid, sargaquinoic acid and fucoxanthin (Figure 2.6). Although these non-polar molecules have been shown to display potent antioxidant activity, it is unlikely that they will be extracted under aqueous conditions.

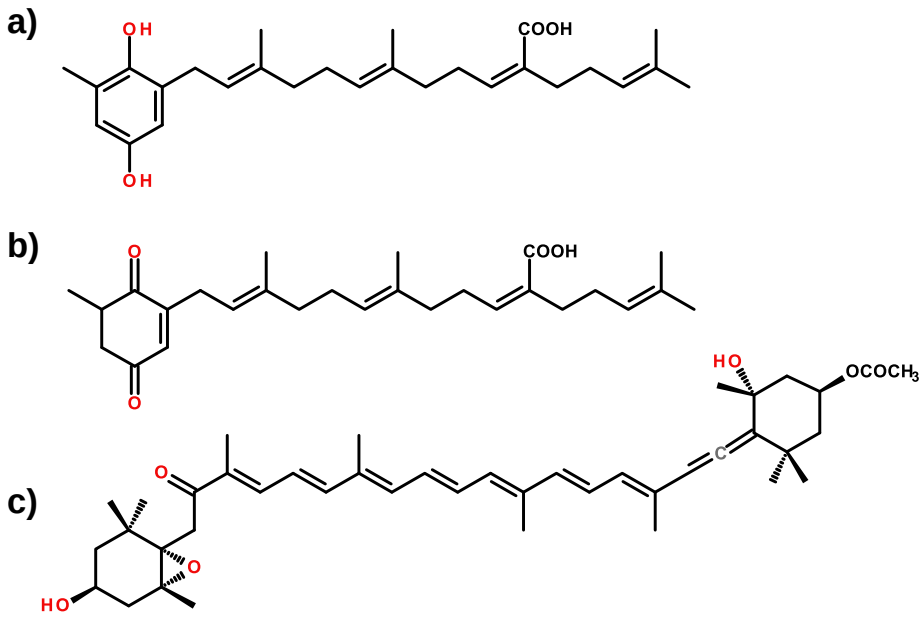

Figure 2.6 Secondary metabolites reported from the organic extract of *S. incisifolium* (Afolayan *et al.*, 2008): a) Sargahydroquinoic acid, b) Sargaquinoic acid, and c) Fucoxanthin.

2.10. Antioxidant activity

Most diseases are caused by inadequate balance between antioxidant defence and oxidant production in cells, a condition termed oxidative stress (Tobwala *et al.*, 2014). Oxidative stress together with free radical production result with reduced amount of antioxidants in the cells. Antioxidants play important role by protecting the body cells from damage induced by reactive oxygen species (ROS) including superoxide radical ($O_2^{\cdot-}$), hydroxyl radical (OH^-), peroxyl radical (ROO^-) and nitric oxide radical (NO^-). Although synthetic antioxidants have shown protective effect against ROS, their use has been nullified by the safety and cytotoxicity issues (Ananthi *et al.*, 2010; Fleita *et al.* 2015). Most studies have evaluated the antioxidant activity exhibited by plants and marine algae in order to counteract the effects of diseases caused by oxidative stress (Huang and Wang, 2004; Lim *et al.*, 2002; Shon *et al.*, 2003; Takamatsu *et al.*, 2003; Tobwala *et al.*, 2014). Polysaccharides from different seaweeds such as *Ulva lactuca* (green), *Sargassum crassifolium* (brown), and *Digenea simplex* (red) were evaluated for antioxidant activity, with the highest activity recorded in polysaccharide from brown seaweed (Al-Amoudi *et al.*, 2009). Ananthi *et al*, (2010) also assessed antioxidant activity of polysaccharide from brown seaweed, *Turbinaria ornata*, which exhibited highest antioxidant and anti-inflammatory activity.

From the best of author's knowledge, antioxidant activity of brown seaweed, *Sargassum incisifolium*, has never been investigated previously. Thus we report for the very first time the antioxidant activity exhibited by *S. incisifolium* in this study.

2.11. Techniques for the characterisation of nanoparticles

The electron microscopy technigues involve the use of transmission electron microscope (TEM) and scanning electron microscope (SEM) which use focused electron beam to study the surface morphology and size of the samples in question. Electron microscopes are usually used to study material in the submicron range and are able to produce images of higher resolution due to the shorter wavelengths of the electrons used as compared to the visible light photon wavelength (Lin *et al.*, 2014). Therefore, traditional optical microscopes are used to study materials at the micron level while nanomaterials can be studied using electron microscopes. There are numerous microscopes used to characterise nanoparticles including, scanning electron microscopes (SEM), transmission electron microscopes (TEM), and atomic force microscopes (AFM) to name a few.

2.11.1. Transmission electron microscope (TEM)

Transmission electron microscope (TEM) uses a beam of electrons to image samples, and the source of the electron beam in TEM is an electron gun. The electron beam in TEM is transmitted through an ultrathin sample of material (Wang, 2001). TEM is the most commonly used electron microscope and it is able to determine size, morphology and topography, composition and crystallography of the sample (Wang, 2001). The image obtained from TEM is magnified and then focused onto a fluorescent screen.. Figure 2.7 shows image obtained from TEM.

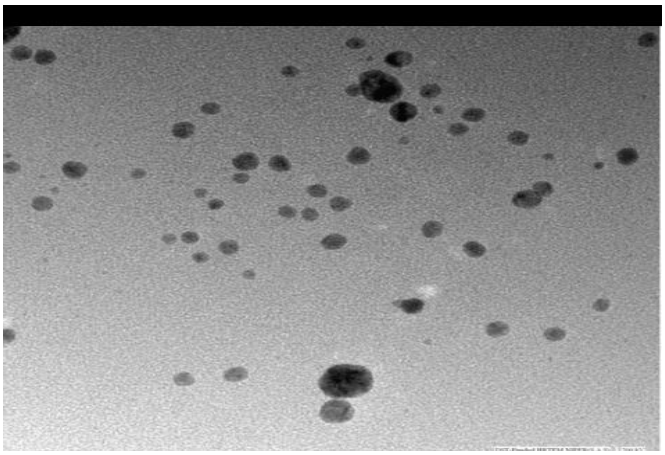

Figure 2.7 TEM image of silver nanoparticles (Kaler *et al*, 2013).

2.11.2 UV-Vis spectroscopy

UV-Vis absorbance spectroscopy is used to determine the size, concentration, aggregation and bioconjugation of nanoparticles should the nanoparticle have characteristic absorption peaks such as the SPR band of AgNPs (Figure 2.1) and AuNPs (Figure 2.2) at ~420 nm and ~532 nm, respectively (Lin *et al.*, 2014, Guo *et al.*, 2015).

The spectrophotometer then records the spectrum of absorbance against wavelength (Joshi *et al.*, 2008). Beer's law is used to help explain the absorbance of a sample at a given wavelength and can be represented in the following equation (2.1):

$$A = \log\left(\frac{Ir}{Is}\right) = \varepsilon cl \qquad (2.1)$$

where: *A* isabsorbance, *Ir* is the intensity of light entering the sample, *Is* is the intensity of light leaving the sample, *C* is concentration of sample in mol/L, *l* is path length of light through the cell in centimeters, and ε is molar absorptivity or molar extinction coefficient of the sample

2.11.3 Fourier transform infra-red (FTIR) spectroscopy

FTIR is a very important spectroscopic technique that can be used to determine the presence and identity of organic or inorganic materials and can be useful in determining the chemical constituents of a mixture and analysing solids, liquids and gases. Figure 2.8 shows FT-IR spectra of silver nanoparticles synthesised from coffee. As can be seen in Figure 2.8, stretching

frequencies corresponding to the various functional groups of molecules found in coffee extract have been recorded. Molecules have time-variant dipole moment whose oscillating frequency corresponds to that of incident IR light to absorb IR radiation. After the absorption of IR radiation, the energy is transferred to the molecule which then causes the stretching of a covalent bond, bending or twisting which can be described by a stationary state of molecular vibrational Hamiltonian. An IR spectrum is therefore then produced which can function like a molecular fingerprint. Those molecules which lack a dipole moment, for example, O_2 and N_2, do not absorb IR radiation (Lin *et al.*, 2014).

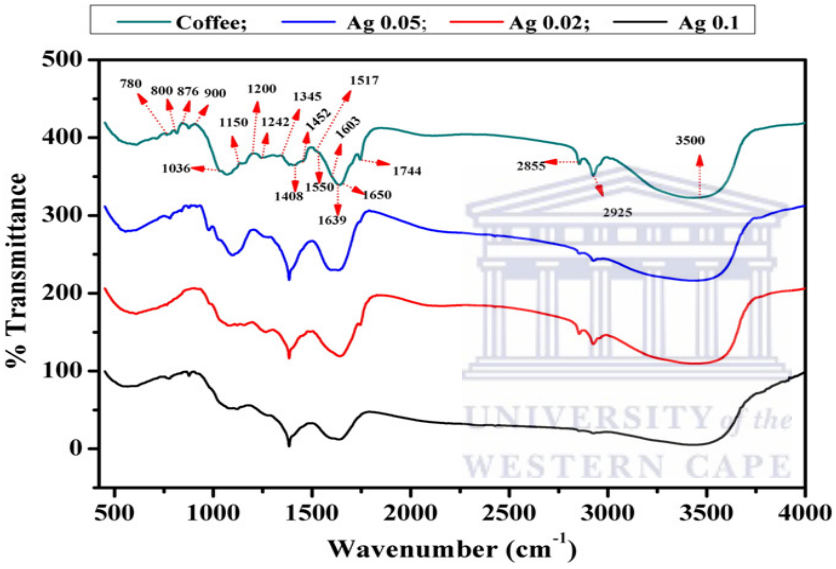

Figure 2.8 FT-IR spectra of AgNPs synthesised using a coffee extract (Dhand et al., 2016).

2.11.4 X-Ray Diffractometry

X-ray diffraction (XRD) was initially used to examine the crystalline form of powder samples and therefore it is originally called x-ray powder diffractometry. Data obtained from XRD reveals information about crystallinity, crystalline size, shape and lattice distortion (Joshi *et al.*, 2008; Lin *et al.*, 2014). Figure 2.9 shows XRD spectrum of silver nanoparticles and the *hkl* values assigned to different peaks. Peaks arise corresponding to certain angles (θ) giving information on the crystal lattice and can also be used to determine the crystallite size. The particle size is determined using the Debye-Scherrer equation (equation 2.2) according to the following formula (Park *et al.*, 2016):

$$d = \frac{k\lambda}{\beta cos\theta} \tag{2.2}$$

where: d is the size, k is the Scherrer constant (0.9), λ is the X-ray wavelength, β is the width of XRD peak at half height determined from the graph, and θ is the Bragg diffraction angle

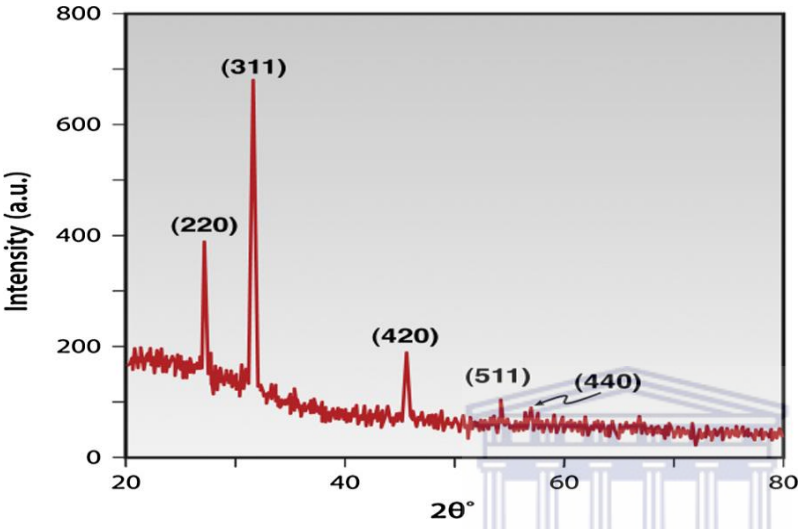

Figure 2.9 XRD spectrum of silver nanoparticles (Mollick et al, 2015).

2.11.5 Dynamic light scattering

The size of nanoparticles can also be determined through the use of the dynamic light scattering technique, which has become popular for determining the size of nanoparticles. Figure 2.10 shows the size distribution of silver nanoparticles determined from DLS. A monochromatic light is shone into the particle solution that are undergoing Brownian motion. The monochromatic laser beam is then scattered by the nanoparticles, undergoing constructive or destructive interference. The intensity of light is detected by a photomultiplier (de Kanter *et al*., 2016).

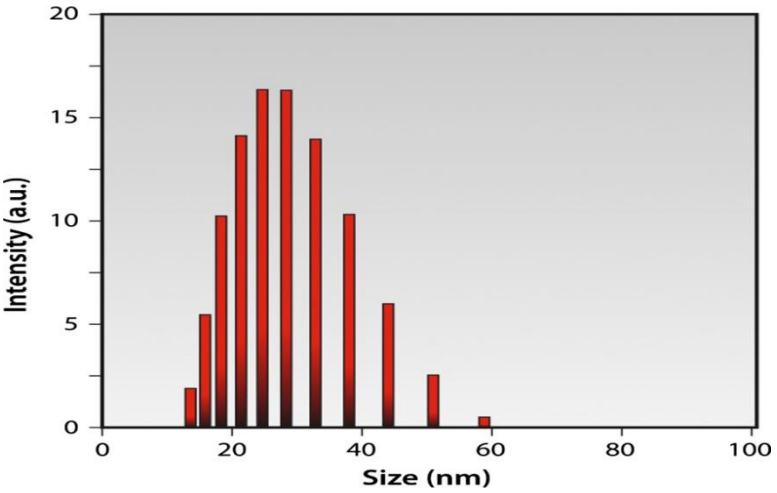

Figure 2.10 Size distribution of nanoparticles as determined by DLS (Mollick et al, 2015).

2.3 Discussion

Nanoscience is an emerging field of science which involves disciplines such as biology, chemistry and physics. Nanoscience is the study of materials at the nanoscale, while the manipulation of these materials at the nanoscale is called nanotechnology and provides an alternative path for the development of drugs, in many cases offering solutions to issues such as solubility and drug delivery. Also, through nanotechnology, new antimicrobial agents can be developed. Different nanoparticles have been synthesised for different purposes in all sectors of life including diagnostics, drug delivery, computing, transport, communication and energy. Of interest to this study is the development of an antimicrobial agent with low toxicity to normal body cells, whilst exhibiting the highest toxicity to microorganisms. Microorganisms have developed drug resistant strains over the years and this makes currently available drugs ineffective. For this reason, there definitely is a need for development of alternative antimicrobial agents, paving the way for the use of nanoscience.

Among the nanoparticles reported in the literature, AgNPs have been found to possess antimicrobial activity against almost all microorganisms. The traditional method employed for the synthesis of AgNPs (termed the chemical method in this thesis) is associated with a high cost, and highly toxic chemicals are utilised. For these reasons, the employment of a “green” synthetic method for the synthesis of nanoparticles by making use of plant extracts is advantageous. Though some work has been done on the synthesis of nanoparticles using plant

extracts, not much has been done using seaweeds. To the best of the author's knowledge, there has never been any work done on the synthesis of Ag- and AuNPs using an aqueous extract from *S. incisifolium.* The fucoidans isolated from seaweed are thought to play a role in the reduction of silver ions (Ag^{+}) to form (Ag^{0}). For this reason, pure fucoidans from different seaweeds were used in this research project to evaluate the significance of the fucoidans in the formation of nanoparticles. Ag and Au NPs synthesised in this project were tested against different microorganisms including two gram-negative bacteria, two gram positive bacteria and one yeast microorganism as well as against cancer cell lines.

CHAPTER 3

3. SYNTHESIS AND CHARACTERISATION OF NANOPARTICLES

3.1. Introduction

This chapter focuses on the synthesis and characterisation of nanoparticles. Several activities were covered in this chapter, including: 1) aqueous extraction; 2) synthesis of nanoparticles with different reducing agents; and 3) characterization of the nanoparticles using different techniques including UV-Vis absorbance spectrophotometry, transmission electron microscopy (TEM) and EDX, Zetasizer, X-Ray powder Diffraction and FTIR-spectrometry. The reducing agents employed for the NP synthesis included: a) aqueous extracts from the seaweed (*S. incisifolium*), b) a variety of pure fucoidans from different brown alga, and lastly c) $NaBH_4$ was used to synthesise silver nanoparticle and sodium citrate was used to synthesise gold nanoparticles.

The nanoparticle synthesis using seaweed extracts was performed using a modified method according to Vivek *et al.* (2011). The properties of the nanoparticles synthesised using this method are thus presented and discussed in the sections to follow. The role of major biomolecules (such as fucoidans) in the reduction of ions and the capping of nanoparticles was evaluated by using pure fucoidans from different seaweeds. The confirmation of these biomolecules on the surface of nanoparticles was carried out by analysis of FTIR-spectra.

3.2. Materials and methods

3.2.1 Chemicals and reagents

The materials used in this study include Sodium borohydride, sodium citrate, gold (III) chloride tryhidrate, silver nitrate, fucoidan from *Fucus vesiculosus* (Fv), *Undaria pinnatifida* (Up), and *Macrocystis pyrifera* (Mp) were purchased from Sigma Aldrich and used without further purification. Folin-Ciocalteu reagent, Na_2CO_3, gallic acid, phosphate buffer (pH 6.6), potassium ferricyanide, trichloroacetic acid (TCA), ferric chloride ($FeCl_3.6H_2O$), ascorbic acid, and 1,1-Diphenyl-2-Picryl-Hydrazyl (DPPH) were purchased from sigma Aldrich. All solvents were redistilled before use. Milli-Q water (15.0 $M\Omega cm^{-1}$) was used for all reactions, including

extraction procedures, dissolving salts and for the synthesis of nanoparticles as well as washing of glassware.

3.2.2. Seaweed extraction

S. incisifolium[1] was collected from the coast of the Western Cape Province, South Africa and stored frozen (-20 °C) until use.

Two different aqueous extracts were prepared from the alga. Firstly, the alga (27.5 g) was extracted directly in boiling water (1 L) for 1 h. A portion aqueous extract (AR) was freeze-dried and stored in a desiccator while the other portion was stored as liquid at -20 °C. Secondly, the alga (27.5 g) was sequentially extracted with methanol(1 L) and dichoromethane-methanol (2:1). The volumes of methanol was 900 ml whilst that of DCM was 1800 ml. Afterwards, the alga was dried, crushed and extracted with boiling water for 1 h. A portion of aqueous extract (AC) was freeze-dried and stored in the desiccator while the other portion was stored as liquid at -20 °C.

3.2.3. Synthesis of silver nanoparticles

a) AgNP synthesis from S. incisifolium aqueous extract (AC and AR)

i) The preliminary method was adapted from Vivek *et al.* (2011). Briefly, 10 ml of aqueous extract (before freeze drying) was added to 90 ml of $AgNO_3$ (0.001 M) and the solution was gently stirred for 18 hours.

ii). In the second method, the freeze-dried extract (2 mg) was dissolved in 10 ml of distilled water. The solution was allowed to mix for 10 minutes after which 500 µl of $AgNO_3$ (0.1 M) solution was added and the reaction was allowed to proceed for 18 hours. This method was applied for both the AR and AC extracts.

[1] Synonymous with *S. heterophyllum*

b) AgNP synthesis from commercially available fucoidans Fv-AgNP, Mp-AgNP and Up-AgNP

The fucoidans from *F. vesiculosus* (*Fv*), *U. pinnatifida* (*Up*),and *M. pyrifera* (*Mp*) were used to synthesise the following nanoparticles. Briefly, 10 mg of pure fucoidans (*Fv*, *Mp* or *Up)* was dissolved in 10 ml of distilled water. To this solution, 500 µl of 0.1 M $AgNO_3$ was added. The solution was then allowed to stir at 100 ºC for 15 minutes for *F. vesiculosus*, 30 minutes for *M. pyrifera*, and 60 minutes for *U. pynatifeda*.

c) AgNPs synthesised from $NaBH_4$ (SB-AgNP)

The method used for the chemical syntheses of AgNP using $NaBH_4$, was carried out using a method developed by Solomon *et al.* (2007). Briefly, 10 ml of 1 mM $AgNO_3$ solution and 30 ml of a 2 mM of $NaBH_4$ solution were first chilled at 0 ºC for 1 hour before mixing. The $AgNO_3$ solution was added $NaBH_4$ solution drop wise with vigorous stirring until all silver nitrate was added. The reaction was stopped immediately after the last addition of silver nitrate, (approximately 3 minutes total reaction time).

3.2.3.1. The rate of nanoparticle formation

The rate of nanoparticle formation was determined by making use of the SPR band of the Ag or Au NPs in UV-Vis spectrophotometry (GBC Cintra 202 UV-Vis spectrophotometer). An aliquot (4 ml) of each sample was taken for UV-Vis analysis every 30 minutes for 150 minutes. The reaction was then allowed to proceed until 18 hours after which UV-Vis absorbance spectrum was collected, using the software, Cintral version

3.2.4 Synthesis of gold nanoparticles

The same biological protocol was followed for the synthesis of AuNPs as for AgNPs to give D-AC-AgNP, D-AR-AuNP, L-AC-AuNP, L-AR-AuNP, Fv-AuNP, Mp-AuNP and Up-AuNP.

a) Synthesis of AuNPs using sodium citrate

The chemical synthesis of AuNPs was accomplished by following the method used by Ojea-Jimenez *et al.* (2010). Sodium citrate (2.2 mM, 150 ml) was heated to 90 ºC before adding a

solution of $HAuCl_4.3H_2O$ (25 mM, 1 ml). After the addition of gold, the solution was allowed to stir for 10 minutes after which the solution was placed in ice to speed up the cooling process.

3.2.5 Characterization of aqueous extracts and commercially available fucoidans

a) UV spectra

UV spectra of the crude extracts and fucoidans were collected using a GBC Cintra UV-Vis spectrophotometer. Briefly, 2 mg of freeze-dried aqueous extract was dissolved in 10 ml of distilled water. Then, 4 ml of this solution was taken for UV-Vis analysis. For the fucoidans, 10 mg was dissolved in 10 ml distilled water and then 4 ml of each solution was taken for UV-Vis analysis.

b) IR spectra

The portion of freeze-dried aqueous extract (AC and AR) was taken for IR analysis in powder form. Similarly, the fucoidans were taken for IR analysis in powder form.

c) NMR spectroscopy

NMR spectra (^1H and HSQC) were acquired on a Bruker 400 MHz Avance IIIHD Nanobay spectrometer equipped with a 5 mm BBO probe at 333 K using standard 1D and 2D NMR pulse sequences. All spectra were referenced to residual undeuterated solvent peaks.

3.2.6 Characterization of nanoparticles

a) UV-Vis spectroscopy

UV-Vis absorbance spectroscopy was carried out to monitor the formation of nanoparticles (with a GBC Cintra 202 UV-Vis spectrophotometer). For nanoparticles (both silver and gold nanoparticles) synthesised using the aqueous extract from *S. incisifolium*, the UV-Vis absorption spectra were measured after 18 hours, which was the expected complete end-point of the reaction. The UV-Vis absorbance spectra were measured immediately after complete reaction for the nanoparticles synthesised from pure fucoidans, $NaBH_4$ and sodium citrate. The samples were

measured in a quartz cuvette with a path length of 1cm. The visible range for the measurements was set to be from 600 nm to 300 nm for AgNPs and 800 nm to 300 nm for AuNPs.

b) FTIR spectroscopy

The NPs synthesized were centrifuged at 10 000 rpm for 20 minutes. The supernatant was then discarded, the pellet was collected and re-suspended in distilled water where it was centrifuged again at 10 000 rpm. The process was repeated two more times to enable purification. The nanoparticles were then freeze-dried and and their spectra recorded on a ParkinElmer Spectrum 400, FT-IR/FT-NIR spectrophotometer, using the software, Spectrum. The measurements were done using attenuated total reflectance (ATR) accessory.

c) XRD

The structure and crystallinity of lyophilized powder samples of nanoparticles (AgNPs and AuNPs) were analysed using XRD. The XRD patterns were acquired from a Bruker AXS (Germany) D8 Advance diffractometer (voltage 40 KV; current 40 mA). The XRD spectra were recorded in the range 10-90º using an X-ray source of Cu Kα (λ=0.154 nm) monochromatic radiation. The NPs used for XRD analyses were prepared as in section 3.2.6 b. The freeze-dried NPs were submitted for XRD to determine their crystalline size and structure. The size of the NPs was calculated using the Debye-Scherrer equation (equation 2.2) (Park *et al*., 2016) by making use of the FWHM of the most intense peak (the 111 index peak) at ~2θ = 38º for both the Au and Ag NPs samples. The program used to calculate the FWHM was the Program CMPR SVN version 513 (Brian Toby, Advanced Photon Source, Argonne National Lab (Brian.Toby@ANL.gov).

d) Transmission Electron Microscopy (TEM) and Energy Dispersive X-ray (EDX) analysis

Samples were prepared by drop-coating one drop of the specimen solution onto a holey carbon coated copper/nickel grid. The specimen solution was then dried under a xenon lamp for about 10 minutes, where after the sample coated grids were analysed under the microscope. Transmission electron micrographs were collected using an FEI Tecnai G2 20 field-emission gun (FEG) TEM, operated in bright field mode at an accelerating voltage of 200 kV. Energy

dispersive x-ray spectra (EDX) were collected using an EDAX liquid nitrogen cooled lithium-doped silicon detector. The size of the nanoparticles was determined with ImageJ software.

e) Dynamic light scattering (DLS) spectroscopy and Zeta potential measurements

The hydrodynamic size of nanoparticles was also determined by making use of a Zetasizer (Malvern zetasizer, nano series instrument). After the synthesis of nanoparticles, an aliquot (3 ml of nanoparticle solution in water) from each solution was taken for determination of the hydrodynamic size by the Zetasizer. Three measurements were determined in triplicate and averaged to obtain the mean size of the nanoparticles. Similarly, the zeta potential of the nanoparticles was determined, where an aliquot (1 ml of nanoparticle solution in water) from the nanoparticle solution was taken and measured. The zeta potential was determined in triplicate, averaged and then recorded.

3.2.7. Determination of antioxidant activity

a) ***Determination of total polyphenolic content***

To determine total phenolic content of *S. incisifolium,* method described by Tobwala *et al*. (2014) was performed which involves the use of Folin-Ciocalteu (FC) reagent. Of the two *S. incisifolium* aqueous extracts (AC and AR), 125 µl of each was mixed with 625 µl of FC reagent, which was diluted 10-fold. Then, 500 µl of 75 mg/ml of Na_2CO_3 was added after 5 minutes of incubation at room temperature. The solutions were vortexed followed by incubation at room temperature for 90 minutes in dark. After incubation, the absorbance was measured at 760 nm (BMG Labtech) and gallic acid was used as standard. The results were recorded as µg of gallic acid equivalents (GAE)/mg of dried seaweed.

b) ***Determination of total reducing power***

Method described by Tobwala *et al.* (2014) was carried out in the lab for determination of total reducing power of the two *S. incisifolium* extracts (AC and AR). Briefly, 2.5 ml of 0.2 M phosphate buffer (pH 6.6) and 2.5 ml of 1% potassium ferricyanide were added to 1 ml of each extract, followed by incubation at 50 ºC in water bath for 20 minutes. Thereafter, 2.5 ml of 10% Trichloroacetic acid (TCA) was added to each solution. The solutions were then centrifuged at

6000 rpm for 10 minutes. From the supernatant obtained, 2.5 ml was added to solution comprising 2.5 ml of distilled water and 0.5 ml of 0.1 % ferric chloride ($FeCl_3.6H_2O$). The absorbance was read after 5 minutes at 700 nm (BMG Labtech). The ascorbic acid was used as the standard and the results were recorded as µg of ascorbic acid equivalents (AAE)/mg of dried seaweed.

c) ***Determination of radical scavenging power***

The method described by Tobwala *et al.* (2014) was used to assess the radical scavenging power of aqueous extracts (both AC and AR) of *S. incisifolium*. Shortly, 2.9 ml of DPPH (1×10^{-4} M) was mixed with 0.1 ml of each extract. The solutions were incubated at room temperature in dark for 30 minutes. The absorbance was read at 520 nm (BMG Labtech). Radical scavenging power was calculated with the use of equation 1.

$$RSP = [1-(A1/A2)] \times 100\ \% \qquad (3.1)$$

Where **RSP** is radical scavenging power, **A1** is the absorbance of sample with seaweed extract and **A2** is the absorbance of sample without seaweed extract.

3.3. RESULTS AND DISCUSSION

3.3.1. Spectroscopic characterisation of the Sargassum incisifolium aqueous extract and fucoidans used in the synthesis of the NPs

As described in section 3.2.2, the aqueous extracts were performed in two different ways. The two extracts differed in colour; where a dark brown colour was obtained for the L-AC extract, a normal brown colour was obtained in the L-AR extract (Figure 3.1 D and E). A possible explanation for the dark colour of L-AC extract could be that the prior organic extraction removed all water insoluble organic biomolecules leaving the water soluble polysaccharides and polyphenols in this marine algal extracts.

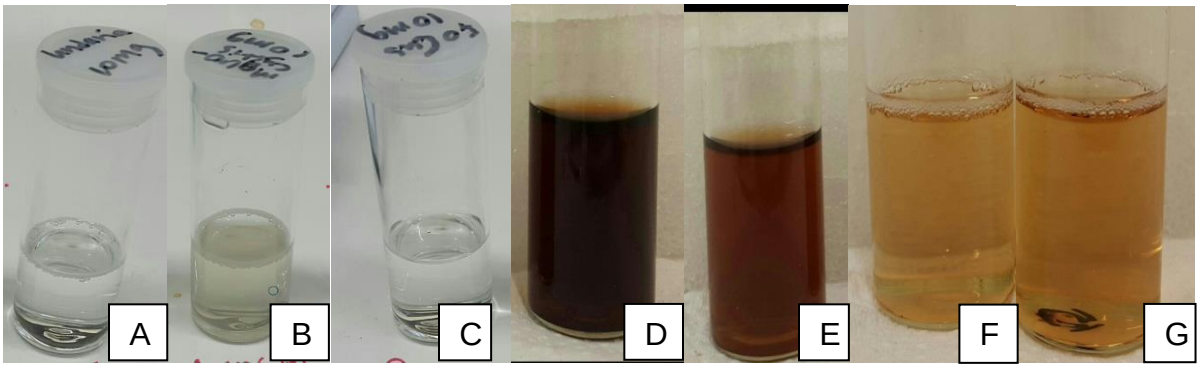

Figure 3.1. Photographs showing the colours of aqueous extracts of *S. incisifolium* as well as commercially available fucoidans A) Up, B) Mp, C) Fv, D) L-AC, E) L-AR, F) AR, G) AC.

Before the synthesis of the nanoparticles, the aqueous extract (AE) and fucoidans dissolved in distilled water were subjected to UV-Vis analysis (Figure 3.2). From Figure 3.2 it can be seen that the pure fucoidan samples Fv and Up are featureless which is expected as these are polysaccaharides and they are optically transparent. The fucoidan isolated from *Macrocystic pyrifera* (Mp), on the other hand, displays a broad peak between 250 and 350 nm, as does the aqueous extract (AE). However, the peaks at this region for the aqueous extract are more pronounced and this may be due to the presence of polyphenols which could also explain the dark brown colour of the extract. Nevertheless, it is clear that the extracts or fucoidans will not mask the observation of Ag or Au NPs as the SPR bands associated with these NPs are expected to occur between 400 and ~530 nm (Gherbawy *et al*., 2013; Huang & El-Sayed, 2010; Jones *et al*., 2011).

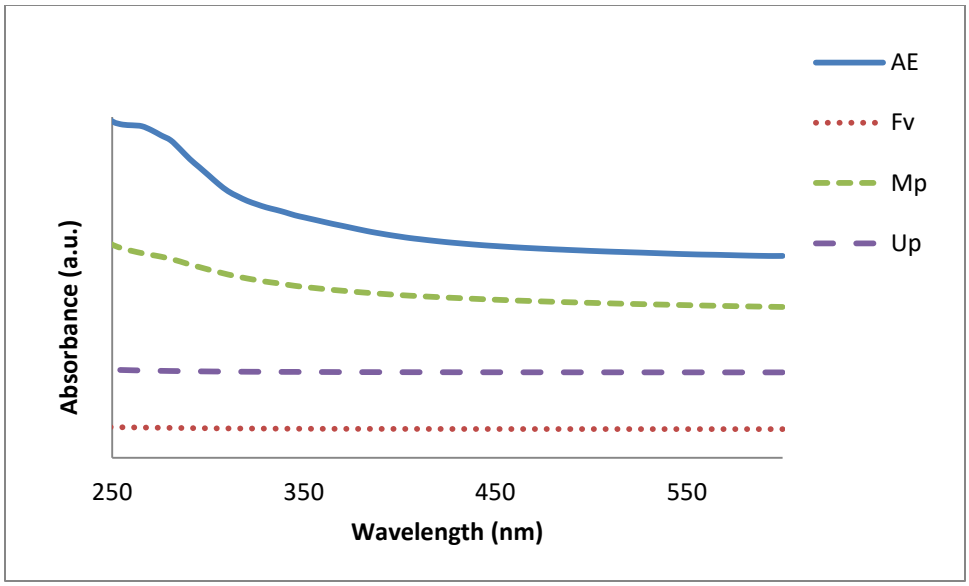

Figure 3.2 UV-Vis absorption spectra for *S. incisifoium* aqueous extracts (AE) and commercially available fucoidans Up, Mp, and Fv.

Further comparison of these reducing agents was done by NMR and the edited HSQC spectra are shown in Figures 3.3-3.6. The HSQC NMR spectra provide information about direct ^{1}H-^{13}C correlations. The purpose of this analysis was not to assign the structures of the fucoidans and aqueous extract but rather to provide a basis to allow one to identify different structural features of the different extracts. In addition, one can distinguish between methyl, methylene and methine signals. Figure 3.3 shows an overlay of the HSQC NMR spectra of *S. incisifolium* aqueous extract (black) and that of the fucoidan from *F. vesiculosus* (red). The large number of overlapping proton signals makes the analysis of the ^{1}H NMR spectrum (x-axis) very difficult. However, the carbon signals (y-dimension) provide a significant amount of information. Firstly, a methyl signal at ~ δ 18 is clearly apparent as are the sugar oxymethine carbons between δ 60 and 80. Finally, the anomeric carbons of sugars are visible around δ 100. Most importantly, an overlay of the two spectra (red and black dots) clearly shows significant differences in carbon and proton signals suggesting that different major monosaccharides are present in these extracts. Interestingly, only low intensity signals are present at δ_C/δ_H 102/6.2 (characteristic of phlorotannins) suggesting that phlorotannins are present as minor constituents in the *S. incisifolium* crude extract.

Similar trends were observed when comparing the HSQC spectra of the *S. incisifolium* aqueous extracts and the other fucoidans (Figures 3.4 and 3.5). Figure 3.6 shows an overlay of all three commercially available fucoidan HSQC spectra and the significant overlap of the signals suggest very similar monosaccharide composition of these fucoidans.

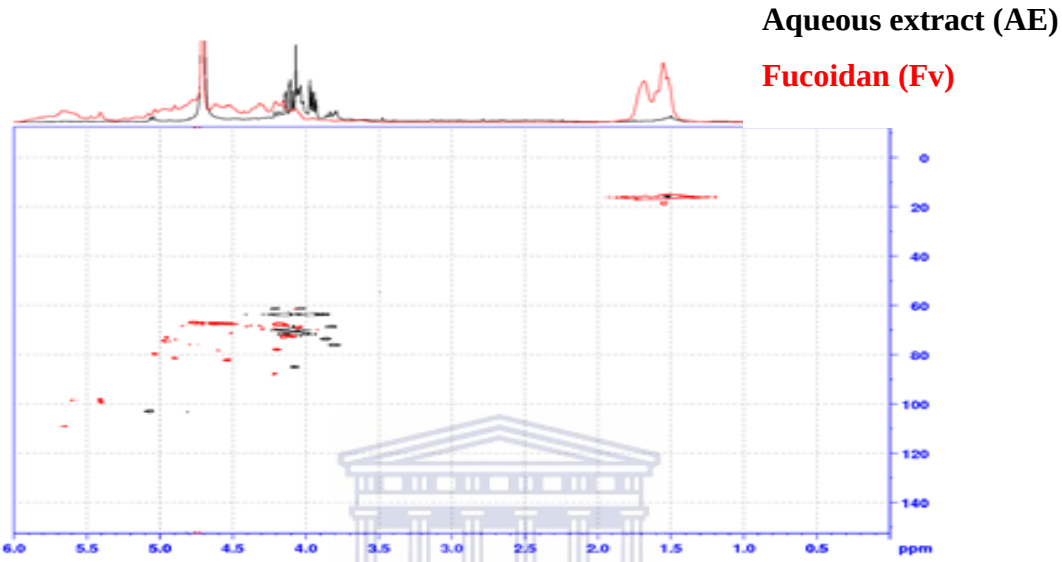

Figure 3.3. HSQC NMR spectra showing the comparison between AE and Fv.

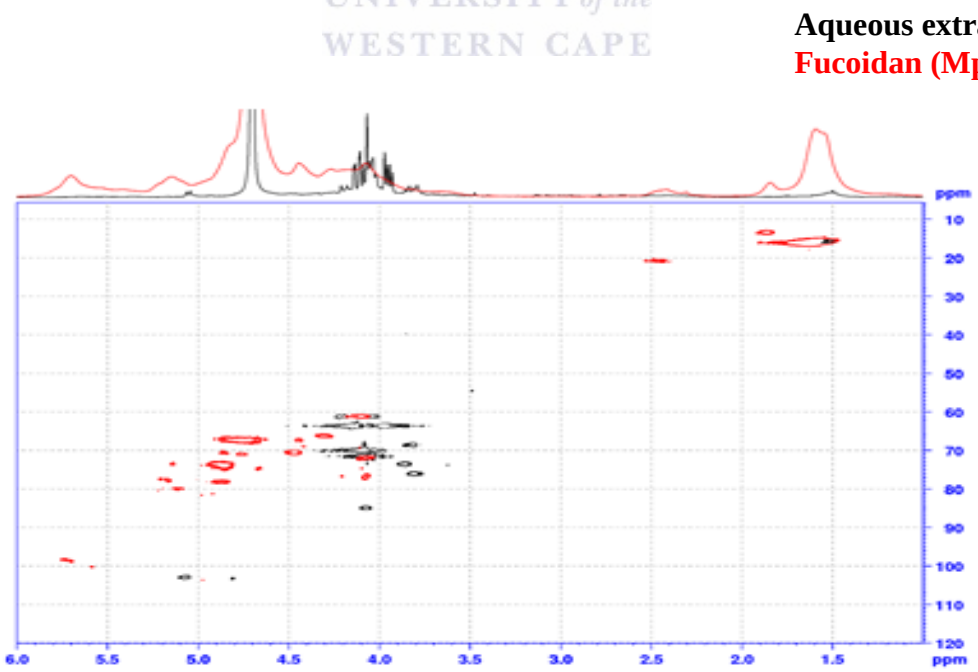

Figure 3.4 HSQC NMR spectra showing comparison between AE and Mp.

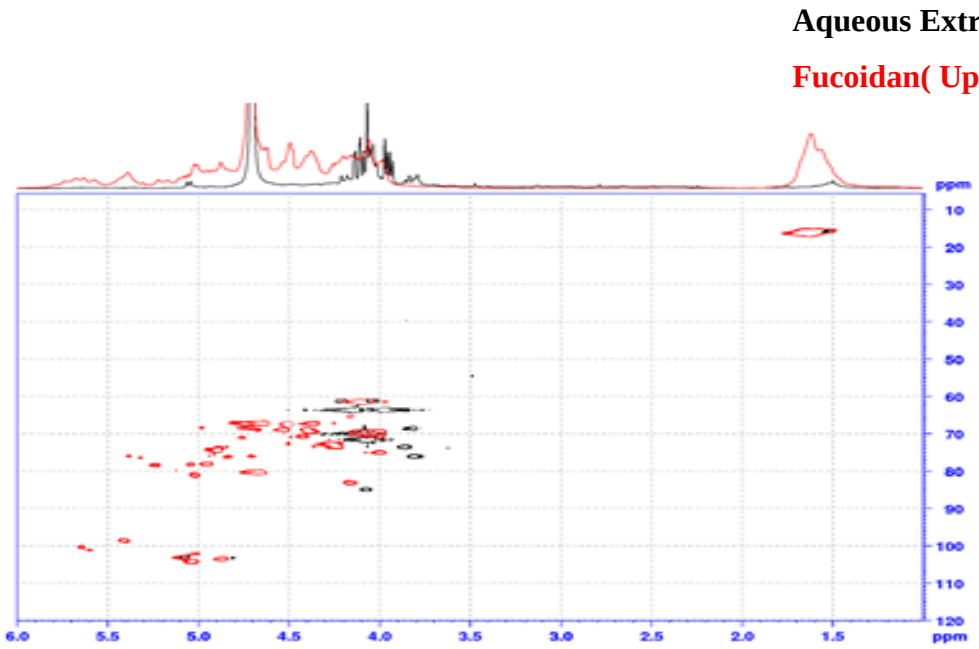

Figure 3.5 HSQC NMR spectra showing comparison between AE and Up.

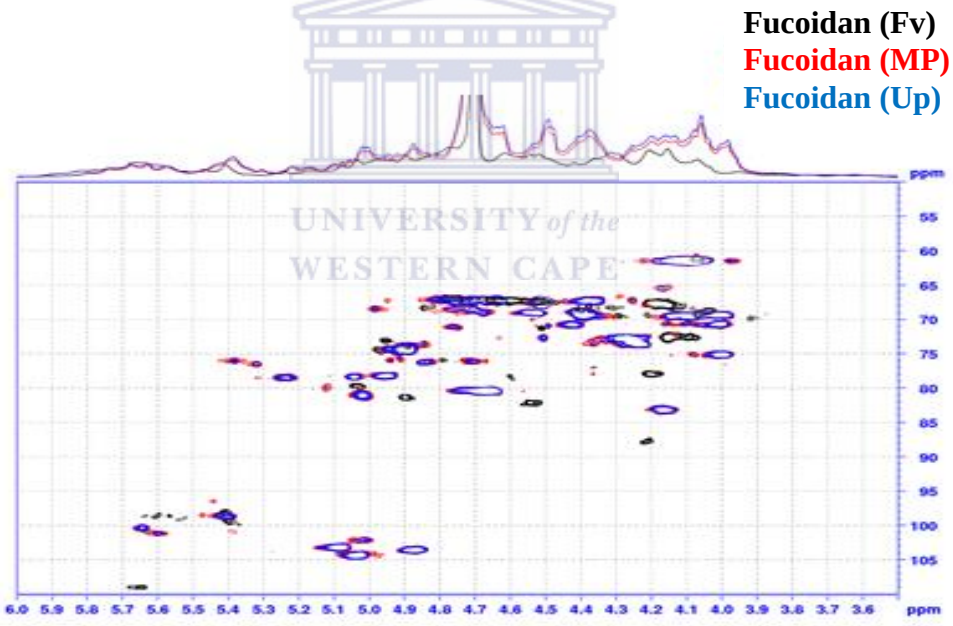

Figure 3.6 HSQC NMR spectra showing comparison between fucoidans Fv, Mp, and Up.

FT-IR spectroscopy was also used for comparison of the AE and fucoidan samples (Figure 3.7). The C-O-C group of monosaccharides was detected at around 800 cm^{-1} (Schulz & Baranska, 2007) in all the spectra except in AC extract. Other similarities are observed between Mp and Up at the peak around 1026 cm^{-1} which indicates the presence of C-N functional group of aliphatic

amines (Kannan et al, 2013). Also AR and AC had similar peaks at 1599 cm^{-1} which may represent amide II bond (Princy & Gopinath, 2013). AR further had a peak at 1038 cm^{-1} which may show the presence of carboxylic acid in the extract (Princy & Gopinath, 2013). Mp and Fv had a peak at around 1200 cm^{-1} which may signal the stretching of sulfated polysaccharides (Kannan et al, 2013). C=N is detected in Mp at 1628 cm^{-1} and at 1636 cm^{-1} in Fv (Kannan et al, 2013). All the reducing agents had the OH group which is usually detected at around 3200-3400 cm^{-1} (Princy & Gopinath, 2013).

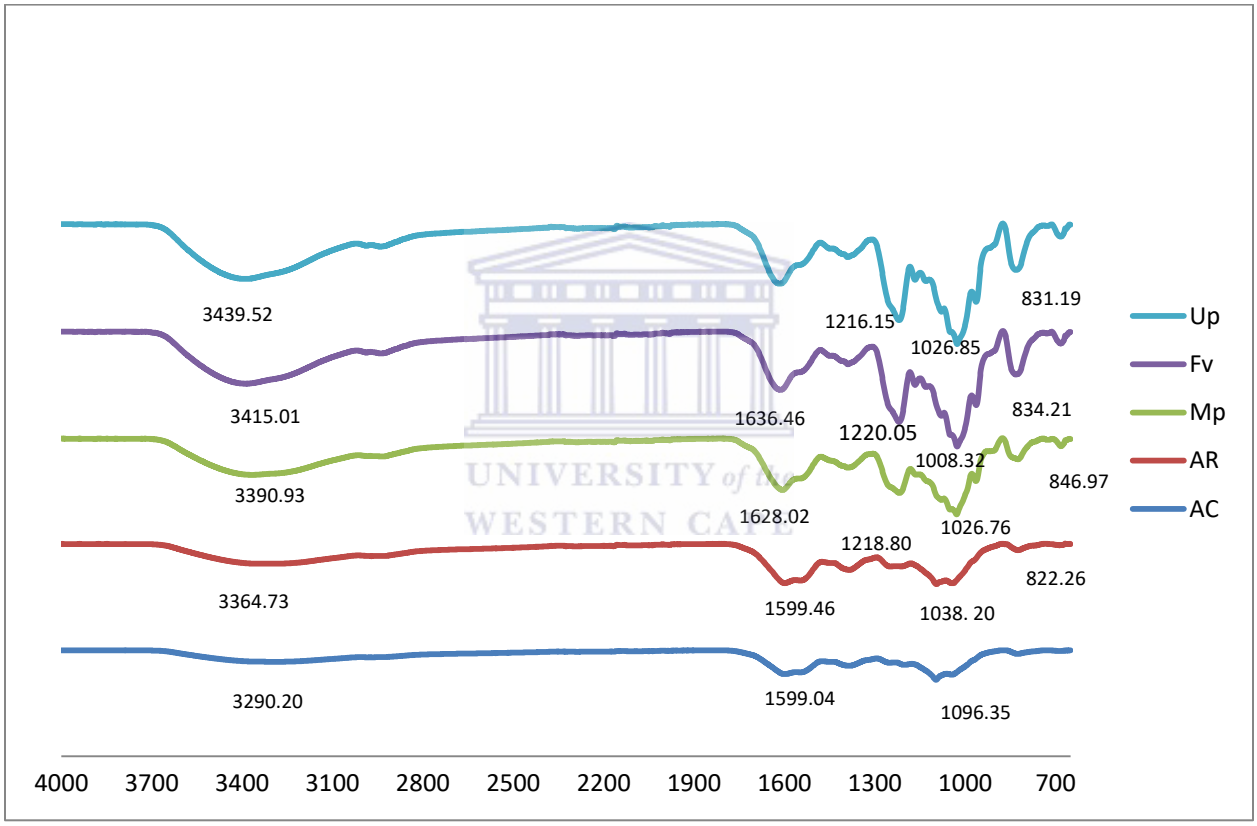

Figure 3.7 FT-IR spectra of A) *S. incisifolium* crude extract and fucoidans.

Determination of the antioxidant activity, polyphenolic content and total reducing power of the aqueous extracts of* S. incisifolium *and fucoidans

The polyphenolic content, total reducing power and antioxidant activity of the two aqueous extracts of *S. incisifolium* and pure fucoidans (Fv, Mp, Up) were evaluated according to Topiwala *et al.* (2014) and the results are presented in Table 3.1. The total phenolic contents of the samples were recorded as gallic acid (a standard) equivalents (GAE) in µg/mg of dried

seaweed. The study was carried out in order to give insight into a) the polyphenolic content of the reagents used and their reducing power (and therefore their ability to form nanoparticles) and b) their antioxidant activity. Prior extraction of the seaweed with organic solvents rendered the AC extract (which is a darker brown in colour) a higher phenolic content and reducing power compared to the AR extract. The pure fucoidans, as polysaccharides isolated from brown seaweeds, possessed significantly lower phenolic contents than the aqueous extracts with Fv, at 1 µg/mg GAE, having the lowest content (Table 3.1). The total phenolic content of the AC extract was significantly higher and the following order was observed: AC>AR>Mp>Up>Fv (with $p < 0.05$).

Table 3.1 Total polyphenolic content and reducing power of the *S. incisifolium* aqueous extracts, and the fucoidans from *F. vesiculosus* (Fv), *M. pyrifera* (Mp) and *U. pinnatifida* (Up).

Extract	Total polyphenolic content (GAE, in µg/mg of dried seaweed / fucoidin)*	Total reducing power (AAE, in µg/mg of dried seaweed / fucoidin)*
AC	235 ± 0.013	95 ± 0.008
AR	150 ± 0.019	75 ± 0.003
Fv	1 ± 0.0007	10 ± 0.001
Mp	10 ± 0.007	15 ± 0.001
Up	10 ± 0.048	15 ± 0.003

*p<0.05

The total reducing power of these samples was also assessed and a similar trend observed. In this assay, the total reducing power of the samples depends on the capability of the antioxidants in the samples to reduce Fe^{3+} (and give an indication of the ability of the samples to reduce the Ag and Au salts to form nanoparticles). The results obtained (Table 3.1) are presented as ascorbic acid equivalents (AAE) in µg/mg of dried seaweed and pure fucoidans. The AC extract boasted a higher total reducing power content (at 95 µg/mg AAE of dried seaweed) than that of the AR sample and pure fucoidans (Table 3.1). The pure fucoidans exhibited much lower values, with the lowest values recorded for the Fv fucoidan (at 10 µg/mg AAE). The total reducing power

was greatest for the *S. incisifolium* aqueous extracts followed by the pure fucoidans in the following order: AC>AR>Mp>Up>Fv.

The trends observed above were echoed in the radical scavenging assays conducted. The DPPH scavenging method is dependent on the reduction of the DPPH to a more stable form (DPPH-H) by the antioxidants (Shon *et al*., 2003). The AC extract once again exhibited a higher radical scavenging power (60% DPPH scavenging) compared to the AR extract (28% DPPH scavenging, Figure 3.8). However, this time the % radical scavenging ability was found to be lowest for the Mp fucoidan. The following order was observed with the radical scavenging ability: AC>AR>Up>Fv>Mp.

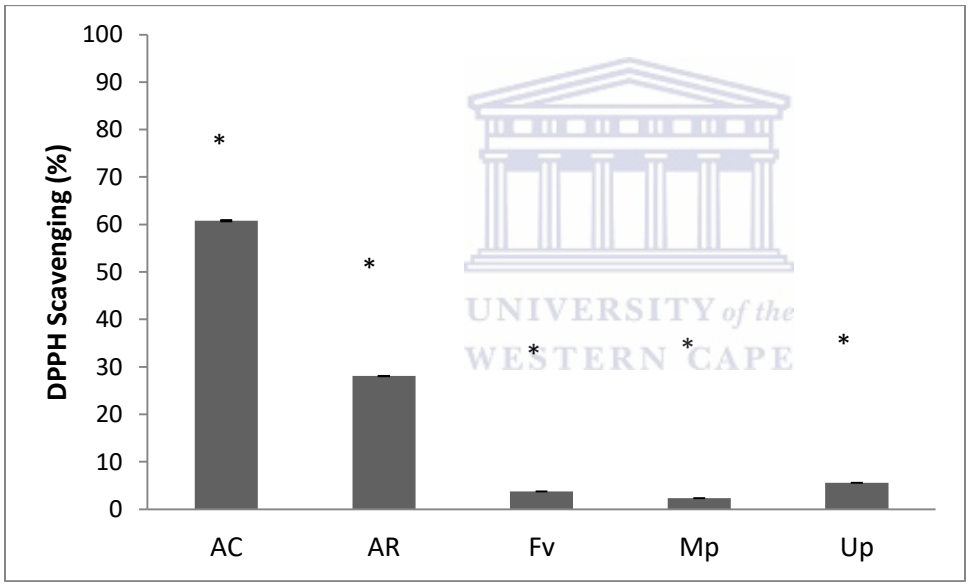

*p< 0.05

Figure 3.8 The DPPH radical scavenging power of the *S. incisifolium* aqueous extracts (AC and AR), and fucoidans from *F. vesiculosus* (Fv), *M. pyrifera* (Mp) and *U. pinnatifida* (Up).

3.3.1. Synthesis of nanoparticles

3.3.1.1. Synthesis of AgNPs using S. incisifolium aqueous extracts and sodium borohydride

The synthesis of AgNPs using sodium borohydride as reducing agent was used as a control reaction at room temperature. The formation of nanoparticles was very quick with colour change

appearing with immediate contact of silver nitrate and sodium borohydride. The colour changed gradually from colourless to dark yelleow within three minutes which is an estimated time of the complete reaction. The solution was subjected to UV-Vis analysis immediately after reaction (Figure 3.9).

The synthesis of AgNPs was initially investigated using the liquid extract *of S. incisifolium* (L-AC). A standard literature protocol was followed in which 10 mL of aqueous seaweed extract was added to 90 mL of a 1 mM solution of silver nitrate solution (Vivek *et al.* (2011). Unfortunately, the dark colour of this extract made visual inspection of the progress of the reaction very difficult. However, confirmation of the presence of AgNPs in the solution was easily obtained by the presence of a UV-Vis absorption band at 405 nm. This is due to the SPR band attributed to AgNPs (Song & Kim, 2009). The spectrum of the solution was measured after 18 hours and is shown in Figures 3.10. The reaction progresses rapidly at room temperature and is complete in 18 h.

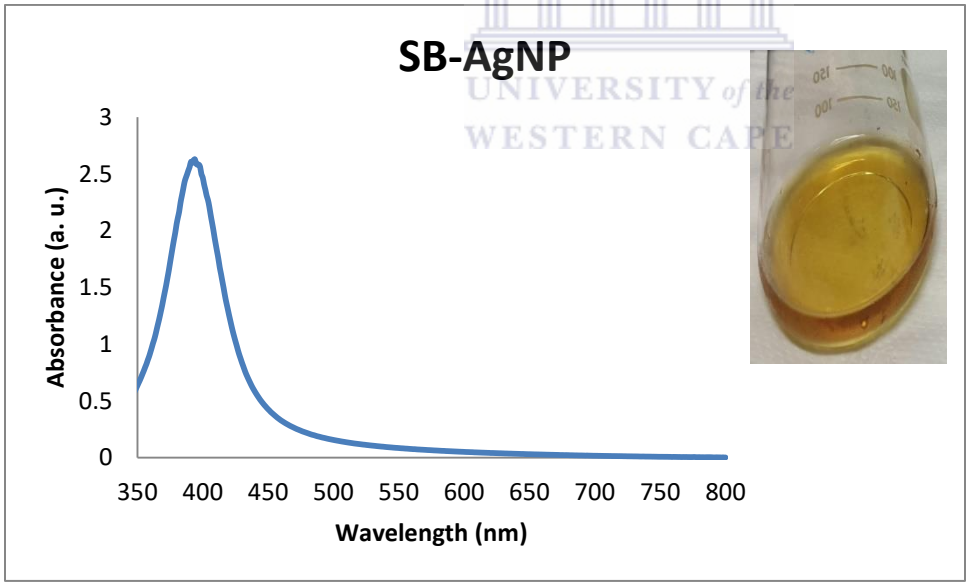

Figure 3.9 UV-Vis absorbance spectrum of SB-AgNP and the colour of the solution in water.

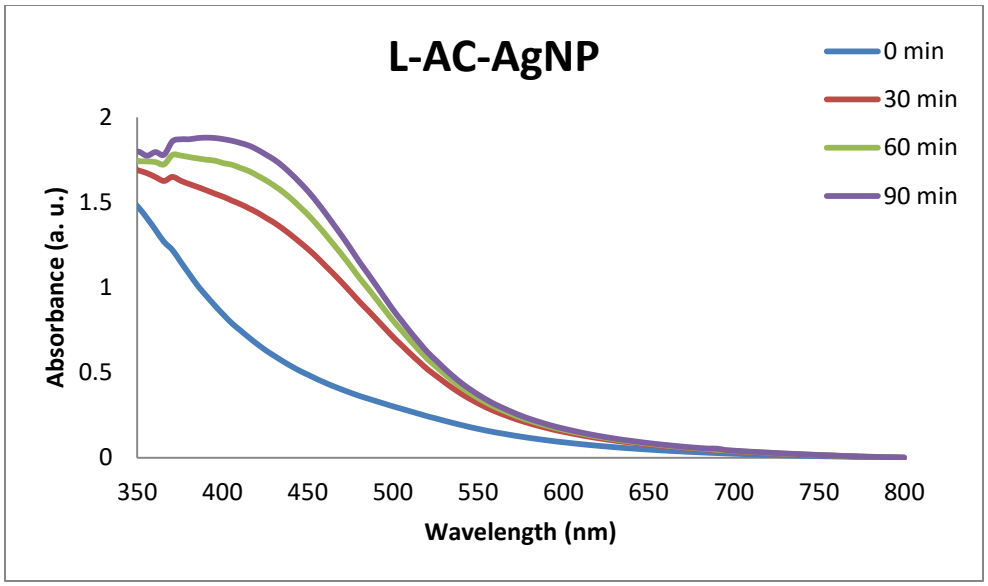

Figure 3.10 UV-Vis absorbance spectrum of L-AC-AgNP from time 0 to 90 minutes in water.

Although the reaction with the L-AC extract proceeded smoothly we were concerned about the potential variability in the amount of organic component extracted from the seaweed and thus added to the reaction mixture. We therefore freeze-dried the *S. incisifolium* aqueous extracts and after several trials developed an optimised method in which 2 mg of crude extract is taken up in 10 mL of water to which 500 µl of 0.1 M sodium nitrate was added. These reactions also proceeded at room temperature and at a rate comparable that of the liquid extracts (Figures 3.11 A & B). The formation of nanoparticles was found to occur within 30 minutes. The speed of the reaction appeared to slow down after 120 minutes in both reactions but was allowed to proceed for a further 18 hours to ensure completion. The plateau was observed whereby the absorbance seemed to level off (Figure 3.12).

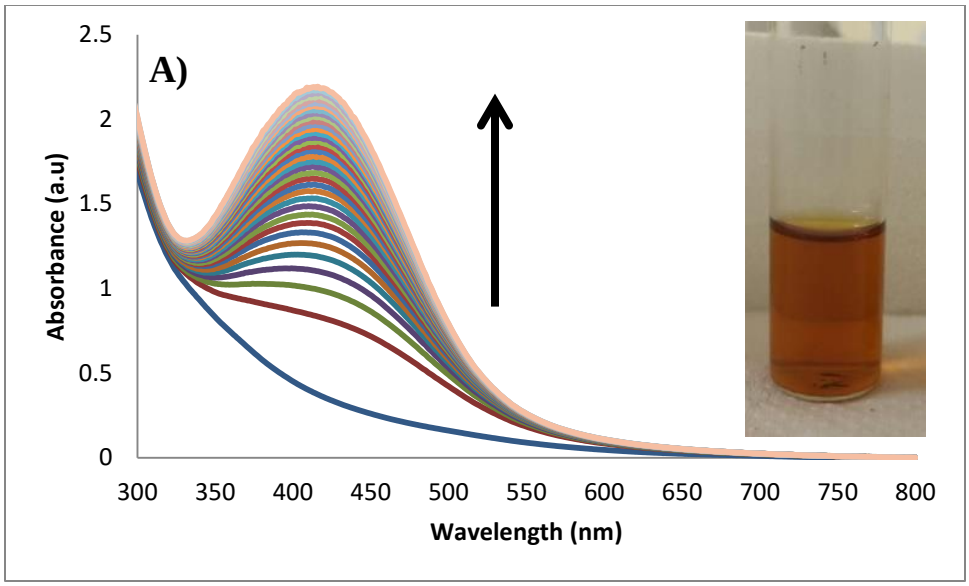

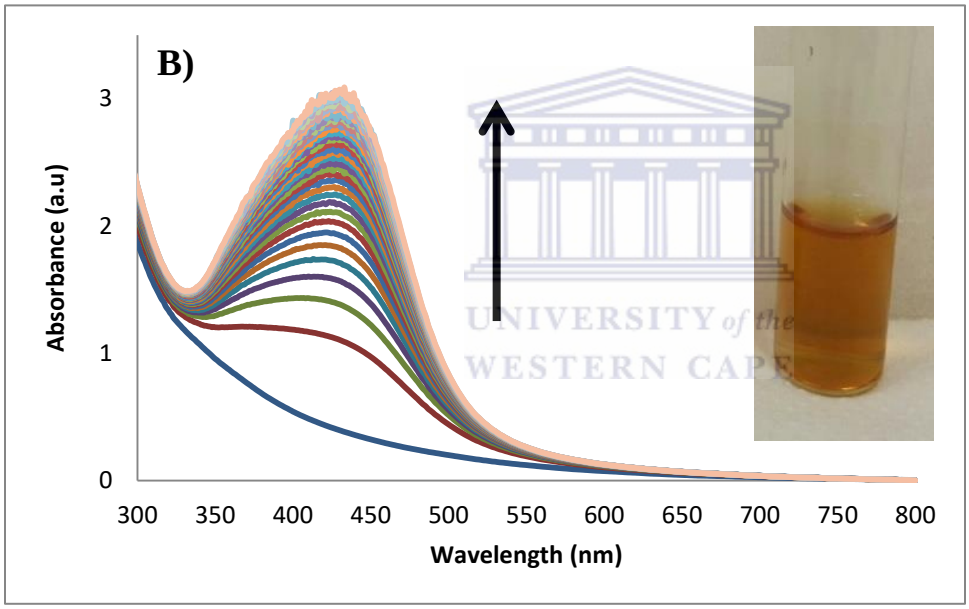

Figure 3.11 UV-Vis absorption spectra of a) the AC-AgNPs and b) the AR-AgNPs from time 0 to 18 hours. Inset: Photograph of the colour of the solution after 18 hours (in water).

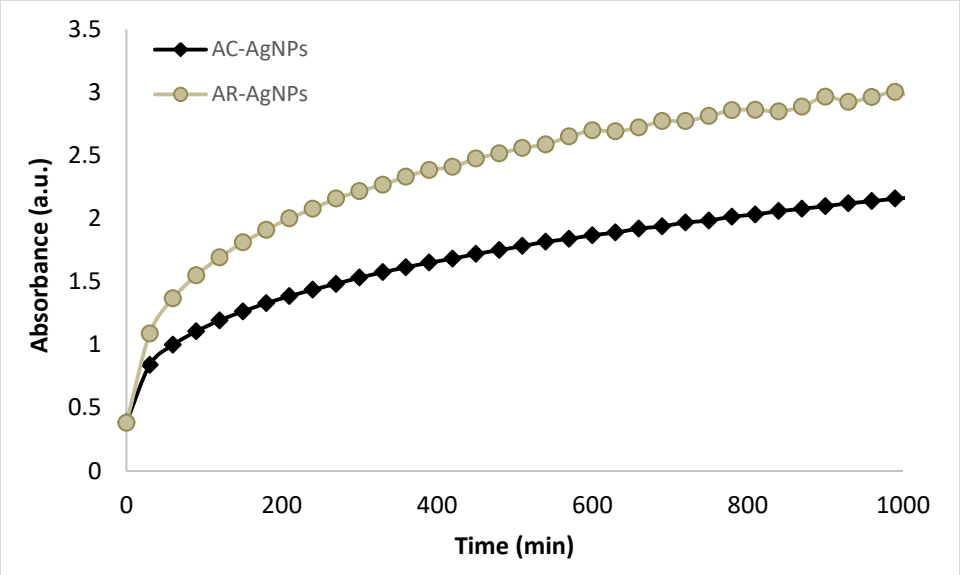

Figure 3.12 Change in absorbance with time during AC-AgNP and AR-AgNP formation as observed at the λ_{max} at 413 nm and 433 nm, respectively (in water).

The aqueous extract of *S. incisifolium* effectively reduces silver nitrate solutions to AgNPs at room temperature and pressure conditions and eliminates any other additional steps as seen in intracellular green synthesis of nanoparticles (Shankar *et al.*, 2004). Additionally, the only solvent used is water which is non-toxic and safe to use too. No ancillary chemicals are used in the synthesis of these NPs.

3.3.1.2. Synthesis of AgNPs using commercially available fucoidans

Fucoidans are fucose rich polysaccharides which are usually isolated from brown seaweeds. They are sulfonated and it is these sulfur groups that make fucoidans good capping agents for nanoparticles synthesis. As outlined in section 3.2.3 (b), the synthesis of AgNPs was also carried out using pure fucoidans from *F. vesiculosus, M. pyrifera* and *U. pynatifida* to determine if these compounds are indeed responsible for the formation of the NPs. The optimized reaction conditions required 10 mg of fucoidan in 10 ml of water to which 500 µl of silver nitrate solution (0.1 M) is added. Firstly, the synthesis of silver nanoparticles using fucoidans as reducing and capping agents was carried out at room temperature (25 ºC) for 18 hours, as shown in the UV-Vis spectra in Figures 3.13 to 3.15. As can be observed in the spectra, nanoparticle formation was not detected under room temperature conditions, suggesting that the pure fucoidans are not

responsible for the reduction of the silver ions at room temperature to form the AgNPs. Increasing the reaction temperature to 100 °C resulted in the formation of some AgNPs by these fucoidans. To determine if the fucoidans could play a role in the reduction of silver ions to form nanoparticles, the same reaction was carried out at 100 ºC. The time taken for the AgNP to form was found to vary from 15 minutes to 1 hour. *F. vesiculosus* showed a greater potential for AgNP formation, followed by *M. pyrifera*; with *U. pynatifida* being the slowest as observed by the change in colour of the solutions and the UV-Vis spectra (Figures 3.13 to 3.15). The reaction using the Up fucoidan was allowed to proceed for 1 hour. However, there was little or no change in colour suggesting that the pure fucoidan from *U. pynatifida* is not a good reducing agent. Higher temperatures could prove to yield AgNPs, however this was beyond the scope of this project due to time constraints. As mentioned in the previous section, the change in colour occurs due to the appearance of the SPR band with AgNP formation. The formation of the nanoparticles was faster in the reaction solution containing *F. vesiculosus*. The colour changed to dark yellow within 5 minutes and the reaction was allowed to take place for 15 minutes. The formation of nanoparticles in solution containing *M. pyrifera* was slower, with the colour change appearing after 10 minutes confirming the formation of AgNPs.

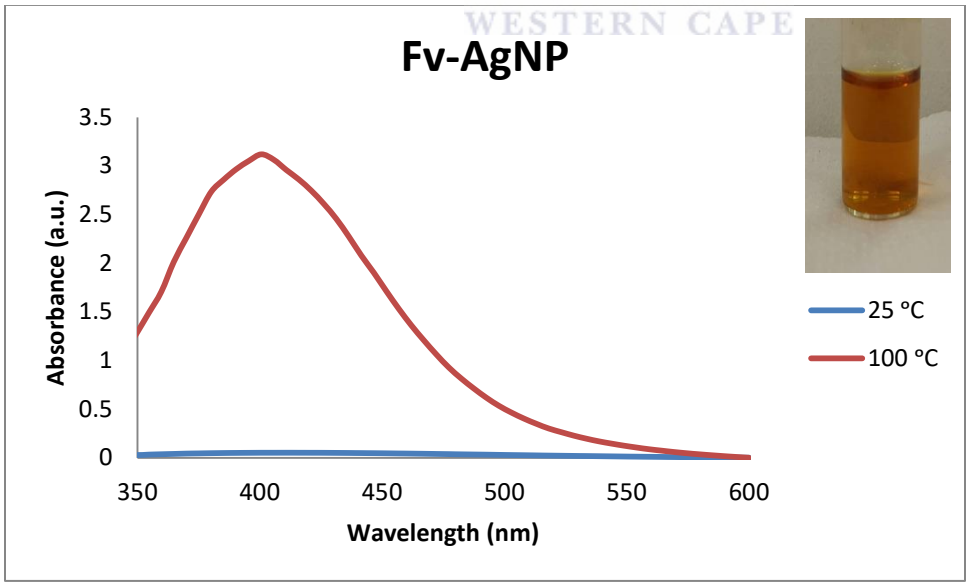

Figure 3.13 UV-Vis absorption spectrum of Fv-AgNP after 18 hours of stirring at room temperature in water.

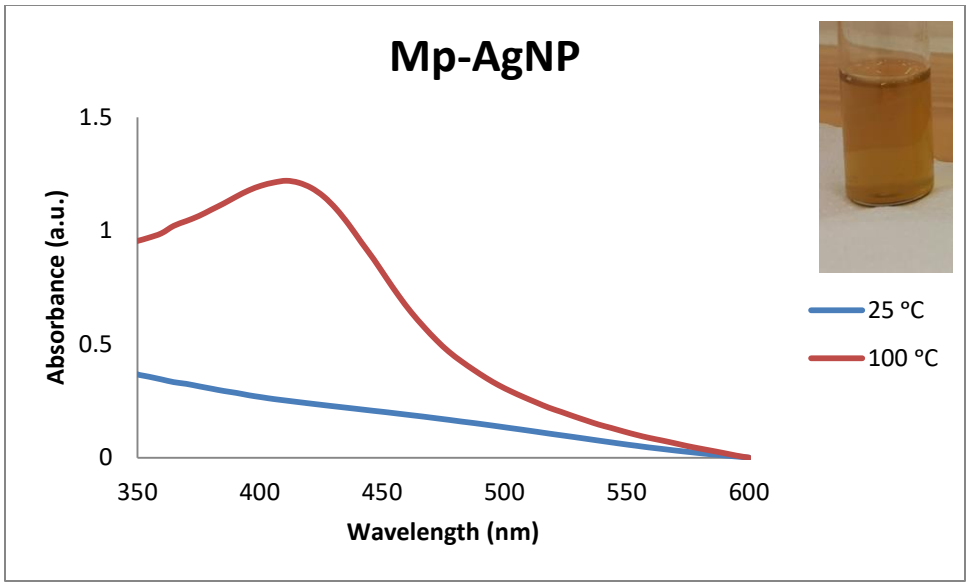

Figure 3.14 UV-Vis absorption spectrum of Mp-AgNP after 18 hours of stirring at room temperature in water.

The concentration of the NPs for the Fv- reaction solution was higher than that of the Mp reaction solution with little or no nanoparticle formation with the Up fucoidan solution (Figures 3.13 to 3.15). For this reason, *U. pynatifida* was not pursued further.

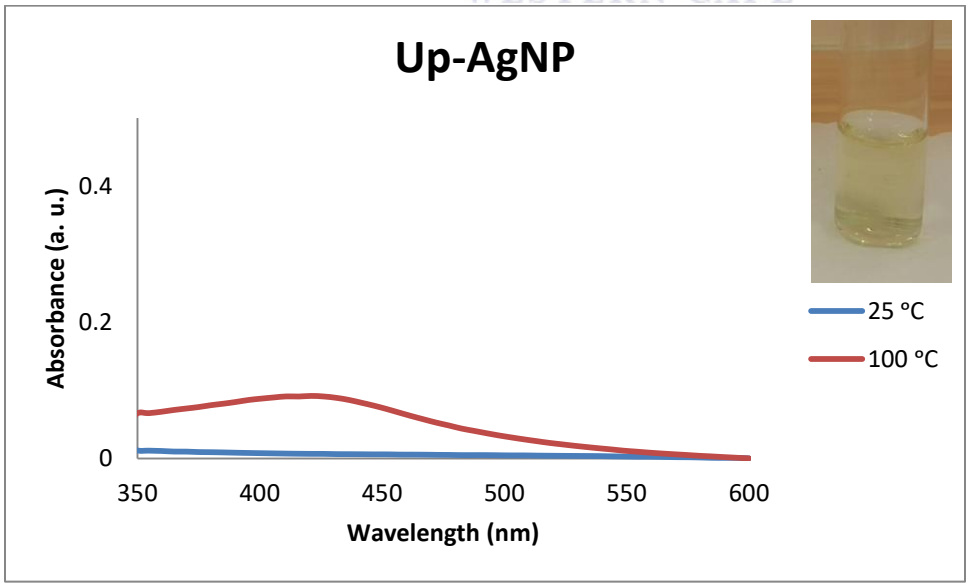

Figure 3.15 UV-Vis absorption spectrum of Up-AgNP after 18 hours of stirring at room temperature in water.

3.3.1.3 Summary of AgNP synthesis

Given the results obtained, it can be concluded that certain fucoidans have the capability of reducing silver ions to form AgNPs at higher temperatures. Since our original aim of this study was to synthesise AgNP using green methodologies, it could be argued that using fucoidans did not follow the 'green' method of nanoparticle synthesis since high temperatures were needed. An additional objective was to evaluate the major metabolites involved in the reduction of silver ions to form nanoparticles. Though fucoidans may be involved in the formation of nanoparticles at room temperature, additional metabolites are obviously at play with regards to the aqueous extracts of the brown alga. Based on our results it appears that fucoidans do not accomplish this purpose alone and require the assistance of other compounds. It is likely that the increased temperatures may break down the fucoidans into reducing sugars capable producing AgNPs. Fucoidans might still be involved in the capping of nanoparticles, even though other metabolites are obviously responsible for reduction of ions to form nanoparticles at room temperature. The synthesis of AgNPs using crude extracts obtained from S. *incisifolium* exhibited exceptional reducing qualities of silver ions at room temperature and pressure conditions.

3.3.2. Synthesis of gold nanoparticles

3.3.2.1 Synthesis of AuNPs from S. incisifolium aqueous extracts and sodium citrate

Gold nanoparticles (AuNPs) were also synthesised initially as a control in this study since the SPR band of AuNPs (at ~530 nm) is much easier to visualise than the AgNP SPR band. Like the AgNPs synthesised previously, gold nanoparticles were synthesised using the AC and AR extracts as described in section 3.2.4. The formation of AuNPs was easily observed by the change of colour from yellow to dark purple (Figure3.16 A & B). The plateau was observed whereby the absorbance seemed to level off (Figure 3.17).

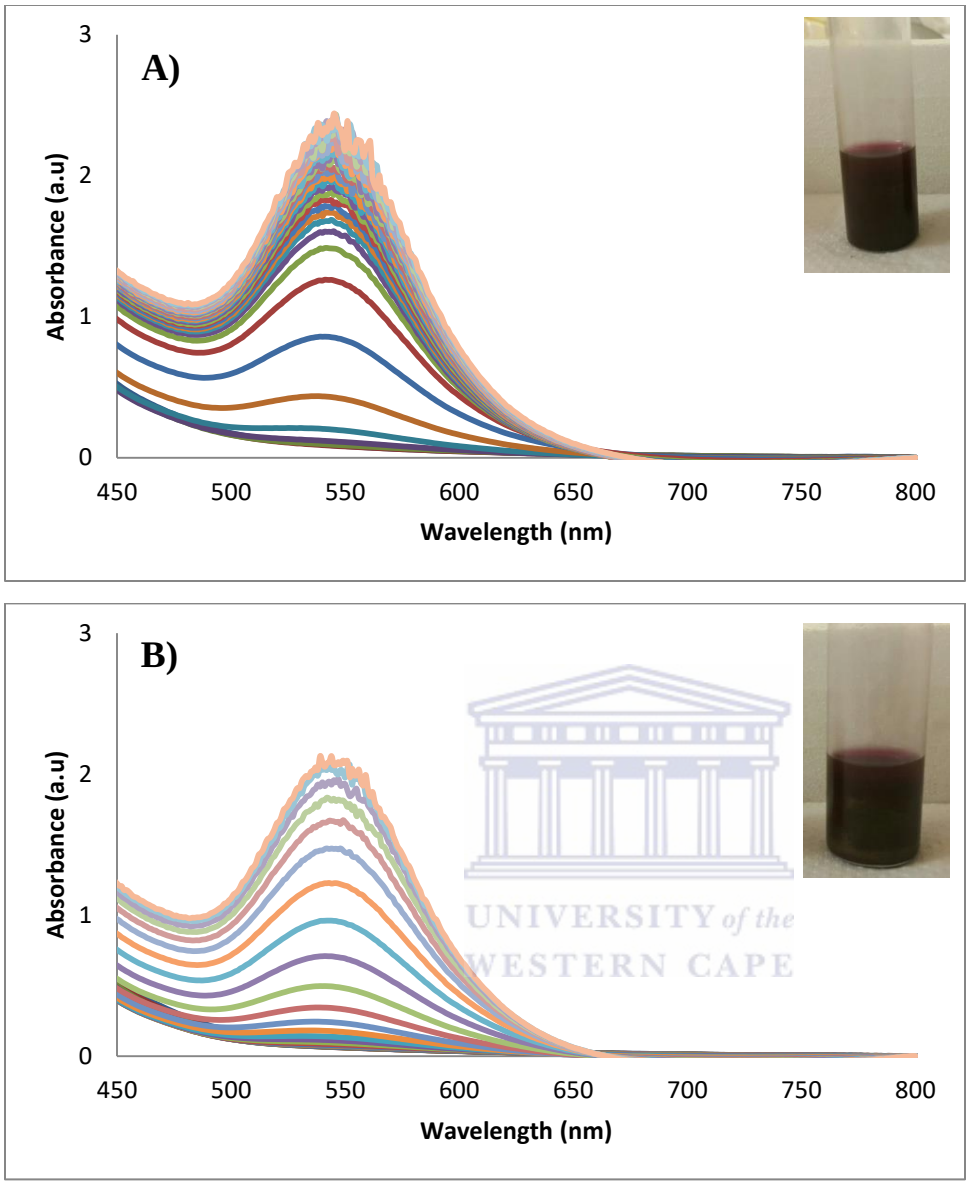

Figure 3.16 UV-Vis absorption spectra of a) AC-AuNPs and b) AR-AuNPs formed after 5 hours at room temperature (in water). Inset: Photograph of the colour of the solution after 5 hours.

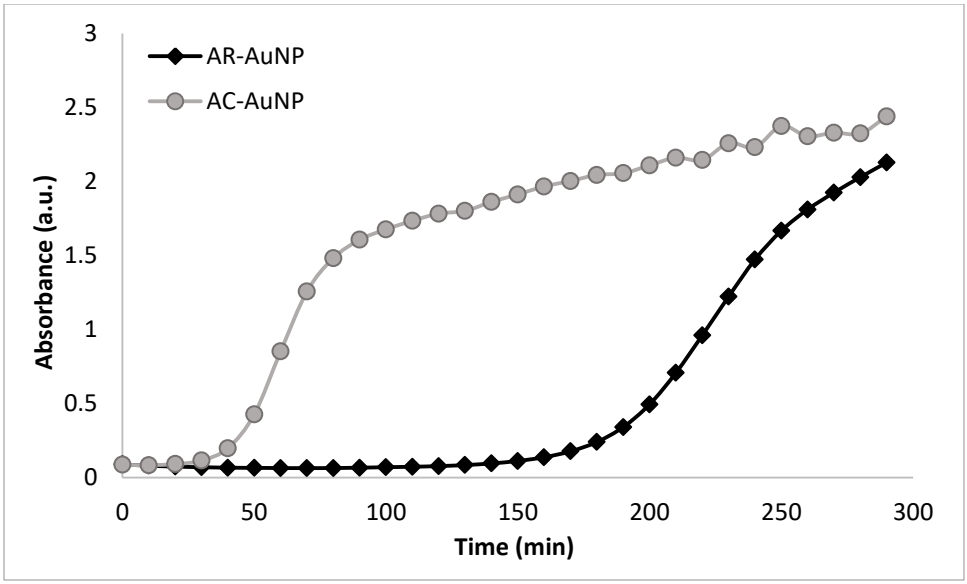

Figure 3.17 Change in absorbance with time during the syntheses of both the AC-AuNPs and AR-AuNPs at the λ_{max} 545 and 544 nm respectively (spectra taken in water).

The synthesis of sodium citrate capped AuNPs (SC-AuNPs) were only successfully synthesised at high temperatures (90 ºC) and the formation of nanoparticles was only apparent after 5 minutes (Figure 3.18). The formation of L-AC-AuNPs was fast, with the appearance of the characteristic purple colour attributed to AuNPs appearing within 5 minutes (UV-Vis spectra in Supplementary information, Figure S3.9b). The difference between this method and that employed for the SC-capped AuNPs is that these L-AC-AuNPs were synthesised at room temperature. Moreover, it appears that the concentration of the nanoparticles formed in AC-extract is higher than that observed for the SC-AuNPs (based on the absorbance at 525 nm in the UV-Vis spectra).

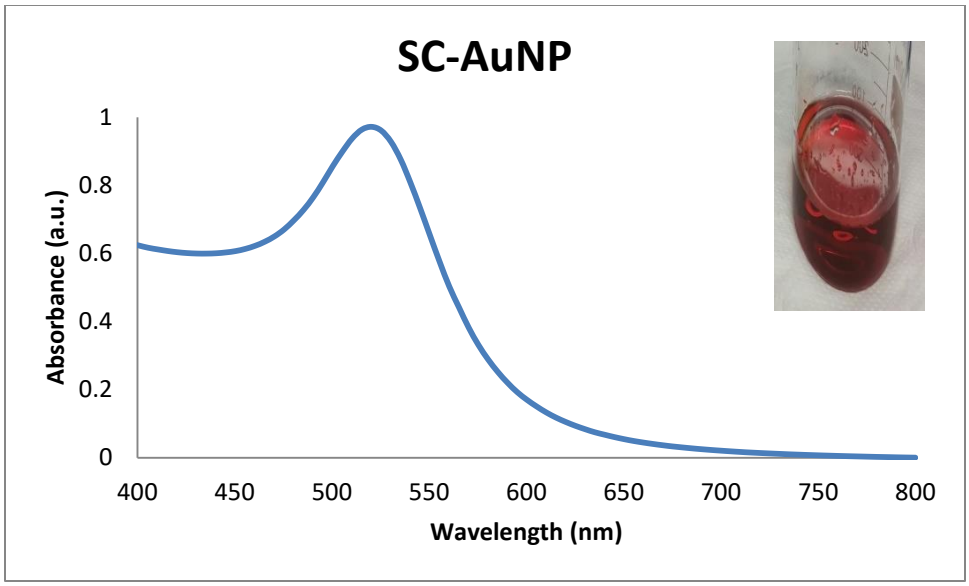

Figure 3.18 UV-Vis absorption spectrum of SC-AuNP after 10 minutes in water.

Inset: Photo of the colour of the solution after 10 minutes.

An interesting difference in reaction rates was observed for the AC and AR extracts (Figure 3.16). The formation of nanoparticles appeared only after 20 minutes of reaction for the AC extract (Figure 3.16), while the AuNPs were only formed after 50 minutes for the AR extract (Figure 3.16). The measurements were taken every 5 minutes. The rate of NP formation was observed to slow down after 35 minutes in the AC extract and after 90 minutes in AR extract implying that the reaction was approaching completion.

In conclusion, as was expected, the AC extract was found to be highly efficient at reducing the gold metal salt as found previously for the silver salt. The synthesis of the nanoparticles using this route is faster than using aqueous extract from seaweed that was not previously extracted with organic solvents as performed by Vivek and colleagues (2011).

3.3.2.2. Synthesis of AuNPs from commercially available fucoidans

The pure fucoidans which were used in the synthesis of AgNPs were also used to synthesise gold nanoparticles at room temperature. However, no AuNPs were observed to form at room temperature (as indicated by the lack of colour change from yellow to purple). The reactions were thus allowed to proceed for an hour at 100 ºC in order to observe any changes that can take

place at elevated temperatures. As can be seen in Figures 3.19 to 3.21, all three fucoidans used in this study were not capable of reducing the gold ions to gold nanoparticles. This, however, shows that our initial hypothesis for this study was wrong. As we believed that the fucoidans may play a major role in the reduction of the gold ions to form nanoparticles. This is not true for gold nanoparticles; even at high temperatures (100 ºC). However, even though the fucoidans could not reduce the gold ions to form nanoparticles *per se*, it appears that the aqueous extract which contains the fucoidans, in concert with other metabolites in the seaweed extract, were indeed capable of producing AuNPs efficiently at room temperature and pressure conditions. Further attempts could be exercised where even higher temperatures could be used for the synthesis of gold nanoparticles with pure fucoidans, but this would be out of the scope of this study which focused on the green synthesis of nanoparticles at ambient temperature.

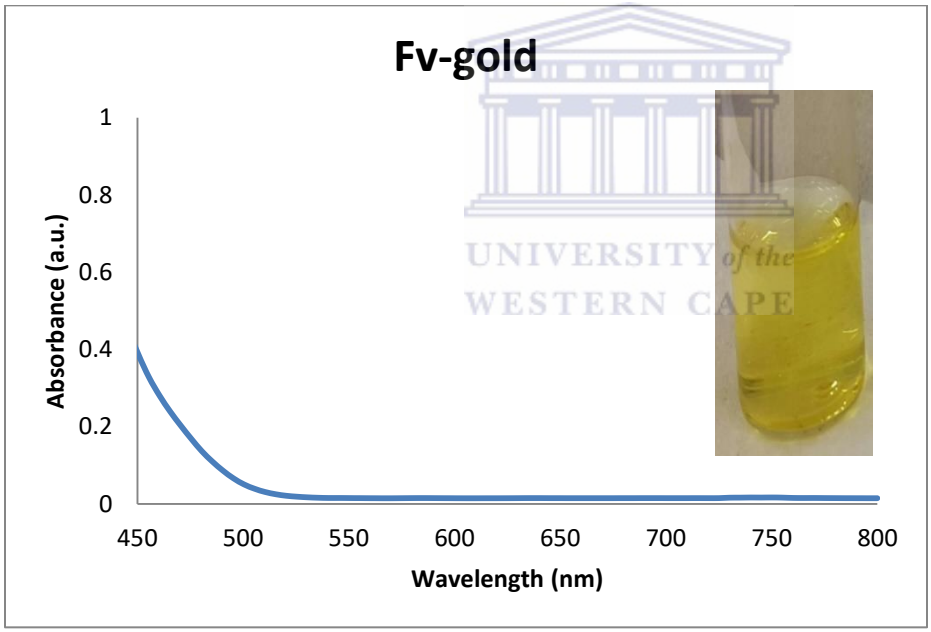

Figure 3.19 UV-Vis absorption spectrum of Fv-gold after 1 hour in water.

Inset: Photo of the colour of the solution after 1 hour.

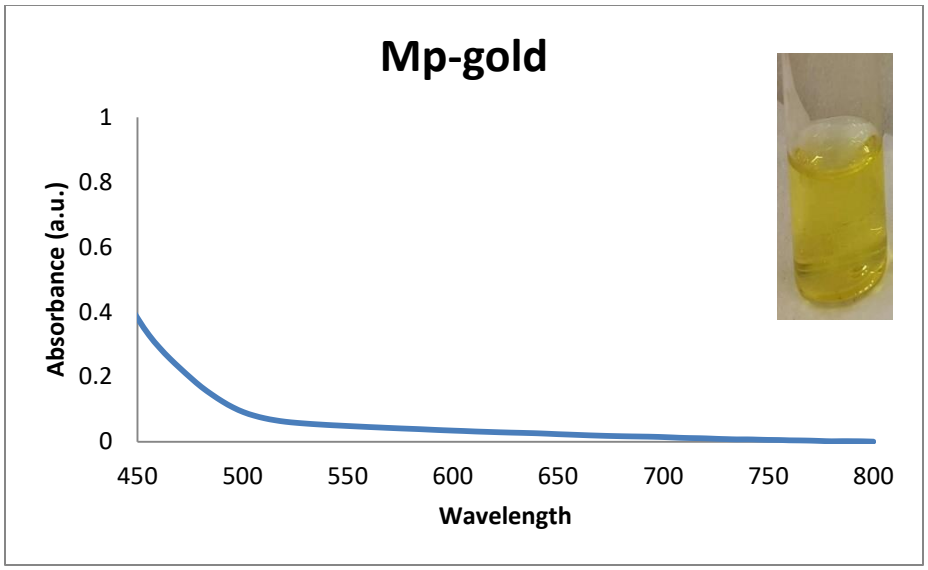

Figure 3.20 UV-Vis absorption spectrum of Mp-gold after 1 hour in water.

Inset: Photo of the colour of the solution after 1 hour.

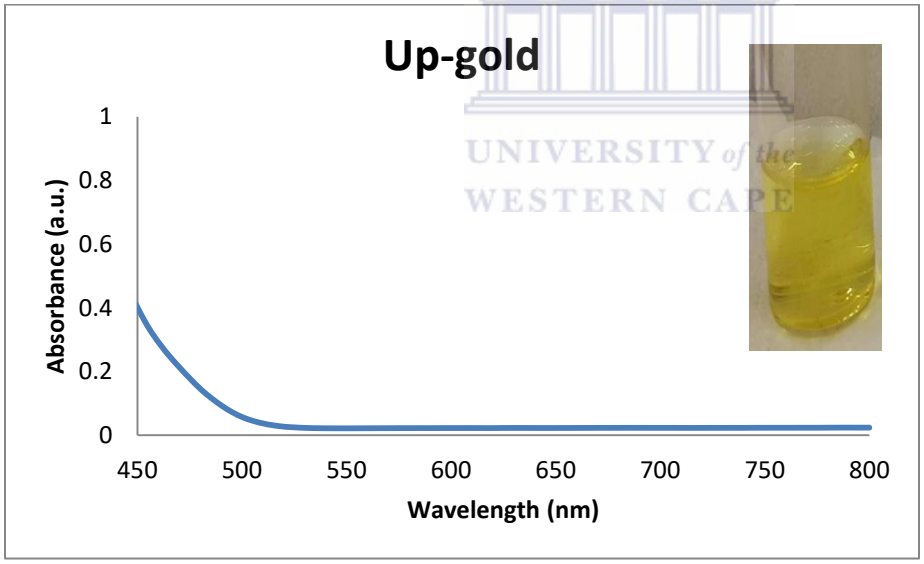

Figure 3.21 UV-Vis absorption spectrum of UP-gold after 1 hour in water.

Inset: Photo of the colour of the solution after 1 hour.

Although we have shown that none of the fucoidans used could reduce the gold ions to AuNPs, it is, however, contrary to the results obtained by Soisuwan *et al.* (2010) who were able to synthesise gold nanoparticles with pure fucoidans at room temperature and at 80 ºC. The nanoparticles were reportedly obtained from both reaction mixtures containing fucoidans from

Cladosiphon okamuranus and *kjellamaniella crassifolia*. While it might be true that fucoidans from *F. vesiculosus*, *M. pyrifera* and *U. pinatifida* do not reduce metal ions to nanoparticles at room temperature, not all pure fucoidans are incapable of reducing metal ions into nanoparticles at room temperature (Soisuwan *et al*., 2010).

3.3.3 Characterization of synthesised nanoparticles by TEM

3.3.3.1. Silver nanoparticles

The results obtained from TEM (with size distribution presented on graphs alongside each TEM micrograph) and EDX analyses are given in Figures 3.22-27 (and Supplementary information, Figures S3.1-7). As can be observed, spherically shaped nanoparticles dominate for the AgNPs in particular. Since different reducing agents were used for the synthesis of AgNPs, the nanoparticles are as expected different both in size and shape. AgNPs were also synthesised using a traditional reducing agent, sodium borohydride. TEM images revealed the morphology and shape of these nanoparticles to be spherical with an average size of 13.90 ± 9.56 nm (Figure 3.23 & Table 3.2).

For better comparison, silver nanoparticles synthesised from L-AC and L-AR extracts were included in this section. Silver nanoparticles synthesised from L-AC extracts are oval in shape and highly aggregated (Figure 3.24), whereas those synthesised from L-AR extract are spherical (Figure 3.25). Moreover, the mean size of L-AC-AgNPs, for example, as determined from the TEM data is 13.96 ± 5.27 nm (Table 3.2). Again, the AgNPs synthesised from AC and AR extracts are different in terms of both the shape and size (Figure 3.26). With AR-AgNPs, the nanoparticles appear to be larger in size. The AgNPs synthesised from the AC extracts are not closely spaced which may be due to some form of electrostatic repulsion brought about by the seaweed metabolites (Tengdelius *et al.*, 2015). The AgNPs formed from the AC extracts are predominantly spherical and polydisperse, while the AgNPs formed from the AR extracts are polydisperse and unusually shaped, clearly displaying some grooves in the NPs which were likely formed during growth of the NP. Interestingly, sizes of AgNPs from these extracts (AC and AR) were almost the same (Table 3.2). Furthermore, smaller nanoparticles were imaged for the AR extract (3.36 – 50.99nm), while slightly bigger nanoparticles were found for the AC extracts (6.67 – 53.08). Though from the same brown, marine seaweed, *S. incisifolium*, the AR

and AC extracts clearly have different properties which offer different degrees of stability and effect on size to the nanoparticles synthesised.

Only two of the pure fucoidans could reduce silver ions to produce AgNPs – then again only at high temperatures. The two fucoidans resulted in differently sized nanoparticles. TEM images were recorded for the AgNPs synthesised from the pure fucoidans obtained from different brown seaweeds (Figures 3.26-3.27). The nanoparticles obtained from the reaction were spherical in shape. However, as shown on Figures 3.26-27 and Table 3.2, the Fv-AgNPs are smaller than Mp-AgNPs (8.69 ± 3.85 and 20.03 ± 10.97 nm, respectively). The nanoparticles obtained from these fucoidans were not observed to be aggregated. The fucoidan is thought to bind to several nanoparticles if its structure is highly branched, especially if there are sulfonated functional groups on these side chains which are likely to result in bigger, agglomerated nanoparticles (Soisuwan *et al.*, 2010). Sulfur is known to be the site for nanoparticle formation. Therefore, the position and the amount of sulfur group can possibly influence the size and agglomeration state of the nanoparticles. The size of nanoparticles is expected to be large if the fucoidan is highly branched with sulfonated groups in its branches (Soisuwan *et al.*, 2010).

Table 3.2 Mean AgNP sizes as determined by TEM, XRD and DLS

Nanoparticle type	TEM Size (nm)		XRD Size (nm)	DLS Size (nm)**	
	Mean size	Range		d_H	PdI
SB-AgNP	13.90 ± 9.56	2.04 – 29.72	25.71	83.65	0.320
AC-AgNP	22.44 ± 11.85	6.67 – 53.08	7.29	82.56	0.264
AR-AgNP	22.94 ± 8.41	3.36 – 50.99	9.54	76.29	0.568
Mp-AgNP	20.03 ± 10.97	1.65 – 46.31	15.28	316.3	0.515
Fv-AgNP	8.69 ± 3.85	2.35 – 20.44	-*	126.6	0.326
L-AC-AgNP	13.97 ± 5.72	1.60 – 25.78	7.53	33.41	0.397
L-AR-AgNP	12.52 ± 5.89	3.51 – 19.18	7.41	209.0	0.554

*Sample quantities obtained were too small for XRD analyses

** This is discussed in Section 3.3.5.

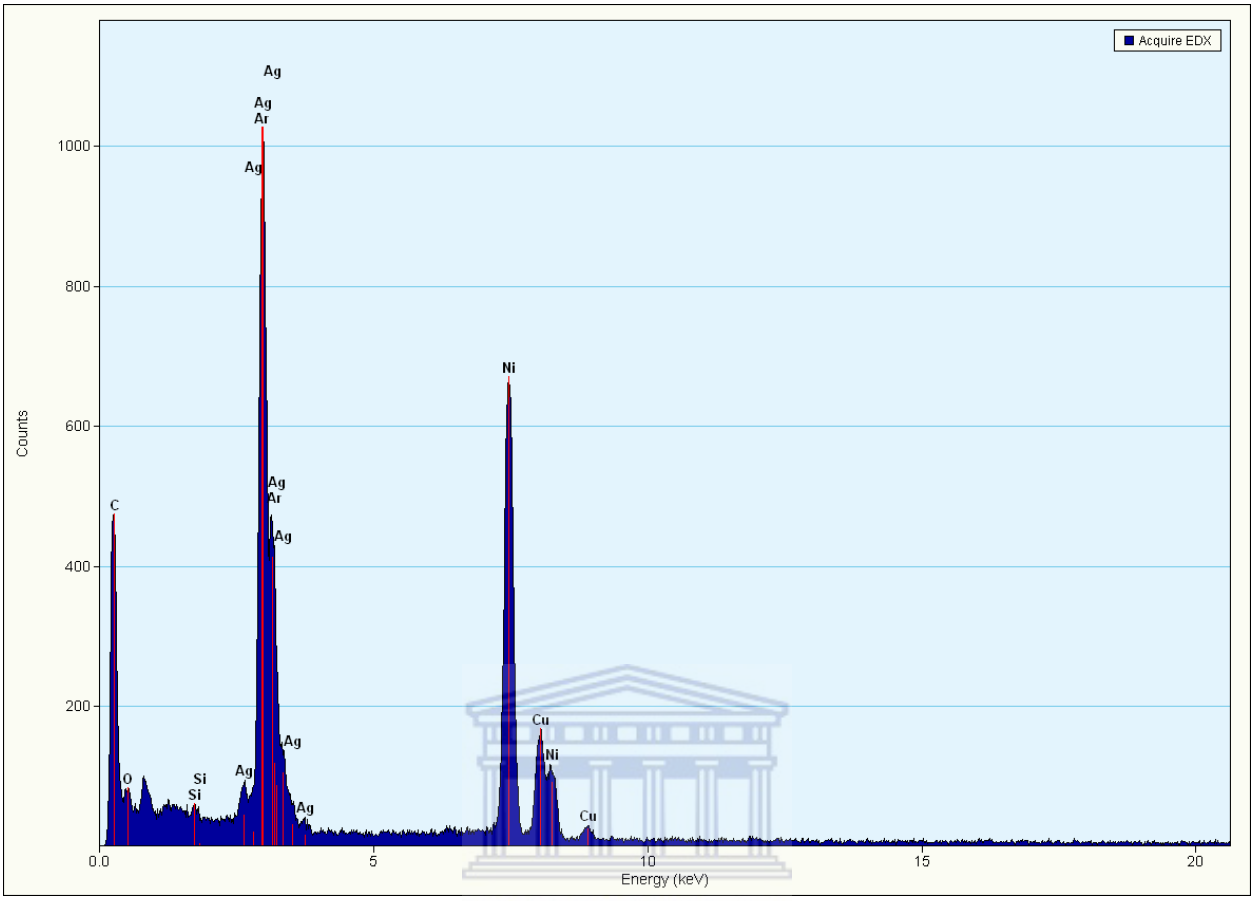

Figure 3.22 Representative EDX graph of SB-AgNP. The peaks due to Ag is detected at 3 keV.

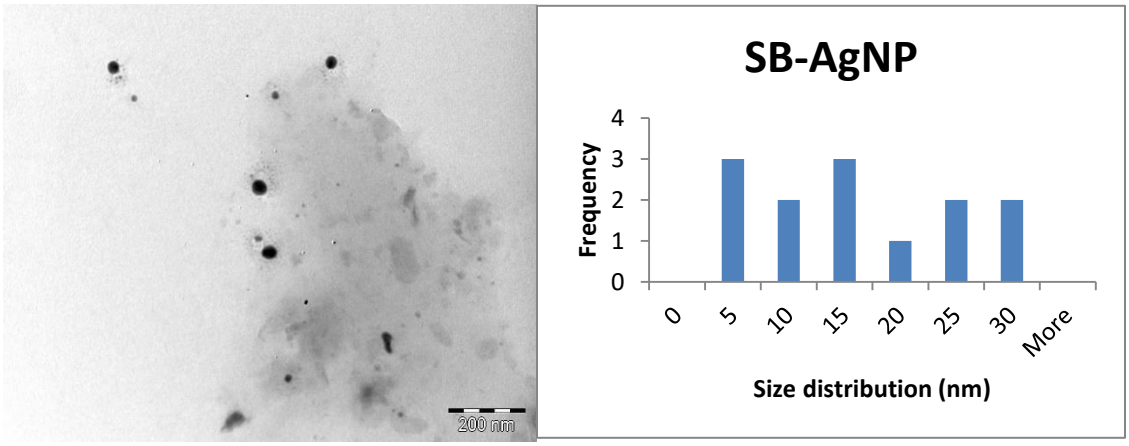

Figure 3.23 TEM image and NP size distribution obtained for SB-AgNP.

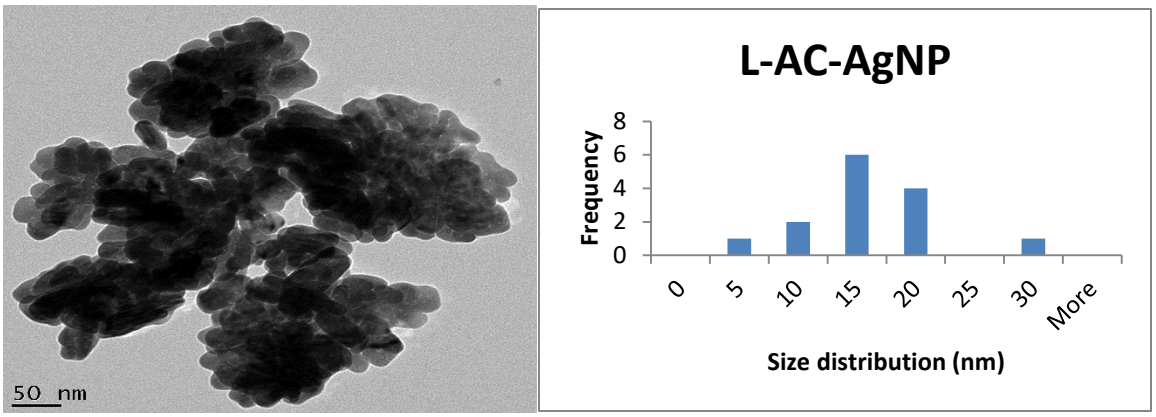

Figure 3.24 TEM image and NP size distribution obtained for L-AC-AgNP.

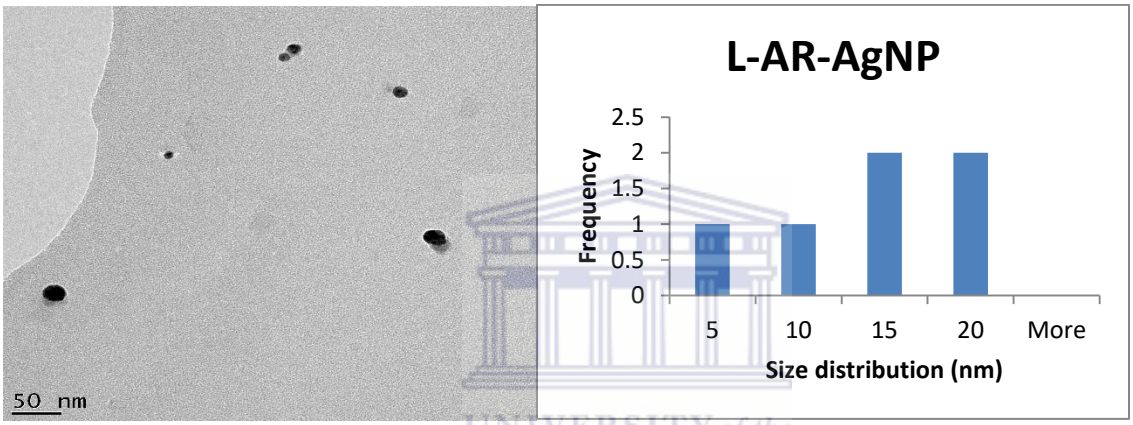

Figure 3.25 TEM image and NP size distribution obtained for L-AR-AgNP.

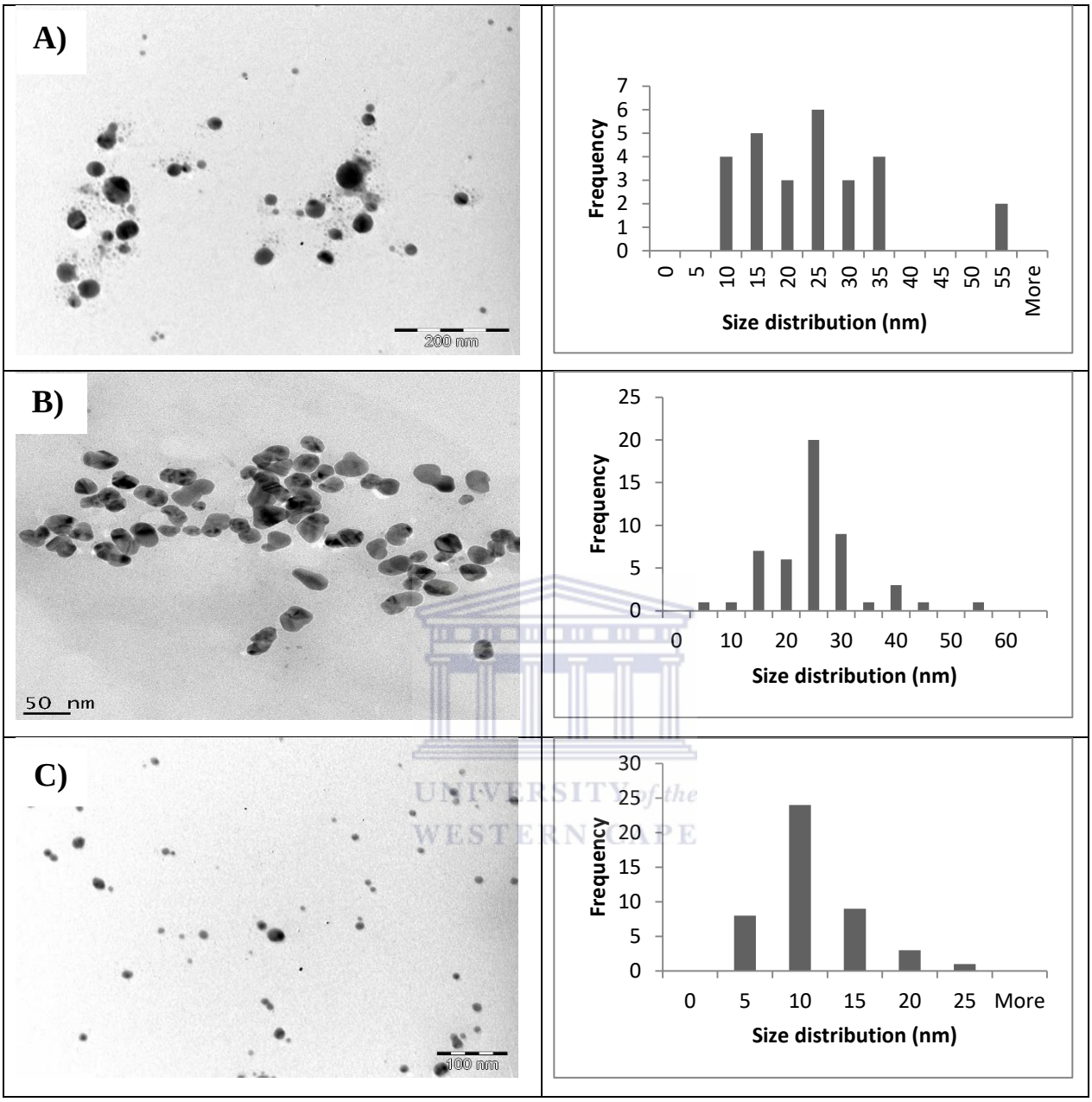

Figure 3.26 TEM images and NP size distributions obtained for a) AC-AgNPs, b) AR-AgNPs and c) Fv-AgNPs.

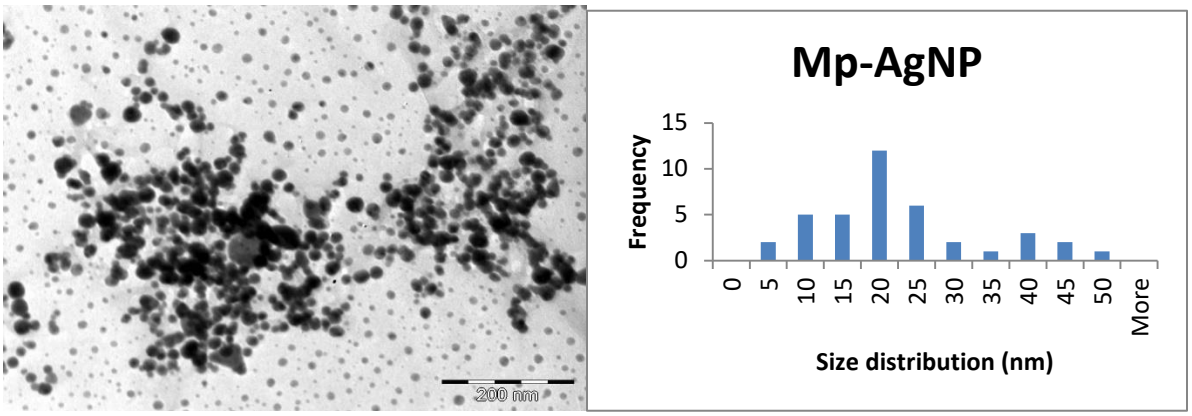

Figure 3.27 TEM image and NP size distribution obtained for Mp-AgNP.

Table 3.3 Zeta potential of silver nanoparticles determined by the Zetasizer

Nanoparticle type	Zeta potential (mV)*
SB-AgNP	-26.4 ± 17.8
L-AC-AgNP	-27.8 ± 8.91
L-AR-AgNP	-35.9 ± 9.67
AC-AgNP	-35.0 ± 4.95
AR-AgNP	-40.0 ± 7.62
Mp-AgNP	-32.9 ± 3.95
Fv-AgNP	-44.1 ± 11.0

*Data are vaule of triplicate determinations ± standard deviation

3.3.3.2. Gold nanoparticles

Gold nanoparticles were also characterised by TEM and EDX (Figures 3.28-32 and Supplementary Information Figures S3.8-12). The shape of the sodium citrate synthesised AuNP was found to be spherical as revealed by the TEM image (Figure 3.29) with the size of the SC-AuNPs ranging from 3.00-21.38 nm, and a mean size of 12.38 ± 0.94 nm (Table 3.4). The AuNPs synthesised from the L-AC extract were found to be polydisperse (Figure 3.30). Furthermore, as observed in Figure 3.30, there is a transparent layer of material around the nanoparticles which might be attributable to the plant extract which is functioning as a capping agent. Contrary to the NPs produced by the L-AC, the L-AR-AuNP sample was found to be

polydisperse, but with some NPs possessing a hexagonal shape with some spherical nanoparticles too (Figure 3.31). The size of L-AR-AuNPs was thus found to be bigger than that of L-AC-AuNPs as given in Table 3.4. The same trend is observed for the AuNPs synthesised from the AC and AR extracts (Figure 3.32 A & B), with the latter sample showing even larger nanoparticles as opposed to its counterpart. Another intriguing observation is the presence of triangular and hexagonal shaped AuNPs which were produced with the D-AR extract. Thus it is possible to produce differently shaped nanoparticles by using the freeze-dried aqueous extract of *S. incisifolium*.

TEM results revealed the morphology and size of nanoparticles formed. Though the layer of biomolecules from the seaweed is not observable in TEM images, it is interesting to note that the NPs in most of the TEM pictures are not aggregated. The reason for this may be due to the fact that the extract (which is known to contain polysaccharides and polyphenols) is capping the nanoparticles and provides the electrostatic repulsion between the nanoparticles needed to keep them apart from each other (Tengdelius *et al.*, 2015). In contrast, other TEM images obtained for the AgNPs showed that the nanoparticles are aggregated. To the best of the author's knowledge, no pure fucoidan has been isolated from *S. incisifolium* and therefore its structure is unknown. However, as per literature, brown seaweeds possess fucose rich polysaccharides which are different in structure and chemical composition (Li *et al*., 2008; Sellimi *et al.*, 2014; Soisuwan *et al.*, 2010). It is unknown if fucoidan from *S. incisifoliun* is a highly branched or a simple branched polysaccharide. However, since it is believed that fucoidans play a role in the capping of nanoparticles, which imparts stability to the NP (Asmathunisha & Kathiresan, 2013), and based on TEM results obtained, it could be surmised that the fucoidan from *S. incisifolium* might be branched with sulfursulphonate groups on its side chains. Also it has to be noted that different metabolites are involved in the bioreduction of the metal ions to form nanoparticles before capping could take place. The size of nanoparticles from both the AC and AR extracts (and similarly the AC and AR extracts) are different, with the AR extract resulting in bigger nanoparticles compared to the AC extract. The different sizes and shapes of nanoparticles synthesised biologically are not uncommon (Shanker *et al*., 2003). Also, in other samples, the shapes of nanoparticles were irregular due to the different phases of nanoparticle formation (Rajathi *et al.*, 2012). The rate for the formation of nanoparticles revealed that the reaction was

quicker in AC solution than it was in AR solution. Therefore, as bioreduction took place in AC reaction, the capping agent was immediately available to cap the nanoparticles and stabilize them. The slow reaction rate in AR may have resulted in many nanoparticles aggregating before capping could take place, subsequently producing large nanoparticles.

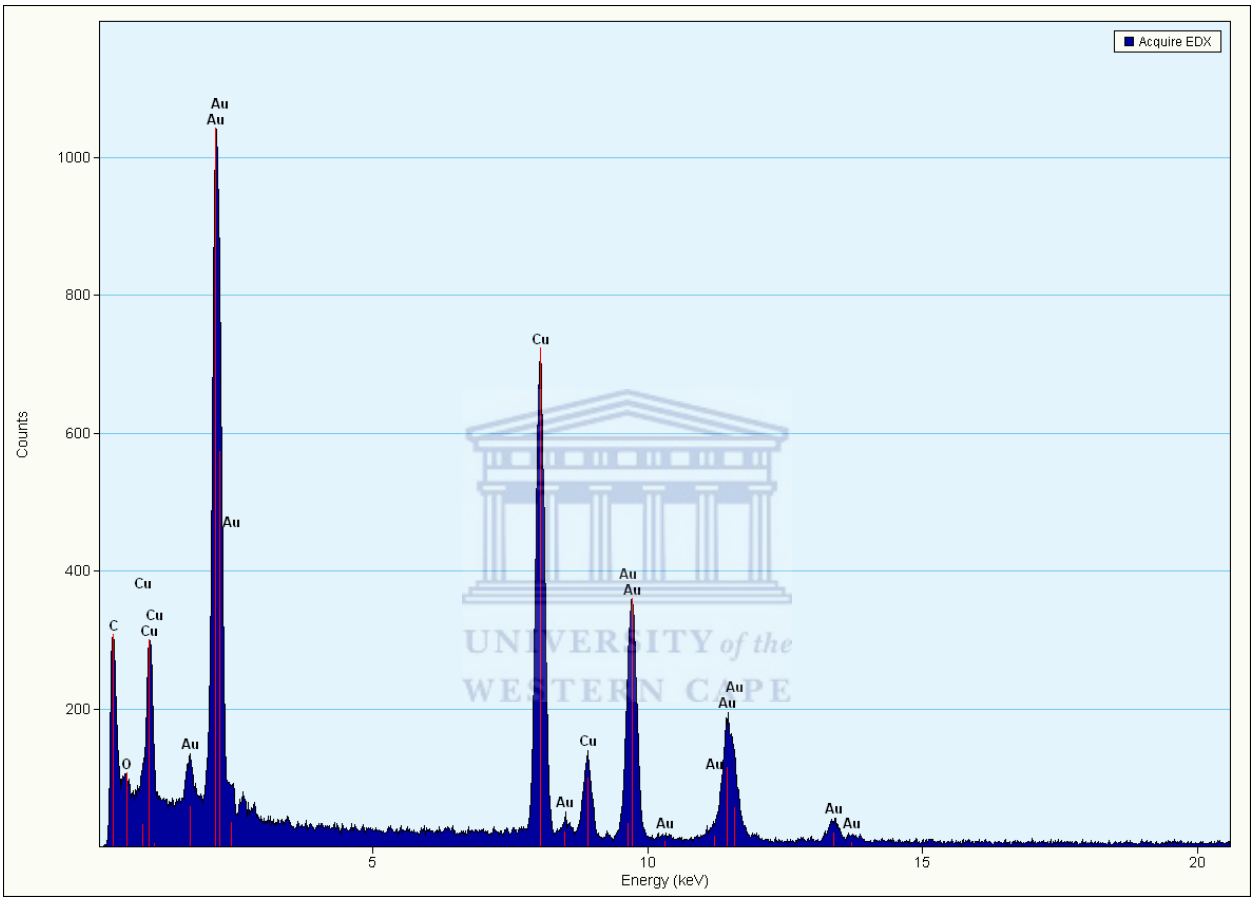

Figure 3.28 Representative EDX graph of the D-AR-AuNP synthesised.

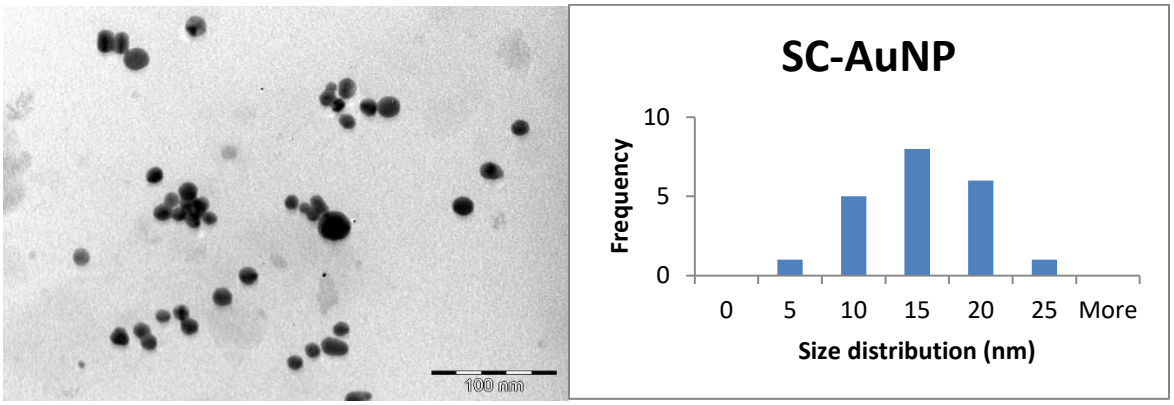

Figure 3.29 TEM image and NP size distribution obtained for SC-AuNP.

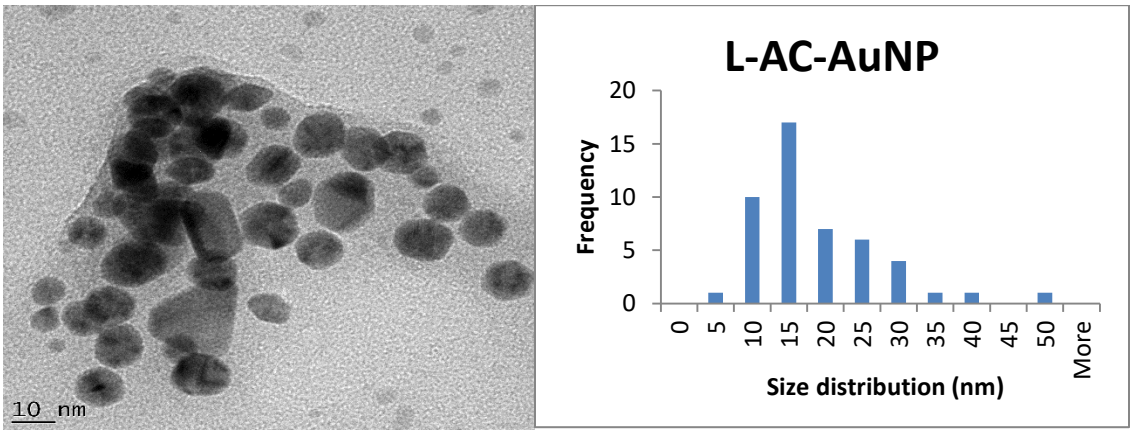

Figure 3.30 TEM image and NP size distribution obtained for L-AC-AuNP.

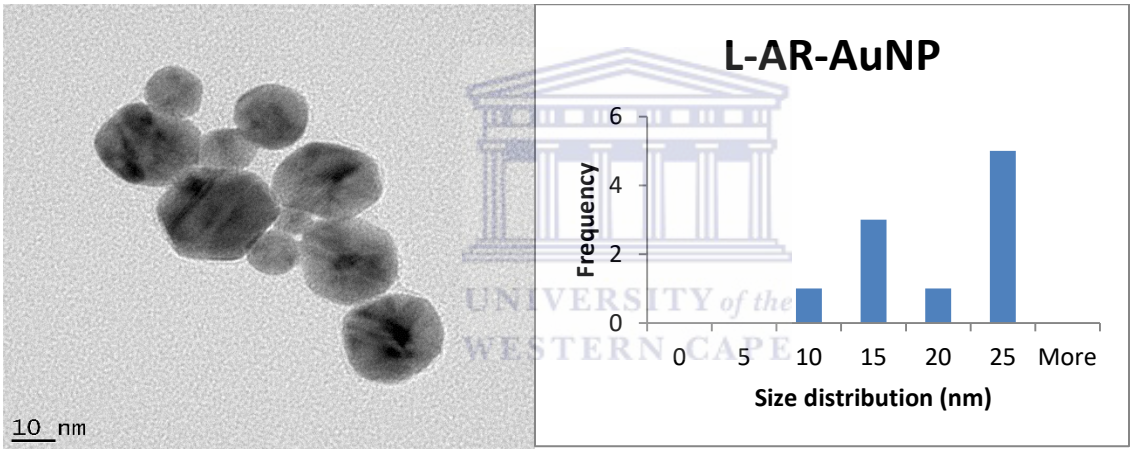

Figure 3.31 TEM image and NP size distribution obtained for L-AR-AuNP.

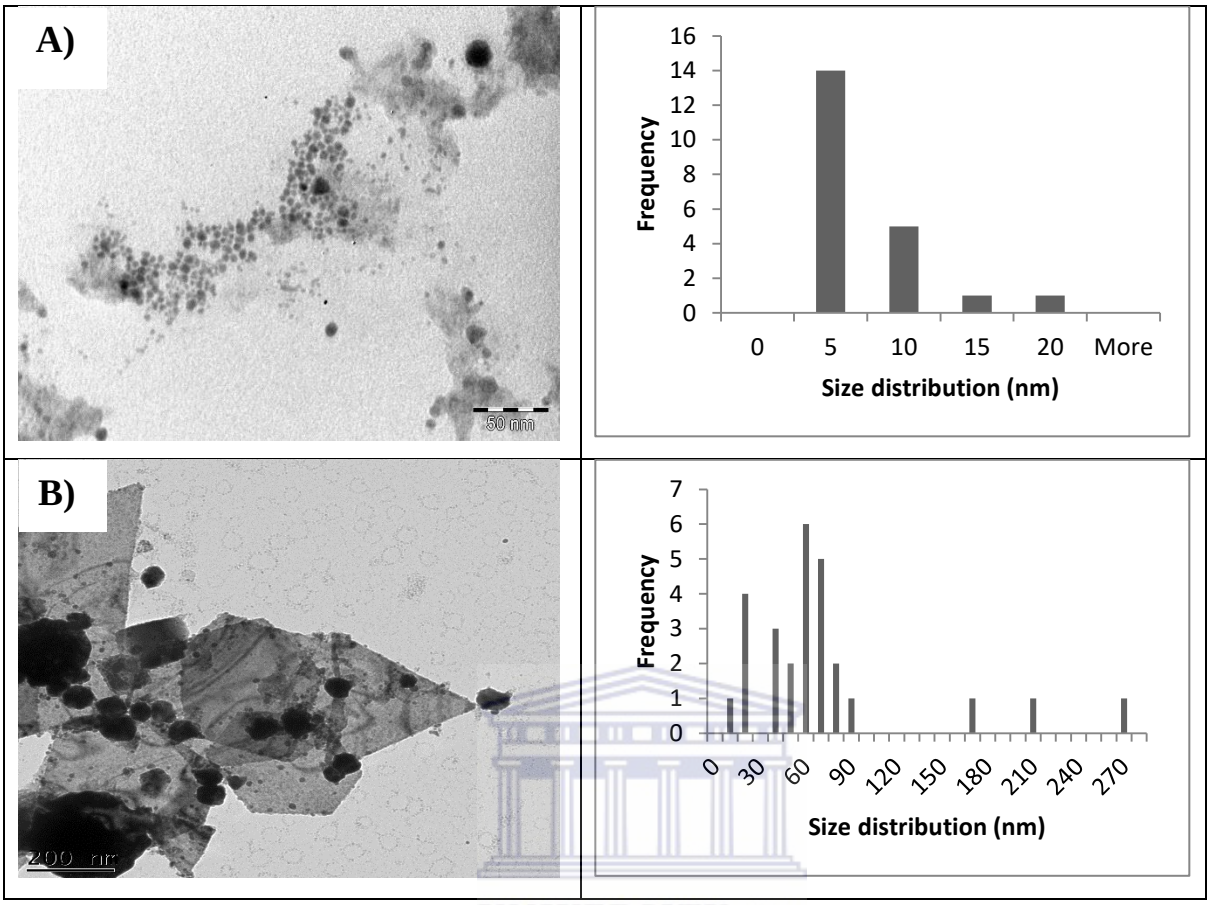

Figure 3.32 TEM images and NP size distributions obtained for a) AC-AuNPs and b) AR-AuNPs.

3.3.4. Characterization of synthesised nanoparticles by EDX

Elemental analysis of the nanoparticles was determined with energy dispersive x-ray spectroscopy (EDX) which is part of the TEM instrument. Elemental Ag and Au were detected in all samples as expected and are shown in Figures S3.1-3.12 of Supplementary information. Figures 3.22 & 3.28 serve as representative EDX graphs obtained for AgNP and AuNP respectively. There are, however, traces of other elements which may or may not be impurities. These elements include copper, nickel, chlorine and oxygen. Copper and nickel are the result of using the holey carbon coated copper/nickel grids which are used to support the samples. Oxygen and chlorine may be due to the starting materials $AgNO_3$ and $HAuCl_4.3H_2O$, respectively or due to sea salt (NaCl and KCl) which may still be present in the seaweed extract. Also, oxygen is easily adsorbed onto sample surfaces, resulting in some detection. So it is

possible that some of the elements from these precursors were still present in the solutions when taken for EDX analyses.

3.3.5. Characterization of synthesised nanoparticles by DLS and the Zetasizer

The size of nanoparticles was also determined by Dynamic Light Scattering (DLS) using the Zetasizer and the data is shown in Table 3.1 & 3.3. Compared to the sizes of nanoparticles determined by TEM, the sizes determined by DLS for the nanoparticles determined are much larger because DLS determines the hydrodynamic (d_H) radius of the nanoparticles (Kato *et al*., 2009). Also, the polydispersity index (PdI) of nanoparticles was determined through the use of the Zetasizer. A PdI index of less than 0.1 represents monodisperse NPs, while a PdI index of between 0.1 but less than 0.2 indicates a narrow size distribution, and a PdI index between 0.2 but less than 0.5 indicates a broad size distribution for the sample. From the results obtained, the nanoparticles all had a broad size distribution with a PdI index ranging from 0.264 to 0.568, except for SC-AuNP which had narrow size distribution, i.e. a PdI index of 0.158. This can also be confirmed with the nanoparticle size distribution determined from TEM results, Figures 3.23-27 & Figures 3.29-32.

Table 3.4 Mean AuNP sizes as determined by TEM, XRD and DLS

Nanoparticle type	**TEM Size (nm)**		**XRD Size (nm)**	**DLS Size (nm)****	
	Mean size**	**Range**		**d_H**	**PdI**
SC-AuNP	12.38 ± 0.94	3.00 – 21.38	10.96	37.46	0.158
AC-AuNP	5.35 ± 3.13	2.17 – 16.38	22.39	89.62	0.551
AR-AuNP	66.13 ± 58.30	7.91 – 268.67	40.12	92.85	0.512
L-AC-AuNP	15.83 ± 8.81	2.96 – 47. 76	5.64	22.14	0.348
L-AR-AuNP	17.87 ± 6.53	6.98 – 24.19	22.52	37.59	0.464

**This is discussed in Section 3.3.5

The zeta potential of nanoparticles was also determined by the Zetasizer, Tables 3.3 & 3.5 for AgNPs and AuNPs respectively. From the data listed in Table 3.3 & 3.5, it is clear that all the nanoparticles have a negative potential charge on the surface. The nanoparticles synthesised from D-AC and D-AR extracts exhibited the largest negative charge (with the latter having the largest negative charge at -40.0 mV) when compared to the other nanoparticles synthesised using

the aqueous extracts. Upon comparison to the fucoidans, the Fv-AgNP sample exhibited the largest charge at -44.1 mV. However, it should be noted that sodium citrate capped AuNPs exhibited the largest negative charge of all, implying that these NPs were the most stable (Koteswari *et. al.*, 2011). The AgNP synthesised with $NaBH_4$ did not show a high zeta potential (Table 3.3). However, all the nanoparticles synthesised had a zeta potential within the cut-off range. The stability of nanoparticles is correlated to zeta potential values which are greater than +30 mV or lower than -30 mV (Koteswari *et. al.*, 2011). The zeta potential of the nanoparticles synthesised was in the range of -27.8 to -44.1 mV for the AgNPs synthesised with seaweed extract and pure fucoidans; excluding SB-AgNPs. For the AuNPs synthesised with seaweed extracts, the zeta potential was within the range -16.0 to -39.3 mV. From this, it is evident that most of the nanoparticles were stable.

Table 3.5 Zeta potential data of the gold nanoparticles determined with the Zetasizer

Nanoparticle type	**Zeta potential (mV)***
SC-AuNP	-56.3 ± 13.9
L-AC-AuNP	-16.0 ± 6.29
L-AR-AuNP	-26.8 ± 11.0
AC-AuNP	-39.3 ± 13.5
AR-AuNP	-39.3 ± 14.8

*Data value of triplicate determination ± standard deviation

3.3.6. Characterization of synthesised nanoparticles by FT-IR spectroscopy

FTIR spectroscopy was used to identify the characteristic peaks associated with the metabolites present in aqueous extract of *S. incisifolium* as well as the pure fucoidans involved in capping of nanoparticles. The IR spectra of nanoparticles synthesised are compared with the IR spectra of the reducing agents/metabolites.

From figure 3.33, it can be observed that the C-O-C group was detected in all the samples at around 800 cm^{-1} (Schulz & Baranska, 2007) although with some slight shifts. Furthermore, similarities were observed between AR-AgNP and Mp-AgNP at 1028 cm^{-1} and 1025 cm^{-1} which

may both show the C-N group of aliphatic amines (Kannan *et al*., 2013). C-OH of polysaccharide was also detected at 1041 cm^{-1} in AC-AgNP (Philip, 2009). The peaks at 1296 cm^{-1} and 1292 cm^{-1} in AC-AgNP and AR-AgNP respectively represent the C-N group in peptides (Schulz & Baranska, 2007). The IR spectra of all the samples had the peak at around 3200-3300 cm^{-1} which may indicate OH group (Princy & Gopinath, 2013).

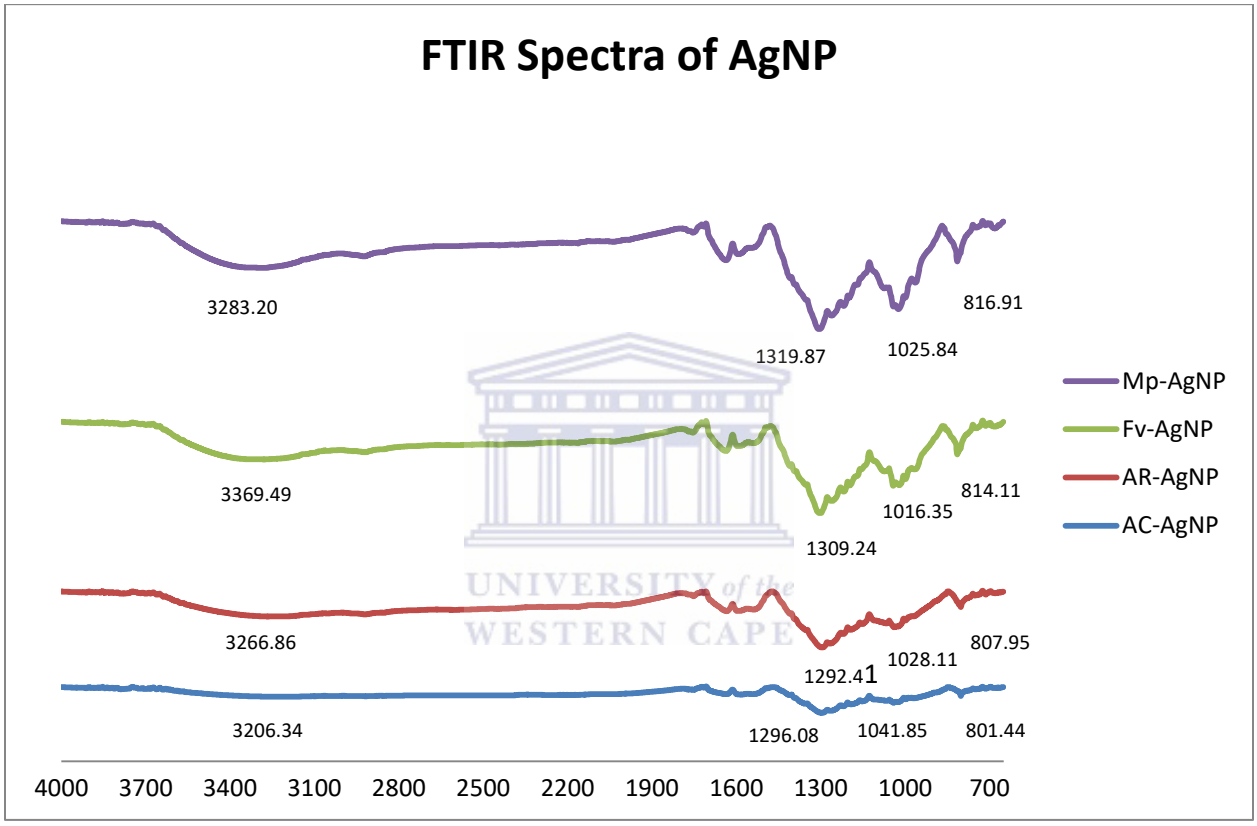

Figure 3.33 FT-IR spectrum obtained for AgNP synthesised from different reducing agents.

The FT-IR spectra shown in Figure 3.34 serves as a representative spectrum for the IR spectra obtained for AuNPs. The C-O-C group which is characteristic of monosaccharides was detected at 800 cm^{-1} in AC-AuNP (Schulz & Baranska, 2007). AC-AuNP also had a peak at 1040 cm^{-1} which is indicative of C-OH group in polysaccharides (Philip, 2009). Amide II bond was detected at 1595 cm^{-1} (Princy & Gopinath, 2013). The peak at 999 cm^{-1} in AR-AuNP signals the presence of C-O-C group (Philip, 2009). The carbonyls of ketones, aldehydes and esters were detected at 1620 cm^{-1} in AR-AuNP. Both AC-AuNP and AR-AuNP had peak at around 3200-3300 cm^{-1} which may represent the presence of OH group (Princy & Gopinath, 2013).

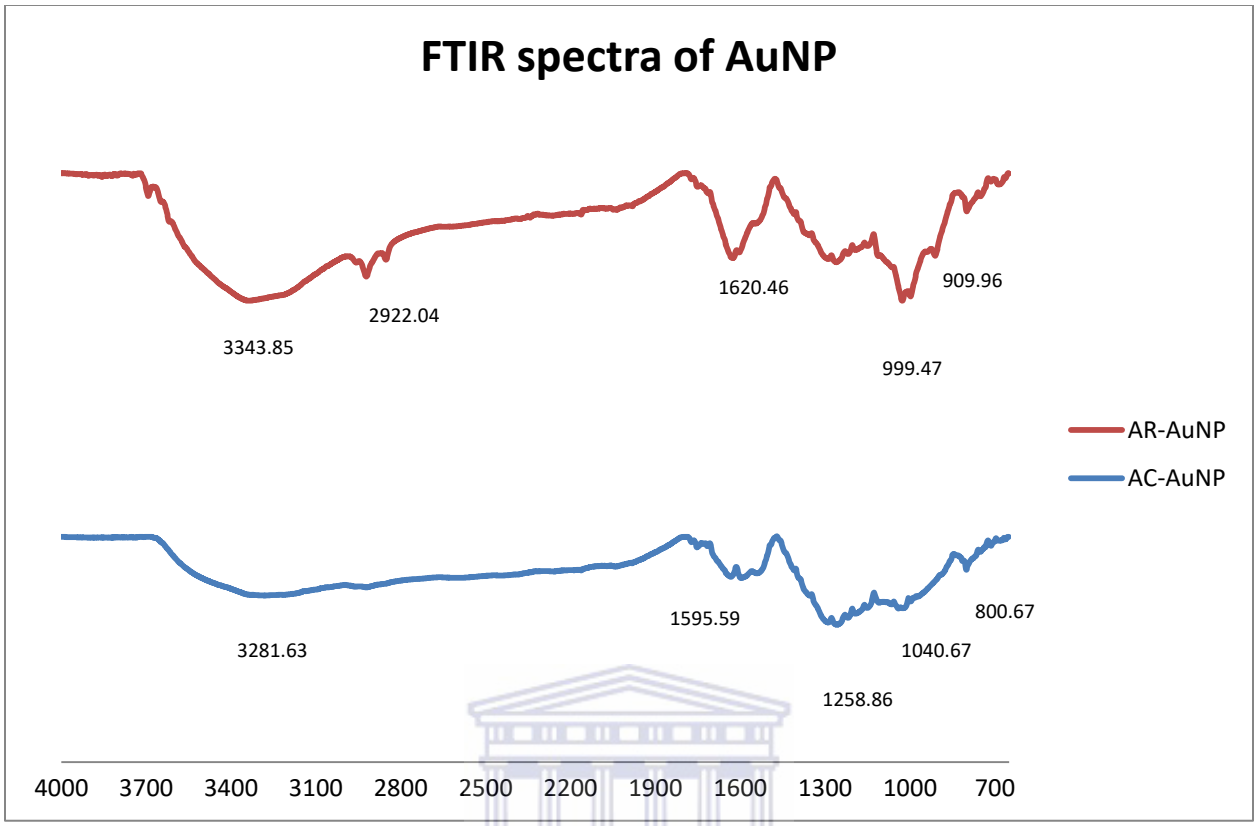

Figure 3.34 FT-IR spectra of AuNP synthesised from different reducing agents.

3.3.7. Characterization of synthesised nanoparticles by XRD

The nanoparticles synthesised using different reducing reagents were also characterized by powder XRD. The X-ray diffractograms for the AgNPs are shown in Figure 3.35. From this figure it is clear that Ag is not the only component present – there are additional peaks. Some additional peaks may be attributed to sea salt which is present in the seaweed. The XRD peaks at 2θ degrees can be attributed to the (111), (200), (220), and (311) crystalline planes of the face-centered-cubic (fcc) crystalline structure of metallic silver, respectively (JCPDS file no. 00-004-0783). The individual reflections are labelled in the X-ray diffractograms of each sample.

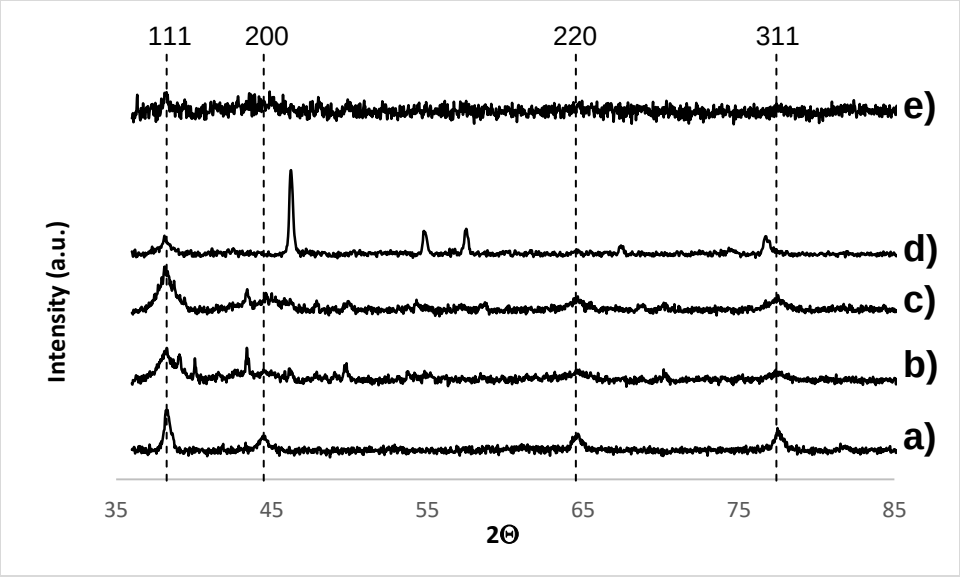

Figure 3.35 X-ray diffractograms obtained for the AgNPs synthesised using a) sodium borohydride, b) AC extracts, c) AR extracts, d) Mp fucoidan and e) Fv fucoidans.

Similarly, the AuNPs synthesised using different reducing agents were also characterised by powder XRD as shown in Figures 3.36. The X-ray diffractograms obtained for the AuNPs were all clean and the reflections clearly observed. The peaks at 2θ degrees can be attributed to the (111), (200), (220), and (311) crystalline planes of the face-centered-cubic (fcc) crystalline structure of metallic gold, respectively (JCPDS file no. 00-004-0784). From the X-ray diffractograms shown it is obvious that the intensity of the (111) diffraction peak is greater than the others and as such these were the peaks that were used to calculate the NP sizes using the Debye-Scherrer equation (2.2). The (111) facets dominate the X-ray diffractograms of nanoparticles synthesised (Liu *et. al.*, 2005). Therefore, calculations of crystalline size of nanoparticles was done using the (111) facet to determine whether the dater from XRD compares fairly with that of TEM. From the results presented in Tables 3.1 and 3.3, the XRD does not fit in TEM range. This could be due to the fact that the XRD measures the crystalline structure of the nanoparticle, not the whole nanparticle resulting in smaller sizes compared to those obtained from TEM. It is important to note that the Debye-Scherrer equation (2.2) should only be applied to spherical nanoparticles that are smaller than 100 nm, thus the size determined by XRD for the AR-AuNP sample is useful.

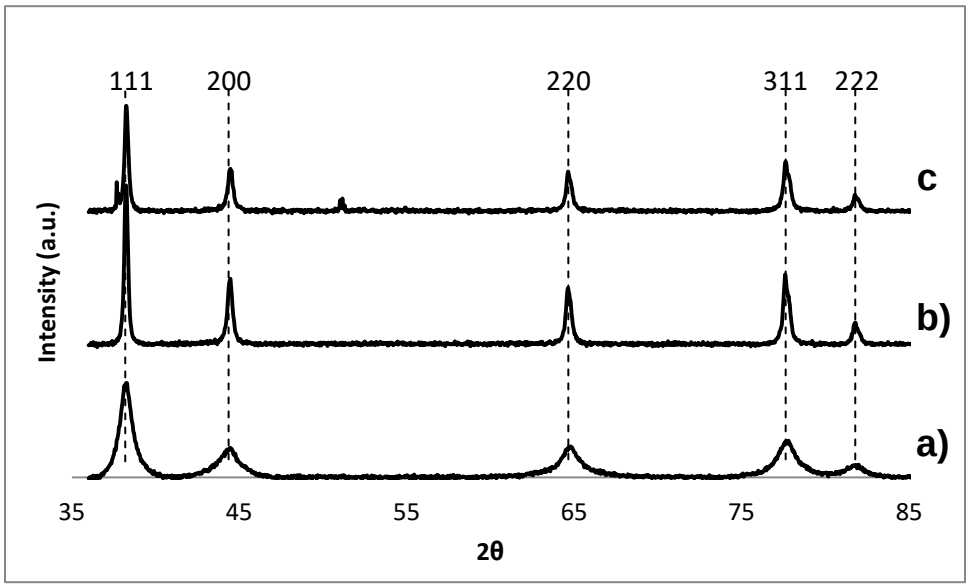

Figure 3.36 X-ray diffractograms obtained for the AuNPs synthesised using a) sodium citrate, b) AC extracts and c) AR extracts.

3.4. CONCLUSION

A green method of synthesis for Au and Ag nanoparticles was achieved in this study using different reducing agents. For example, nanoparticles that were synthesised using the AC extracts were found to produce higher concentrations of nanoparticles compared to the AR extract under the same conditions. Moreover, the rate of nanoparticle formation was faster with the AC extract compared to the AR extract. FT-IR spectroscopy confirmed the presence of the extract metabolites on the surface of the NPs. Clear differences were observed for the AgNPs synthesised compared to the extract alone. However, the AuNP samples did not show such distinct differences. The formation of the nanoparticles using $NaBH_4$ and sodium citrate for the Ag and AuNPs respectively was fast compared to biological method of synthesis, especially for the AgNPs. The reaction was complete after the addition of $AgNO_3$ to $NaBH_4$ whereas the reaction seemed to take longer than 18 hours when seaweed extract was used. However, in case of AuNP syntheses, the biological synthetic method can permanently replace the chemical synthesis since it is as fast and does not require high temperatures, thus the biological method is

more energy efficient. Moreover, the concentration of nanoparticles formed in the latter method is greater than that of chemically synthesised AuNPs.

Although fucoidans are thought to play role in capping of nanoparticles, based on the results obtained in this study, it could be said that fucoidans are not likely able to reduce the metal ions to form nanoparticles at room temperature.

From antioxidant activity results, it is conclusive that *S. incisifolium* has high antioxidant activity, even though we only compared two differently extracted aqueous extracts. The lower total phenolic content, reducing power and radical scavenging power of pure fucoidans assessed in this study may explain why the pure fucoidans were not able to reduce Ag^{+} and Au^{+} to form nanoparticles at room temperature. This further confirms that fucoidans per se, do not contribute in the formation of nanoparticles as evidenced by the results obtained from total reducing power. The size of the nanoparticles was determined using different techniques and the results differ. However, this could be explained by the technique itself and the drawbacks associated with it. For example, the sizes determined by DLS were found to be bigger than the sizes determined by TEM as these are hydrodynamic diameters. The DLS size determination will take into account the capping agent of the NP, whereas in TEM carbon based materials are transparent to the electron beam. The sizes determined by XRD were found to be smaller than the sizes of the nanoparticles determined by TEM. This may be due to the fact that the size determination given by XRD will be an average of the whole sample, while TEM is focussed on a small area of a sample. Factors such as hydration of nanoparticles, dry state of nanoparticles and crystallinity may have had effect on different sizes of nanoparticles determined from the technigues employed.

Lastly, it seems that different methods of extractions have an impact of the characteristics of nanoparticles synthesised. These include the size, shape and crystallinity. The sizes of nanoparticles were found to be big when AR is used as a reducing agent ad small when AC is used as a reducing agent. Furthermore, the speed of reaction differs between different reducing agents with AC being the fastest among other reducing agents at room temperature.

CHAPTER 4

4. ANTIMICROBIAL ACTIVITY AND CYTOTOXICITY OF SYNTHESISED SILVER AND GOLD NANOPARTICLES

4.1. INTRODUCTION

In this chapter we evaluated the antimicrobial and cytotoxic activities of the synthesised nanoparticles. Antimicrobial studies were done by the author in the laboratory of Dr Marilize le Roes-Hill at the Cape Peninsula University of Technology (CPUT). For the antimicrobial studies five drug resistant strains were selected. These included two gram positive strains, *Enterococcus faecalis* and *Staphylococcus aureus*, two gram negative strains, *Acinetobacter baumannii* and *Klebsiella pneumoniae* subsp. *pneumoniae*, and a yeast, *Candida albicans*.

All five microorganism strains included in this study are biomedically important and exhibit resistance to a number of current antibiotics. *Enterococcus faecalis* and *Staphylococcus aureus* are two important bacteria responsible for a number of nosocomial infections. *E. faecalis* is a gram-positive bacterium responsible for urinary tract infections, intra-abdominal, pelvic and soft tissue infections. This bacterium is found in intestines of many animals and insects, beach sand, fresh and marine water sediments, soil and aquatic and terrestrial plants (Higuita & Huycke, 2014). Methicillin resistant *S. aureus* commonly colonizes the nasal passage and axillae. *S. aureus* induces illness and tissue damage in the host by the use of its virulence factors such as capsule, immunoglobulin binding protein A, which protect the bacteria from destruction by phagocytosis in the host (Baron, 1996). *Acinetobacter baumannii* is an opportunistic pathogen especially in immune-compromised individuals. This microorganism is responsible for 80% of all infections caused by species that belong to *Acinetobacter* (CDC, 2016). However *A. baumannii* rarely causes diseases outside health care settings even though it is resistant to many antibiotics that are commonly prescribed for patients. *Klebsiella pneumoniae* subsp. *Pneumoniae,* also gram-negative bacteria, causes infections such as pneumonia, blood infections,

wound or surgical site infections and meningitis. This bacterium is commonly found in human intestines where it does not cause any damage. *K. pneumoniae* has developed antimicrobial drug resistant strains (CDC, 2016). *Candida albicans* is yeast causes a fungal infection called candidiasis. It is commonly found in skin and mucous membranes. However, they only cause infection when they overgrow (CDC, 2016).

Silver nanoparticles have excellent antibacterial activity (Abbaszadegan *et al.*, 2014; Zargar *et al.*, 2011). Bacteria are usually unable to develop resistance to AgNPs because they can interact with a variety of targets in the microorganism. AgNPs interact specifically with proteins through thiol groups, cell membranes and cell walls (Zargar *et al*., 2011). Similarly, Park *et al.*. (2016) recently synthesised AuNP and AgNP with resveratrol for antimicrobial activity. The resultant AuNPs were reportedly active against a panel of microorganisms (gram-negative and gram-positive bacteria). In their study, Hayden and colleagues showed that AuNP are capable of interacting with cell membranes of gram-positive and gram-negative bacteria, subsequently leading to the lysis of the bacterial cell (Hayden *et al.*, 2012).

Given the critical need for new antibiotics we screened our green synthesised silver and gold nanoparticles for activity against five microorganisms. In order to adequately assess the potential of the synthesised nanoparticles as antimicrobials it is essential to also assess their cytotoxicity against human cells. Thus, we also evaluated the cytotoxicity of our synthesised nanoparticles against a human colon adenocarcinoma cell line (HT-29) (Cacicedo *et al*., 2016), a human breast cancer cell line (MCF-7) (Nune *et al*., 2009) and a non-tumorigenic breast epithelial cell line (MCF-12A) (Vorster *et al*., 2012).

4.2 MATERIALS AND METHODS

4.2.1. Antimicrobial Assay

The antimicrobial activity of the synthesised nanoparticles was evaluated by the agar well-diffusion method (Dhand *et al.*, 2016).

4.2.1.1. Nanoparticle sample preparation

The nanoparticle reaction mixture was centrifuged at 10 000 rpm and the pellet collected and washed with milliQ water. The pellet was then re-suspended in 3 ml of distilled water. The final concentrations of samples prepared are presented in Table 4.1.

Table 4.1 Sample concentrations used for the antimicrobial and cytotoxicity assays

Sample code	**Sample concentration (*Antimicrobial assay*)***
SB-AgNP	0.053 mM
D-AC-AgNP	0.26 mM
D-AR-AgNP	0.26 mM
D-AC-AuNP	0.21 mM
D-AR-AuNP	0.21 mM
SC-AuNP	0.105 µM
Fv-AgNP	0.26 mM
Fv	0.0.075 mg/ml
Mp-AgNP	0.26 mM
Mp	0.075 mg/ml
D-AC	0.015 mg/ml
D-AR	0.015 mg/ml
Amp	1 mg/ml
Chl	1 mg/ml
Van	1 mg/ml
H_2O	75 µL

SB-AgNP = Silver nanoparticles synthesised using sodium borohydride, D-AC-AgNP =Silver nanoparticlessynthesised using freeze-dried aqueous extract with prior organic extraction, D-AR-AgNP = Silver nanoparticles synthesised from aqueous extract without prior organic extraction, D-AC-AuNP = Gold nanoparticles synthesised from freeze-dried aqueous extract with prior organic extraction, D-AR-AuNP = Gold nanoparticles synthesised from freeze aqueous extract without prior organic extraction, SC-AuNP =Gold nanoparticles synthesised from sodium cutrate, Fv-AgNP = Silver nanoparticles synthesised from pure fucoidan from Fucus vesiculosus, Fv = Pure fucoidan from Fucus vesiculosus, Mp-AgNP = Silver nanoparticles synthesised from pure fucoidan from Macrocystis pyrifera, Mp = pure fucoidan from Macrocystis pyrifera, D-AC = Freeze-dried aqueous extract with prior organic extration, D-AR = Freeze-dried extract without prior organic extraction, Amp = Ampicillin, Chl = Chloramphenicol, Van = Vancomycin

*These values represent the expected theoretical concentrations of NPs, based on the amount used to synthesise NP.

4.2.1.2. Microorganisms and growth conditions

Details of the microorganisms used in this study and their growth media are listed in Table 4.2. *A. baumannii* (ATCC BAA-1605), *K. pneumoniae* (ATCC 700603), *E. faecalis* (ATCC 51299), *S. aureus* (ATCC 33591) *and C. albicans* (ATCC 24433) were obtained from Dr Marilize le Roes-Hill, Cape Peninsula University of Technology (CPUT).

Table 4.2 Microorganisms used in this study and their growth media

Microorganism	Strain	Description[2]	Media	Reference
Acinetobacter baumannii	ATCC BAA-1605	Gram negative, multiple drug resistant opportunistic pathogen, especially with immune-compromised individuals; increased incidence as cause of nosocomial infections [a]	Tryptic soy agar	CDC, 2016
Klebsiella pneumoniae subsp. *pneumoniae*	ATCC 700603	Gram negative, Control for extended spectrum betalactamase production. Important causative agent of nosocomial infections[b]	Nutrient agar	CDC, 2016
Enterococcus faecalis	ATCC 51299	Gram positive, Cause of nosocomial infections [c]	Brain heart infusion broth	Huycke, 2014
Staphylococcus aureus subsp. *aureus*	ATCC 33591	Gram positive, Comon cause of nosocomial infections, can cause range of illnesses [d]	Nutrient agar	Baron, 1996
Candida albicans	ATCC 24433	Yeast, Reference strain for clinical and laboratory standards Institute (CLSI)-developed antifungal susceptibility testing [e]	YM agar	CDC,2016

[a] Resistant to Ceftazidime, Gentamicin, Ticarcillin, Piperacillin, Aztreonam, Cefepime, Ciprofloxacin, Imipenem, and Meropemem. Sensitive to Amikacin and Tobramycin
[b] Resistant to Ampicillin, Aztreonam, Cefoxitin, Cefpodoxime, Ceftazidime, Piperacillin, Ceftriaxone
Sensitive to Amoxicillin-Clavulanate Cefepime, Ciprofloxacin, Impenem, Piperacillin-tazobactam, Inmethoprim-Sulfamethoxazole
[c] Low level Vancomycin-resistant, VanB
Resistant to Vancomycin
Sensitive to teicoplanin

[2] From ATCC product sheet

[d] Methicillin resistant, produces beta lactamase
[e] Assay of amphotericin B. Fungizone, quality control, susceptibility testing

4.2.1.3 Agar well diffusion assay

The agar well-diffusion assay was carried out according to the method of Dhand *et a.* (2016). Each microorganism culture in liquid suspension (100 µl) was spread onto each agar plate depending on the media it grows in (Table 4.2). Four wells were created on each agar plate and 75 µl (refer to Table 4.1 for concentrations of each sample) of each nanoparticle sample was added. Eight replicates, on two separate agar plates (4 replicates per plate), were prepared for each nanoparticle sample. The controls (1 mg/mL) used were vancomycin, ampicillin and chloramphenicol. The plates were then incubated at 37 ºC for 24 hours. The results were obtained by measuring the diameter of the clear zone (zone of inhibition) around the well.

4.2.2. Cytotoxicity Assay

4.2.2.1. Cell culture

All the processes were performed under laminar flow hood. The detailed method is outlined in Apendix A. The cytotoxicity of the synthesised nanoparticles were evaluated by the author against two cancer and one non-cancer cell line in the laboratory of Professor Mervyn Meyer (University of the Western Cape). The cell lines MCF-7, MCF-12a, and HT-29 were obtained from American Type Culture Collection (ATCC) and were grown as follows: MCF-7 and HT-20 cells were grown in Dulbecco's Modified Eagle's Media (DMEM) supplemented with 1% of penstrep (penicillin-streptomycin) and 10% foetal bovine serum (FBS). MCF-12a cells were grown in DMEM-F12 to which 1% penstrep and 10% foetal bovine serum were added. In addition to these supplements, 25 µL of hydrocortisone, 10 µL of epidermal growth factor (EGF) and 80 µL of insulin were added to DMEM-F-12. All three cell lines were grown under standard culture conditions (37 °C, and 5% CO_2).

Cells were trypsinized when they were confluent (70-90%) after which they were counted on a Countess^{TM} cell counting chamber slide. The number of live cells was used to calculate the volume of cells to be cultured in a 96 well plate. To each well, 100 µl of cells was added (1 x 10^5 live cells) and incubated for 24 hours at 37 ºC and 5% CO_2.

4.2.2.2. Sample preparation

Nanoparticles were centrifuged at 10 000 rpm and the pellet was collected and re-suspended in 3 ml distilled water. From this solution, 500 µL was taken and diluted with 500 µL of media. Samples were added to the 96 well plate (100 µL) in triplicate, i.e., 100 µl in three wells for each concentration.

4.2.2.3. MTT assay

The cell viability test was done by using the MTT assay (Nune *et al.*, 2009). The assay was performed in 96-well microtitre plates. To each well, 100 µl of cells was added (1 x 10^5 live cells) and incubated for 24 hours at 37 ºC and 5% CO2. The media was discarded after 24 hours and the nanoparticles were added in triplicate. Cells and media were used as a control. The 96-well microtitre plate was then incubated for 24 hours at 37 ºC, 5% CO2. The nanoparticles were removed from wells using a multi-channel micropipette after 24 hours and the cells were washed with PBS to ensure complete removal of nanoparticles that had not internalised.

MTT stock solution (5 mg/ml) 1 ml was mixed with 10 ml of media and 100 µL of the solution was then added to each well. The plate, covered in foil, was incubated for 4 hours at 37 ºC and 5% CO_2. After incubation, MTT was then discarded before 100 µl of DMSO (>99.5%) was added to each well and incubated again for 15 minutes until a purple colour appeared. The absorbance at 570 nm was read on a multi-plate reader (BMG Labtech).

The percentage viability was calculated as follows:

$$\% \text{ viability} = \frac{OD\ of\ test\ sample}{OD\ of\ control} x\ 100 \qquad (4.1)$$

4.2.2.4. Statistical analysis

The cell viability study was done in triplicate. The results were presented as mean ± standard deviation. The *p* values were calculated on excel using the TTEST function.

4.3 RESULTS AND DISCUSSION

This section focuses on the behaviour of the nanoparticles as they are tested against different microbes and cancer and non-cancer cells. The effectiveness of nanoparticles antimicrobial activity was determined by measuring the zone of inhibition, and percentage viability in the case of cancer and non-cancer cell lines used in this study. Results from both experiments (antimicrobial and cytotoxicity assay) are presented in the following sections.

4.3.1. Antimicrobial assay

The antimicrobial activities based on the well-diffusion test are shown in Figure 4.1. Interestingly, the crude aqueous extracts from *S. incissifolium* (AC and AR) as well as the fucoidans from *F. vesiculosus* (Fv) and *M. pyrifera* (Mp) showed no or negligible activity against the panel of microorganisms. Similarly, the sodium borohydride synthesised nanoparticles (SB-AgN) as well as the gold nanoparticles also showed no or negligible antimicrobial activity. The most potent activity was exhibited by the nanoparticles synthesised from the aqueous extract of *S. incissifolium* (AC-AgNP and AR-AgNP). This is particularly, interesting since the known antibiotics, except for chloramphenicol also showed no or negligible antimicrobial activity.

The selection of microorganisms was done in such a manner that involved two gram negative bacteria namely *A. baumannii* and *K. pneumoniae*, two gram positive bacteria *E. faecalis* and *S. aureus*, and one yeast, *C. albicans*. The greatest inhibition was recorded in the yeast followed by gram negative bacteria and lastly, gram positive bacteria for agar well diffusion assay. These results are only partially congruent with literature, especially between gram positive and gram negative bacteria, in case of *S. aureus*. Liu *et al.* (2014) tested AgNP against *E. coli* and *B. subtilis* which are gram negative and gram positive bacteria, respectively. From their study, they found out that the greatest inhibition of growth was observed in gram positive bacteria. The difference in degree of AgNP toxicity towards gram positive and gram negative bacteria stem from their structural composition. Gram positive bacteria consist of thick peptidoglycan, techoic acid, functional protein and a single bilayer that is wrapped in lipid. The gram negative bacteria, on the other hand, consist of thin peptidoglycan embedded within two lipid bilayers, and lipopolysaccharide (LPS). The LPS plays a major role in protecting the gram negative bacteria.

As such, the gram negative is supposed to be more resistant to nanoparticles than gram positive bacteria (Liu *et al.*, 2014). According to the results obtained, the reverse was true for this study, except for *S. aureus*.

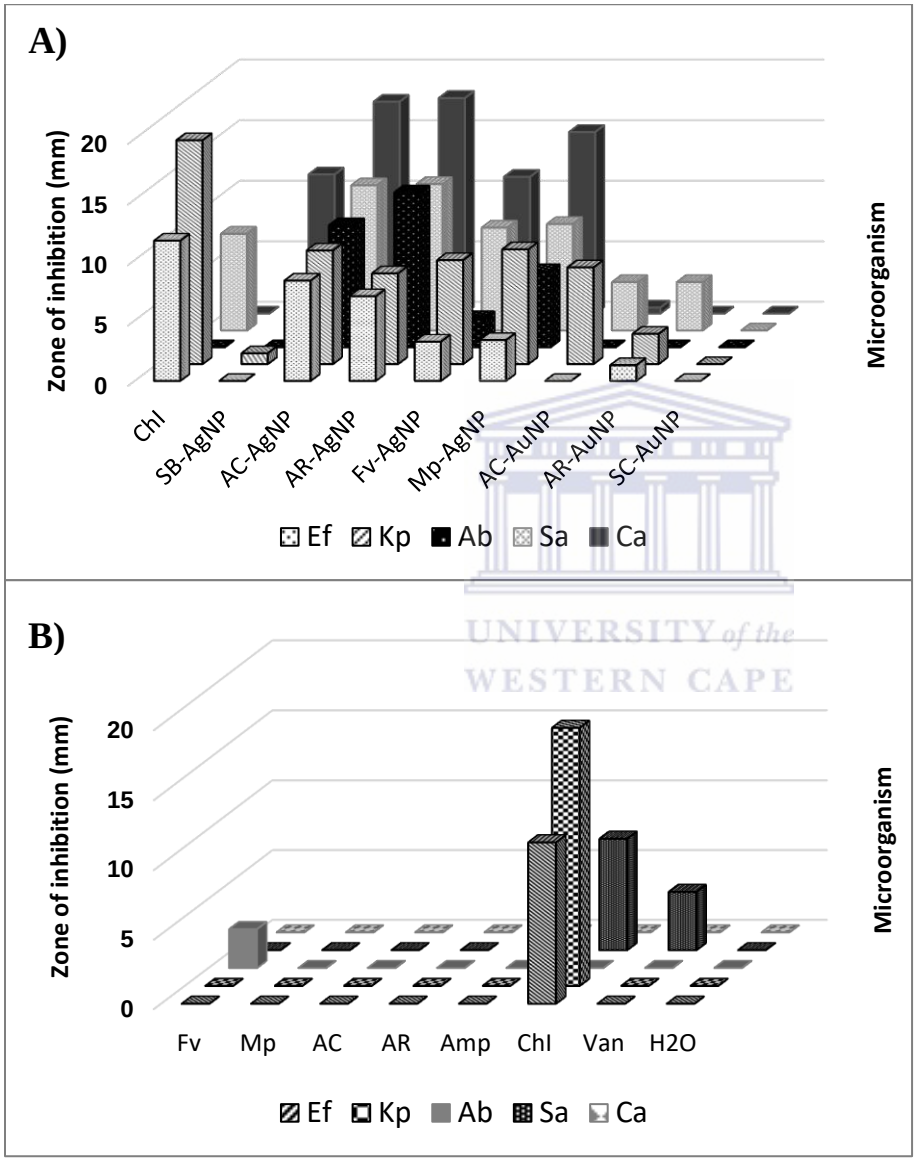

Figure 4.1 Antimicrobial activity (well-diffusion assay) against a panel of microorganisms (Ab = *A. baumannii*, Kp = *K. pneumoniae*, Ef = *E. faicalis*, Sa = *S. aureus*, Ca = *C. albicans*) for a) the synthesised nanoparticles and b) the aqueous extracts (AC and AR), fucoidans (Fv and Mp), and controls: Vancomycin (Van), Ampicillin (Amp), Chloramphenicol (ChI) and water (H_2O). NP concentrations used: ~0.2 mM. [Van], [Amp] and [ChI]: 1mg/ml.

It is well known that seaweeds, particularly brown seaweeds produce molecules that are antiviral (Li *et al.*, 2008). However, very little has been reported on the antibacterial activity of aqueous extracts of marine brown algae. Nevertheless, AgNP synthesised from *S. incisifolium sp.*, the brown seaweed, were very toxic to microbes. Surprisingly, when the aqueous extract was tested against the microorganisms did not show any activity. The other component of brown seaweeds, fucoidan, is known for a various bioactivities, but antimicrobial is not part of them. However, when tested against microbes, fucoidan from *F. vesiculosus* showed activity against only *A. baumannii* which suggests that fucoidan may also possess bactericidal activity. Mp did not show any activity against selected microbes. However, AgNP synthesised from these fucoidans did show activity against the test strains, especially Mp-AgNP.

As a control, AuNP were also tested against different microorganisms as was the case with AgNP. When modified or synthesised by the use of plant extract, AuNP may show bactericidal activity (Bindhu & Umadevi, 2014; Park *et al.*, 2016). Park *et al.* (2016) found that AuNP were toxic against *Streptococcus pneumoniae* when resveratrol was conjugated on their surface. The results obtained in this research do not agree that modified AuNP can be toxic to microorganism, especially chemically synthesised AuNP. Almost all AuNP tested against microorganisms in this study did not show any activity against the microorganisms. However, AC-AuNP and AR-AuNP did show slight activity.

4.3.2. Cytotoxic activity of silver and gold nanoparticles

One of the major concerns in the development of silver nanoparticles as antimicrobial agents is their potential toxicity to humans and the environment. It was therefore important to assess the cytotoxicity of the synthesised nanoparticles. The cytotoxicity was determined using the MTT assay where viable cells reduce the MTT dye which can be measured by absorbance spectroscopy. The cytotoxicity results are presented in Figure 4.1.

Unfortunately, the most active antimicrobial nanoparticles, AC-AgNP and AR-AgNP also showed the most potent cytotoxicity against the cells studied, albeit at a much higher concentration. It also appeared that the nanoparticles themselves may interfere with the absorbance readings of the formazan dye. Care was taken in removing excess nanoparticles

before addition of the MTT dye in order to minimise these effects. However, it may be necessary to develop newer methods for the investigation of the cytotoxicity of nanoparticles. The formazan dye absorbs UV-Vis light at the range of 500-600 nm. To ensure that AuNP and AgNP do not interfere with the absorbance readings, OD were measured at 570 nm.

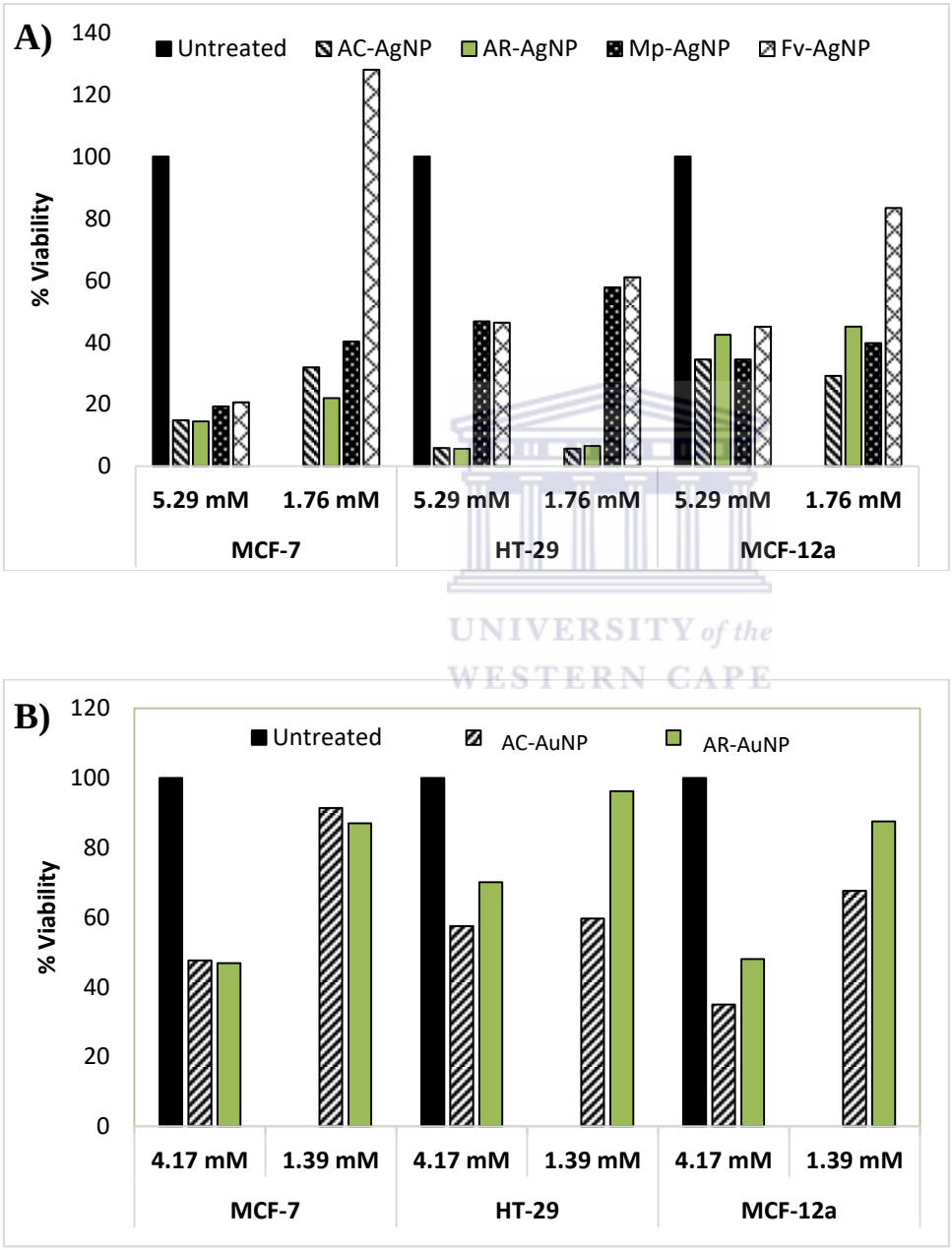

*p<0.05
**p>0.05

Figure 4.2 Percentage cell viability for MCF-7, HT-29 and MCF-12a cell lines after 24 hrs with a) AgNPs and b) AuNPs.

Interestingly, the gold nanoparticles also showed appreciable cytotoxic activity (Figure 4.2). AR-AuNP and AC-AuNP showed more activity against the cancer cell lines which was higher than that recorded for non-cancer cell line. The percentage viability of AuNP for MCF-12a was above 70% which entails less toxicity associated with AuNP against MCF-12. Even though these are *in vitro* studies, this gives hopes in case where green synthesised AuNP are to be used as vehicles for drug delivery because there will be less toxicity against human cells.

From Figure 4.2, it can be seen that AC-AgNP and Mp-AgNP showed excellent inhibition of growth of MCF-7 with a recorded percentage viability just below 20%. Fv-AgNP showed a percentage viability of 20%. Only AR-AgNP had percentage viability just above 20%. Although SB-AgNP showed activity against MCF-7, the toxicity of these nanoparticles was above 40% (Figure 4.2), which is lower than that of nanoparticles synthesised from aqueous extract of seaweed. It is however understandable since the concentration of sodium borohydrite synthesised nanoparticles (SB-AgNP) was lower than the concentrations of green synthesised AgNPs.

AuNPs were also tested for cytotoxicity against MCF-7 cell lines. The different results were obtained when AC-AuNP and AR-AuNP are tested against MCF-7. Both these AuNPs displayed activity against MCF-7, especially AR-AuNP with percentage viability just below 20% (Figure 4.2). AC-AuNP on the other hand is less toxic against MCF-7 with percentage of live cells that is more than 50%. Although the concentration of SC-AuNP is lower than that of any of the green synthesised AuNP, the percentage viability revealed that these nanoparticles are not toxic against MCF-7 (Figure 4.2).

The reducing agents, especially *S. incisifolium* and commercially available fucoidans were also tested against MCF-7 (Supplementary information, Figure 4.11). All of these reducing agents resulted in a percentage viability that is higher than 50 %. Though its percentage viability was just above 50%, *Macrocystis pyrifera* could potentially be toxic towards MCF-7 if slightly higher concentration is used (Table 4.1).

Colorectal cancer cell lines were also tested with nanoparticles to determine whether they are susceptible to nanoparticle toxicity. AC-AgNP and AR-AgNP seem to exert the same toxic effect on HT-29 with percentage viability below 10% (Figure 4.2). Fucoidan nanoparticles seemed to be less toxic against HT-29 with percentage viability just above 40%. SB-AgNP on the other hand did not show any toxicity against HT-29 with percentage viability sitting at 80%.

As was the case with MCF-7, AuNPs were also tested for cytotoxicity against HT-29. From Figure 4.2 it can be noticed that AC-AuNP and AR-AuNP showed comparable cytotoxicity.

From reducing agents tested against HT-29, only *Fucus vesiculosus* seemed to be toxic against HT-29 with percentage viability below 40%.

Non-cancer cell line, MCF-12a (non-cancer breast cell line) was also tested with nanoparticles. Although some were somewhat toxic towards MCF-12a, but the toxicity of all the nanoparticles tested against MCF-12a does not compare to that of other cancer cell lines, MCF-7 and HT-29. Results in Figure 4.2 show that Mp-AgNP showed activity against MCF-12a with percentage viability below 40%. 4AR-AgNP and Fv-AgNP followed with percentage viability just above 40 %. Only AC-AgNP seemed not to be toxic to MCF-12a when compared to other AgNPs. From the reducing agents, only Fv had percentage viability below 40% recorded, D-AR resulted with percentage viability just above 40%. All other reducing agents had percentage viability of at least 60%.

Silver is one of the most versatile substances in the medical field. Silver has been used as bactericidal agent and also as in wound dressing due to its wound healing properties (Nam *et al.*, 2016). Anticancer activity of AgNPs has previously been evaluated (Guo *et al.*, 2015). From the results presented in Table 4.4 it is clear that AgNPs are toxic to MCF-7 and HT-29 cancer cell lines. AC-AgNP and AR-AgNP were found to be more active against HT-29 than they were with MCF-7. Again, the AgNPs tested for cytotoxicity showed somewhat different trend, whereby those AgNPs synthesised from AR, were more toxic than those AgNPs synthesised from AC. The obvious reason for this difference stems from the method of synthesis (and the method of aqueous extraction). Although AC is highly concentrated as was seen in Chapter 3, the

nanoparticles synthesised from this extract are not very toxic. This implies that some toxic organic soluble molecules may be extracted under aqueous conditions and may cap the nanoparticles, thus imparting increased toxicity.

The nanoparticles produced from commercially available fucoidans also showed different degrees of anticancer activity. Mp-AgNP was very active against MCF-7 but less active when tested against HT-29 (Figure 4.2). Also, Mp-AgNP was more toxic when compared to Fv-AgNP on both cell lines. Fv-AgNP also showed the same trend that was shown by Mp-AgNP between MCF-7 and HT-29, i.e., more activity was observed when tested against MCF-7 but less activity was witnessed when tested against HT-29. Both HT-29 and MCF-7 cell lines are susceptible to green synthesised AgNP, but the activity of nanoparticles was found to be less in MCF-7 compared to HT-29 cell lines.

There are several mechanisms through which AgNP may kill cancer cells. One such mechanism is through induction of oxidative stress (Guo *et al.*, 2015; Mollick *et al.*, 2015). Size, shape and zeta potential of metallic nanoparticles (AgNPs) are known to elicit death of cells through the elevation of reactive oxygen species (ROS). The AgNPs are taken inside the cells by endocytosis and end up in endosomes. Guo *et al.*. (2015) used HepG2 to study the internalisation of AgNPs and confirmed that the AgNP were inside the endosomes. Inside the cells, AgNPs are broken down by lysozymes and release Ag^{+} which results in oxidative stress. In addition to induction of oxidative stress in cancer cells, AgNPs also induce apoptosis in cancer cells. AgNPs use ROS to interact with mitochondria thereby inducing apoptosis pathway. Also, apoptosis may be induced by the upregulation of gene p53 (Guo et al., 2015).

Results obtained from the non-cancer cell line, MCF-12a, suggest that AgNPs are selective when it comes to cytotoxicity against different cell lines. Even though Mp-AgNP showed toxicity against MCF-12a, the percentage viability was higher than that recorded for MCF-7. The AgNPs synthesised from *S. incisifolium* are very toxic towards MCF-7 but less toxic towards MCF-12a.

4.4 CONCLUSION

Based on the preliminary results obtained in this study it could be seen that AgNPs possess potent antimicrobial activities. Indeed, the green synthesised AgNPs present with enhanced antibacterial activity as the conventionally synthesised AgNPs did not show competitive activity against microorganisms tested. Also, it seems that the method of green synthesis affects the future bactericidal activity of AgNPs synthesised. This was proved by the AgNPs synthesised from different aqueous extract in this study (AC and AR), with AR synthesised AgNP being more effective in killing the microorganisms tested. Furthermore, it seems that different microorganisms respond differently from the AgNPs. This could possibly be due to the nature of the microbial cell membranes as they are very different between gram-positive and gram-negative bacteria. The results show that gram negative bacteria were very susceptible to AgNP compared to gram-positive bacteria. Methicillin-resistant *S. aureus* on the other hand was the most susceptible among the tested four bacteria. Of all the test strains, the yeast, *C. albicans* was most susceptible to AgNPs.

Although they showed activity against the microorganisms, AuNPs resulted in lower zones of inhibition. However, this entails that if care is ensured during their synthesis with the help of seaweed extract, AuNPs could be modified into antibacterial effective nanoparticles. The highest zone of inhibition was recorded in AC-AuNP against *K. pneumoniae*. The conventionally synthesised AuNPs could hardly show any inhibition of microbial growth.

The preliminary cytotoxicity results suggest that care should be taken when developing these AgNPs, especially for internal use. The highest activity was recorded against HT-29 for AgNPs synthesised from aqueous extract of *S. incisiflolium* while those synthesised from pure fucoidans showed greater activity against MCF-7. The toxicity of AgNPs lowered when the non-cancer cell line was tested. These findings suggest that there could be some selectivity of AgNPs which dictates how they react with cancer and non-cancer cells.

AuNPs did show appreciable toxicity against cancer cell line used in this study. The green synthesised AuNPs showed greater inhibition of cancer cell growth when the conventionally

synthesised AuNPs showed little toxicity towards the cancer cell lines. Like in AgNPs, the toxicity of AuNPs towards non-cancer cell lines was low compared to that of cancer cell lines.

Lastly, the objectives of this study were successfully achieved. The green synthesised AgNPs showed great antibacterial activity.

CHAPTER 5

5. CONCLUSION AND FUTURE WORK

5.1 SYNTHESIS AND CHARACTERISATION OF NANOPARTICLES

A green method of synthesis for Au and Ag nanoparticles was developed in this study using *S. incisifolium* aqueous extracts as reducing agents. The method of preparation of the aqueous extract affects the rate at which nanoparticles are formed. NMR and FT-IR spectroscopic studies confirmed that complex polysaccharides are the major components of the aqueous extracts. FT-IR spectroscopy also confirmed the presence of these polysaccharides on the surface of the NPs. However, it appears that additional components, most likely phlorotannins may play an important role in nanoparticle formation.

The formation of the nanoparticles using $NaBH_4$ and sodium citrate for the Ag and AuNPs respectively was much faster when compared to biological method of synthesis, especially for the AgNPs. The reaction was complete after the addition of $AgNO_3$ to $NaBH_4$ whereas the reaction seemed to take longer than 18 hours when seaweed extract was used. However, in the case of AuNP syntheses, the biosynthetic method appears to afford significant advantages over chemical synthesis since it is as fast and does not require high temperatures. Moreover, the concentration of nanoparticles formed in the latter method is greater than that of chemically synthesised AuNPs.

From antioxidant activity results, it is conclusive that *S. incisifolium* has high antioxidant activity, even though we only compared two differently extracted aqueous extracts. The lower total phenolic content, reducing power and radical scavenging power of pure fucoidans assessed in this study may explain why the pure fucoidans were not able to reduce Ag^+ and Au^+ to form nanoparticles at room temperature. This further confirms that fucoidans per se, do not contribute in the formation of nanoparticles as evidenced by the results obtained from total reducing power.

The size of the nanoparticles was determined using different techniques and the results differ. However, this could be explained by the technique itself and the drawbacks associated with it. For example, the sizes determined by DLS were found to be bigger than the sizes determined by

TEM as these are hydrodynamic diameters. The DLS size determination will take into account the capping agent of the NPs, whereas in TEM carbon based materials are transparent to the electron beam. The sizes determined by XRD were found to be smaller than the sizes of the nanoparticles determined by TEM. This may be due to the fact that the size determination given by XRD will be an average of the whole sample, while TEM is focussed on a small area of a sample. Factors such as hydration of nanoparticles, dry state of nanoparticles and crystallinity may have had effect on different sizes of nanoparticles.

Lastly, it seems that different methods of extractions have an impact of the characteristics of nanoparticles synthesised. These include the size, shape and crystallinity. The sizes of nanoparticles were found to be big when AR is used as a reducing agent and small when AC is used as a reducing agent. Furthermore, the speed of reaction differs between different reducing agents with AC being the fastest among other reducing agents at room temperature.

5.2 ANTIMICROBIAL AND CYTOTOXICITY ASSAYS

Based on the preliminary results obtained in this study it could be seen that AgNPs possess potent antimicrobial activities. Indeed, the green synthesised AgNPs present with enhanced antibacterial activity as the conventionally synthesised AgNP did not show a competitive activity against microorganisms tested. Also, it seems that the method of green synthesis affects the future bactericidal activity of AgNPs synthesised. This was proved by the AgNPs synthesised from different aqueous extracts in this study (AC and AR), with AR synthesised AgNPs being more effective in killing the microorganisms tested. Furthermore, it seems that different microorganisms respond differently to the AgNPs. This could possibly be due to the nature of the microbial cell membranes as they are very different between gram-positive and gram-negative bacteria. The results show that gram negative bacteria were very susceptible to AgNPs compared to gram-positive bacteria. Methicillin-resistant *S. aureus* on the other hand was the most susceptible among the tested four bacteria. Of all the test strains, the yeast, *C. albicans* was the most susceptible to AgNPs.

Although they showed activity against the microorganisms, AuNPs resulted in lower zones of inhibition. However, this suggests that if care is ensured during their synthesis with the help of

seaweed extract, AuNPs could be modified into antibacterial nanoparticles. The highest zone of inhibition was recorded in AC-AuNP against *K. pneumoniae*. The conventionally synthesised AuNP hardly showed any inhibition of microbial growth.

The preliminary cytotoxicity results suggest that care should be taken when developing these AgNPs, especially for internal use. The highest activity was recorded against HT-29 for AgNPs synthesised from aqueous extract of *S. incisifolium* while those synthesised from pure fucoidans showed greater activity against MCF-7. The toxicity of AgNPs lowered when the non-cancer cell line was tested. These findings suggest that there could be some selectivity of AgNPs which dictates how they react with cancer and non-cancer cells.

AuNPs did show appreciable toxicity against cancer cell lines used in this study. The green synthesised AuNPs showed greater inhibition of cancer cell growth when the conventionally synthesised AuNPs showed little toxicity towards the cancer cell lines. Like in AgNPs, the toxicity of AuNPs towards non-cancer cell lines was low compared to that of cancer cell lines. Lastly, the objectives of this study were successfully achieved. The green synthesised AgNPs showed significant antibacterial activity.

5.3 FUTURE WORK

Since commercial fucoidans were used in this study to synthesise nanoparticles, it would be essential to isolate fucoidans and phlorotannins from the aqueous extract of *S. incisifolium* and study their reducing capabilities to those commercially available fucoidans.

Our preliminary studies showed that *S. incisifolium* synthesised AgNPs exhibit activity against several microbial strains used and also against the cancer and non-cancer cells. More detailed antimicrobial and cytotoxic studies are required in order to determine MIC values against the microorganisms and IC_{50} values against cancer cells. At this stage, it appears that the AgNP synthesised in this study is more appropriate for external application. Furthermore, additional studies are required to develop bioassays more suitable for use with nanoparticles that show overlapping absorbance with those of common dyes used in viability studies. *In vivo* studies will

also be essential as that would determine potential toxicity and whether the *in vitro* antimicrobial activity is maintained in *in vivo* studies.

Although there has been suggested mechanism of action of metallic nanoparticles, it is not very clear as to what these nanoparticles interact with in the bacterial cytoplasm. Therefore more work still needs to be done in order to determine the targets in the microorganism that the AgNPs interact with.

6. REFERENCES

Adams, F. C., and Barbabante, C. (2013). Nanoscience, nanotechnology and spectrometry. *Spectrochimica Acta Part B*. **86**, 3-13.

Afolayan, A. F., Bolton, J. J., Lategan, C. A., Smith, P. J., and Beukes, D. R. (2008). Fucoxanthin, tetraprenylated toluquinone and toluhydroquinone metabolites from *Sagarssum heterophyllum* inhibit the in vitro growth of the malaria parasite *Plasmodium falciparum*. *Z Naturforsch C*. **63**, 848-852.

Ahn-Tuan, L., Huy, P. T., Tam, P. D., Huy, T. Q., Cam, P. D., Kudrinskiy, A. A., and Krutyakov, Y. A. (2010). Green synthesis of finely dispersed highly bactericidal silver nanoparticles via modified Tollens technique. *Current Applied Physics* **10**, 910-916.

Aitken, R. J., Candhry, M. Q., Boxal, A. B. A., and Hull, M. (2006). Manufacture and use of nanomaterials: current status in the UK and global trends. *Occupational Medicine* **56**, 300-306.

Akhtar, M. S., Panwar, J., and Yun, Y-S. (2013). Biogenic synthesis of metallic nanoparticles by plant extracts. *ACS Sustainable Chem. Eng* **1**, 591-602.

Al-Amoudi, O., Mutawie, H. H., Patel, A. V., and Blunden, G. (2009). Chemical composition and antioxidant activities of *Jeddah cornice* algae, Soudi Arabia. *Saudi Journal of Biological Sciences* **16**, 23-29.

Ale, M. T., Mikkelsen, J. D., and Meyer, A. S. (2011). Important determinants for fucoidan bioactivity: a critical review of structure-function and extraction methods for fucose-containing sulfated polysaccharides from brown seaweeds. *Mar. Drugs* **9**, 2106-2130.

Ananthi, S., Raghavendran, H. R. B., Sunil, A. G., Gayathri, V., Ramakrishnan, G., and Vasanthi, H. R. (2010). *In vitro* antioxidant and *in vivo* anti-inflammatory potential of crude polysaccharide from *Turbinaria ornata* (marine brown alga). *Food and Chemical Toxicology* **48**, 187-192.

Arokiyaraj, S., Kannaian, U. P. N., Elakkya, V., Kamala, T., Bhuvaneswari, S., and Dinesh, K.V. (2013). Green synthesis of silver nanoparticles using aqueous floral extract of *Nelumbo Nucifera*. *Journal of Material and Science Forum* **756**, 106-111.

Asharani, P. V., Mun, G. L. K., Hande, M. P., and Valiyaveettil, S. (2009). Cytotoxicity and genotoxicity of silver nanoparticles in human cells. *ACS Nano* **3**, 297-290.

Asmathunisha, N., and Kathiresan, K. (2013). A review on biosynthesis of nanoparticles by marine organisms. *Colloids and Surfaces B: Biointerfaces* **103**, 283-287.

Banerjee, J., and Narendhirakannan, R. T. (2011). Biosynthesis of silver nanoparticles from *Syzigium cumini* (L.) seed extract and evaluation of their in vitro antioxidant activities. *Digest Journal of Nanomaterials and Biostructure* **6**, 961-968.

Barbosa, M., Valentão, P., and Andrade, P. B. (2014). Bioactive compounds from macroalgae in the new millennium: implications for neurodegenerative diseases. *Marine Drugs* **12**, 4934-4972.

Baron, S. (1996). Medical Microbiology. 4th edition. Galveston (TX): University of Texas medical branch at Galveston. Chapter 12: Staphylococcus. ISBN-10:0-9631172-1-1.

Begum, N. A., Mondal, S., Basu, S., Laskar, R. A. and Mandal, D. (2009). Biogenic synthesis of Au and Ag nanoparticles using aqueous solutions of black tea leaf extracts. *Colloids and Surfaces B: Biointerfaces* **71**, 113-118.

Benn, T. M., and Westerhoff, P. (2008). Nanoparticle silver released into water from commercially available sock fabrics. *Environmental Science and Technology* **42**, 4133-4139.

Bhatt, P., Tandel, K., Sheter, V., and Rathi, K. R. (2015). Burden of extensively drug-resistant and pandrug-resistant gram-negative bacteria at a tertiary-care centre. *New Microbes and New Infections* **8**, 166-170..

Bhattacharya, R., and Mukherjee, P. (2008). Biological properties of "naked" metal nanoparticles. *Advanced Drug Delivery Reviews* **60**, 1289-1306.

Bhumkar, D. R., Joshi, H. M., Sastry, M., and Pokharkar, V. B. (2007). Chitosan reduced gold nanoparticles as novel carriers for transmission delivery of insulin. *Pharmaceutical Research* **24**, 1415-1426.

Bindhu, M. R., and Umadevi, M. (2014). Antibacterial activities of green synthesized gold nanoparticles. *Materials Letters* **120**, 122-125.

Binupriya, A.R., Sathishkumar, M., Yun, S.-I. (2010b). Biocrystallization of silver and gold ions by inactive cell filtrate of *Rhizopus stolonifer*. *Colloid Surfaces. B: Biointerfaces* **79**, 531-534.

Borm, P.J.A., and Berube, D. (2008). A tale of opportunities, uncertainties, and risks. *Journal of Nano Today* **3**, 56-59.

Buzea, C., Blandino, I. I. P., and Robbie, K. (2007). Nanomaterials and nanoparticles: Sources and toxicology. *Biointerfaces* **2**, MR17-MR172.

Cacicedo, M. L., León, I. E., Gonzales, J. S., Porto, L. M., Alvarez, V. A., and Castro, G. R. (2016). *Journal of Colloids and Surfaces B: Biointerfaces* **140**, 421-429.

Carrillo-Lopez, L. M., Zavaleta-Mancera, H. A., Vilchis-Nestor, A., Soto-Hernandez, R-M., Arenas-Alatorre, J., Trejo-Tellez, L. I., and Gomez-Merino, F. (2014). Biosynthesis of silver silver nanoparticles using *Chenopodium ambrosioides*. *Nanomaterials* **2014**, 1-8.

Center for Disease Control and Prevention. (2016). Fungal disease: Candidiasis. www.cdc.gov/fungal/diseases/candidiasis/ visited on 7 March 2016. Accessed: 12 June 2015

Center for Disease Control and Prevention. (2016). Health care-associated infections (HAIs). *Acinetobacter* in health care settings. www.cdc.gov/HAI/organisms/acinetobacter.htlm Accessed: 7 March 2016.

Center for Disease Control and Prevention. (2016). *Klebsiella pneumoniae* in health care settings. Health care associated infections. www.cdc.gov/HAI/organism/klepsiella/klepsiella.html. Accessed: 24 November 2010.

Chandran, S. P., Chaudhary, M., Pasricha, R., Ahmad, A., and Sastry, M. (2006). Synthesis of gold nanoparticles and silver nanoparticles using *Aloe vera* plant extract. *Biotechnology Progress* **22**, 577-583.

Chen, X., and Schluesener, H. J. (2008). Nanosilver: a nanoproduct in medical applications. *Toxicology Letters* **176**, 1-12.

Cui, Y., Zhao, Y., Tian, Y., Zhang, W., Lu, X., and Jiang, X. (2012). The molecular mechanism of action of bactericidal gold nanoparticles on *Escherichia coli*. *Journal of Biomaterials* **33**, 2327-2333.

Cumberlands, S. A., and Lead, J. R. (2013). Synthesis of NOM-capped silver nanoparticles: size, morphology, stability, and NOM binding characteristics. *ACS Sustainable Chemical Engineering* **1**, 817-825.

Daniel, M-C., and Astruc, D. (2004). Gold nanoparticles: assembly, supramolecular chemistry, quantum-size-related properties, and application toward biology, catalysis, and nanotechnology. *Chemical Reviews* **104**, 293-346.

Dhand, V., Soumya, L., Bharadwaj, S., Chakra, S., Bhatt, D., and Sreedhar, B. (2016). Green synthesis of silver nanoparticles using *Caffea Arabica* seed extract and its antibacterial activity. *Material Science and Engineering C* **58**, 36-43.

Das, P., Williams, C. J., Fulthorpe, R. R., Hoque, M. E., Metcalfe, C.D., Xenopoulos, M.A. (2012). Changes in bacterial community structure after exposure to silver nanoparticles in natural waters. *Environmental Science and Technology* **46**, 9120-9128.

de Kanter, M., Meyer-Kirshner, J., Viell, J., Mitsos, A., Kather, M., Pich, A., and Janzen, C. (2016). Enabling the measurement of particles size in stirred colloidal suspensions by embedding dynamic light scattering into an automated probe head. *Measurement* **80**, 92-98.

Derderian, S. L. (2007). Alexander Fleming's miraculous discovery of penicillin. *River Academic Journal* **3**, 1-5.

Dhand, V., Soumya, L., Bharadwaj, S., Chakra, S., Bhatt, D., and Sreedhar, B. (2016). Green synthesis of silver nanoparticles using *Coffea Arabica* seed and extract and its antibacterial activity. *Material Science and Engineering* C **58**, 36-43.

Elia, P., Zach, R., Hazan, S., Kolusheva, S., Porat, Z., and Zeiri, Y. (2014). Green synthesis of gold nanoparticles using plant extracts as reducing agents. *International Journal of Nanomedicine* **9**, 4007-4021.

Fleita, D., El-Sayed, M., and Rifoat, D. (2015). Evaluation of the antioxidant activity of enzymatically-hydrolyzed sulphated polysaccharides extracted from red algae, *Pterocladia capillacea*. *LWT-Food Science and Technology* **63**, 1236-1244.

Gamal, A. A. (2010). Biological importance of marine algae. *Saudi Pharmaceutical Journal* **18**, 1-25.

Gericke, M., Pinches, A. (2006). Biological synthesis of metal nanoparticles. *Hydrometallurgy* **83**, 132-140.

Gherbawy, Y. A., Shalaby, I. M., El-Sadek, M. S. A., Elhariry, H. M., and Banaga, A. A. (2013). The anti-fasciolasis properties of silver nanoparticles produced by *Trechoderma harzianum* and

their improvement of the anti-fasciolasis drug triclabendazole. *International Journal of Molecular Science* **14**, 21887-21898.

Ghorbani, H. R., Safekordi, A. A., Attar, H., and Sorkhabadi, S. M. R. (2011). Biological and non-biological methods for silver nanoparticles synthesis. *Chem. Biochem. Eng. Q* **24**, 317-326

Gnanojobitha, G., Paulkumar, K., Vanaja, M., Rajeshkumar, S., Malarkodi, C., Annadurai, G., and Kannan, C. (2013). Fruit-mediated synthesis of silver nanoparticles using *Vitis vinifera* and evaluation of their microbial efficacy. *Journal of Nanostructure in Chemistry*. **3**, 1-6.

Guo, D., Duo, D., Ge, L., Huang, Z., Wang, L., and Gu, N. (2015). Caffeic acid mediated facile synthesis of silver nanoparticles with powerful anti-cancer activity. *Colloids and Surfaces B: Biointerfaces* **134**, 229-234.

Handford, C. E., Dean, M., Spence, M., Henchion, M., Ellioh, C. T., and Campbell, K. (2015). Awareness and attitudes towards the emerging use of nanotechnology in the agri-food sector. *Food Control* **57**, 24-34.

Hayden, S. C., Zhao, G., Saha, K., Phillips, R. L., Li, X., Miranda, O. R., Rotello, V. M., El-Sayed, M., Schmidt-Krey, I., and Bunz, U. H. F. (2012). Aggregation and interaction of cationic nanoparticles on bacterial surfaces. *American Chemical Society* **134**, 6920-6923.

He, Y., Du, Z., Li, H., Jia, Q., Tang, Z., Zhang, X., Zang, K., and Zhao, F. (2013). Green synthesis of silver nanoparticles by *Chrysanthemum morifolium* Ramat. extract and their application in clinical ultrasound gel. *International Journal of Nanomedicine* **8**, 1809-1815.

Huang, H-L., and Wang, B-G. (2004). Antioxidant capacity and lipophilic content of seaweeds collected from the Qingdao coastline. *Journal of Agricultural and Food Chemistry* **52**, 4993-4997.

Huang, X., and El-Sayed, M. A. (2010). Gold nanoparticles: optical properties and implementations in cancer diagnosis and photothermal therapy. *Advanced Research* **1**, 13-28.

Huh, A. J., and Kwon, Y. J. (2011). "Nanoantibiotics": a new paradigm for treating infectious diseases using nanomaterials in the antibiotic resistant era. *Controlled Release* **156**, 128-145.

Higuita, N. I. A., and Huycke, M. M.. (2014). Enterococcal disease, epidemiology, and implications for treatment. Boston: Massachusetts Eye and Ear. Infirmary. www.ncbi.nlm.nih.gov/books/NBK190429/

Iravani, S., and Zolfaghari, B. (2013). Green synthesis of silver nanoparticles using *Pinus elderica* Bark extract. *BioMed Research International* **2013**, 1-5.

Isaac, R. S. R., Sakthivel, G., and Murthy, C. (2013). Green synthesis of gold and silver nanoparticles using *Averrhoa bilibi* fruit extract. *Nanotechnology* **2013**, 1-6.

Jones, M. R., Osberg, K. D., Macfarlane, R. J., Langille, M. M., and Mirkin, C. A. (2011). Templated technigues for the synthesis and assembly of plasmonic nanostructures. *Chemical Reviews* **111**, 3736-3827.

Joshi, M., Bhattacharyya, A., and Ali, S. W. (2008). Characterization technigues for nanotechnology applications in textiles. *Indian Journal of Fibre & Textile Research* **33**, 304-317

Kaler, A., Jain, S., and Banerjee, U. C. (2013). Green and rapid synthesis of anticancerous silver nanoparticles by *Saccharomyces boulardii* and insight into mechanism of nanoparticle synthesis. *BioMed Research International* **2013**, 1-8.

Kannan, R. R. R., Stirk, W. A., and Van Staden, J. (2013). Synthesis of silver nanoparticles using seaweed *Codium capitulum* P.C. Silva (*Chlorophyceae*). *South African Journal of Botany* **86**, 1-4.

Kato, H., Suzuki, M., Fujita, K., Horie, M., Endoh, S., Yoshida, Y., Iwahashi, H., Takashi, K., Nakamura, A., and Kinugasa, S. (2009). Reliable size determination of nanoparticles using dynamic light scattering method for in vitro toxicology assessment. *Toxicology in Vitro* **23**, 927-934.

Kim, J. S., Kuk, E., Yu, K. N., Kim, J. H., Park, S. J., Lee, H. L., Kim, S. H., Park, Y. K., Park, Y. H., Hwang, C-Y., Kim, Y-K., Lee, Y-S., Jeong, D. H., Cho, M-H. (2007). Antimicrobial effects of silver nanoparticles. *Nanomedicine: Nanotechnology, Biology, and Medicine* **3**, 95-101.

Kim,D., Jeong, S., and Moon, J. (2006). Synthesis of silver nanoparticles using polyol process and the influence of precursor injection. *Nanotechnology* **17**, 4019.

Klaus, T., Joeger, R., Olsson, E., and granqvist, C-G. (1999). Silver-based crystalline nanoparticles, microbially fabricated. *Proceedings of the National Academy of Sciences* **96**, 13611-13614.

Kora, A. J., and Rastogi, L. (2015). Green synthesis of palladium nanoparticles using gum ghatti (*Anogeissus latifolia*) and its application as an antioxidant and catalyst. *Arabian Journal of Chemistry.* , http://dx.doi.org/10.1016/j.arabjc.2015.06.024

Koteswari, P., Krishna, S. R., Reddy, V. P., Nasaru,L. M. (2011). Formulation and preparation of felodipine nanoemulsion. *Asial Journal of Pharmaceutical and Clinical Research* **4**, 116-117.

Kumar, S., Aaron, J., and Sokolov, K. (2008). Directional conjugation of antibodies to nanoparticles for synthesis of multiplexed optical contrast with both delivery and targeting moieties. *Nature Protocols* **3**, 314-320.

Lara, H. H., Ayala-Nunez, N. V., Turrent, L. C. I., and padilla, C. R. (2010). Bactericidal effect of silver nanoparticles against multidrug-resistant bacteria. *World Journal of Microbiology and Biotechnology* **26**, 615-621.

Le, A-T., Huy, P. T., Tam, P. D., Huy, T. Q., Cam, P. D., Kudrinskiy, A. A., and Krutyakov, Y. A. (2010). Green synthesis of finely-dispersed highly bactericidal silver nanoparticles via modified Tollens technigue. *Current Applied Physics* **10**, 910-916.

Leela, A., and Vivekanandan, M. (2008). Tapping the unexploited plant resources for the synthesis of silver nanoparticles. *Africal Journal of Biotechnology* **7**, 3162-3165.

Levin, A. S., Barone, A. A., Penço, J., Santos, M. V., Marinho, I. S., Arruda, E. A. G., Manrique, E. I., and Costa, S. F. (1999). Intravenous colistin as therapy for nosocomial infectrions caused by multidrug-resistant *Pseudomonas aeruginosa* and *Acinetobacter baumannii*. *Clin Infect Ds.* **28**, 1008-1011.

Li, B., Lu, F., Wei, X., and Zhao, R. (2008). Fucoidan: structure and bioactivity. *Molecules* **13**, 1671-1695.

Lim, S. S., Cheung, P. C. K., Ooi, V. E. C., and Ang, P. O. (2002). Evaluation of antioxidant activity of extracts from a brown seaweed, Sargassum siliquastrum. *Journal of Agricultural and Food Chemistry* **50**, 3862-3866.

Lin, P-C., Lin, S., Wang, P. C., Sridhar, R. (2014). Technigues for physicochemical characterization of nanomaterials. *Biotechnology Advances* **32**, 711-726.

Liu, B., Xie, J., Lee, J. Y., Ting, Y. P., and Chen, J. P. (2005). Optimization of high-yield biological synthesis of single-crstalline gold nanoparticles. *Phys. Chem. B.* **109**, 15256-15263.

Liu, J. and Hurt, R.H. (2010). Ion release kinetics and particle persistence in aqueous nanosilver colloids. *Environmental Science and Technology* **44**: 2169–2175.

Liu, X., Jin, X., Cao, B., and Tang, C. Y. (2014). Bactericidal activity of silver nanoparticles in environmentally relevant freshwater matrices: influences of organic matter and chelating agent. *Environmental Chemical Engineering* **2**, 525-531.

Mollick, M. M. R., Rana, D., Dash, S. K., Chattopadhyay, S., Bhowmick, B., Maity, D., Mondal, D., Pattanayak, S., Roy, S., Chakraborty, M., and Chattopadhyay, D. (2015). Studies on green synthesized silver nanoparticles using *Abelmoschus esculentus* (L.) pulp extract having anticancer (in vitro) and antimicrobial applications. *Arabian Journal of Chemistry*. http://dx.doi.org/10.1016/j.arabjc.2015.04.033

Morones, J. R., Elechiguerra, J. L., Camacho, A. C., Holt, K., Kouri, J. B., Ramirez, J. T., and Yacaman, M. J. (2005). The bactericidal effect of silver nanoparticles. *Nanotechnology* **16**, 2346-2353.

Muralidharan, G., Subramanian, L., Nallamuthu, S. K., Santhanam, V., and Kumar, S. (2011). Effect of reagent addition rate and temperature on synthesis of gold nanoparticles in microemulsion route. *Ind. Eng. Chem. Res*. **50**, 8786-8791.

Nam, G., Purushotman, B., Rangasamy, S., and Song, J. M. (2016). Investigating the versatility of multifunctional silver nanoparticles: preparation and inspection of their potential as wound treatment agents. *Int Nano Lett*. **6**, 51-63.

Narayan, R., and EL-Sayed, A. (2004). Shape-dependent catalytic activity of platinum nanoparticles in colloidal solution. *Nano Letters* **4**, 1343-1348.

Nikaido, H. (2009). Multidrug resistance in bacterial. *Annu Rev Biochem.* **78**, 119-146.

Nune, S. K., Chanda, N., Shukla, R., Katti, K., Kulkarni, R. R., Thikavathi, S., Mekapothula, S., Kannan, R., and Katti, K. V. (2009). Green nanotechnology from tea: phytochemicals in tea as building blocks for production of biocompatible gold nanoparticles. *Mater Chem*. **19**, 2912-2920.

Ojea-Jiménez, I., Romero, F. M., Bastús, N. G., and Puntes, V. (2010). Small gold nanoparticles synthesized with sodiumcitrate and heavy water: insights into the reaction mechanism. *J. Phys. Chem. C.* **114**, 1800-1804.

Pankter, M. S., Oehninger, S., Barnett, T., Williams, J. L., and Clark, G. F. (1993). A revised structure of fucoidan may explain some of its biological activities. *Biological Chemistry* **268**, 21770-21776.

Park, S., Cha, S-H., Cho, I., Park, S., Park, Y., Cho, S., and Park, Y. (2016). Antibacterial nanocarriers of resveratrol with gold and silver nanoparticles. *Material Science and Engineering C* **58**, 1160-1169.

Pavagadhi, S., Sathishkumar, M., and Balasubramanian, R., 2014. Uptake of Ag and TiO2 nanoparticles by zebra fish embryos in the presence of other contaminants in the aquatic environment. *Water Research* **55**, 280–291.

Pedersen, K. (2006). Quantum size effects in nanostructures. Lecture notes to the course organic and inorganic nanostructures. Department of physics and nanotechnology, Aalborg University. 1-33.

Philip, D. (2009). Biosynthesis of Au, Ag and Au-Ag nanoparticles using edible mushroom extract. *Spectrochimica Acta Part A* **73**, 374-381.

Prabhu, S., and Poulose, E. K. (2012). Silver nanoparticles: mechanism of antimicrobial actions, synthesis, medical application, and toxicity effects. *International Nano Letters* **2**, 1-10.

Prathna, T. C., Mathew, L., Chandrasekaran, N., Raichur, A. M., Mukherjee, A. (2010). Biomimetic Synthesis of Nanoparticles: Science, Technology & Applicability, Edited A. Mukherjee, InTech Publishers, Croatia: 1-20.

Princy, K. F., and Gopinath, A. (2013). Ecofriendly synthesis and characterisatio of silver nanoparticles using marine macroalga *Padina tetrastromatica*. *International Journal of Science and Research* **4**, 1050-1054.

Rai, M., Yadav, A., and Gade, A. (2009). Silver nanoparticles as a new generation of antimicrobials. *Biotechnology Advances* **27**, 76-83.

Rajathi, F. A. A., Parthiban, C., Kumar, V. G., and Anantharaman, P. (2012). Biosynthesis of antibacterial gold nanoparticles using brown alga, *Steochospermum marginatum* (Kützing). *Spectruchimica Acta Part A: Molecular and Biomolecular Spectroscopy* **99**, 166-173

Ramesh, P., Rajendran, A., and Meena-Kshisundaram, M. (2014). Green synthesis of zink oxide nanoparticles using flower extract *Cassia auriculata*. *Nanoscience and Nanotechnology* **2**, 41-45.

Ramteke, C., Chakrabarti, T., Sarangi, B. K., and Pandey, R-A. (2012). Synthesis of silver nanoparticles from the aqueous extract of leaves of *Ocimum sanctum* for enhanced antibacterial activity. *Chemistry* **2013**, 1-7.

Rickerby, D. G., and Morrison, M. (2007). Nanotechnology and the environment: a European perspective. *Science and Technology of Materials* **8**, 19-24.

Salem, W. M., Haridy, M., Sayed, W. F., and Hassan, N. H. (2014). Antibacterial activity of silver nanoparticles synthesised from latex and leaf extract of *Ficus sycomurus. Industrial Crops and Products* **62**, 228-234.

Sathishkumar, G., Pradeep, K. J., Vignesh, V., Rajkuberan, C., Jeyaraj, M., Selvakumar, M., Rakhi, J., Sivaramakrishnan, S. (2016). Cannonball fruit (*Couroupita guianensis*, Aubl.) extract mediated synthesis of gold nanoparticles and evaluation of its antioxidant activity. *Molecular Liquids* **215**, 229-236.

Schulz, H., and Baranska, M. (2007). Identification and quantification of valuable plant substances by IR and Roman spectroscopy. *Vibrational Spectroscopy* **43**, 13-25.

Sellimi, S., Kadri, N., Barragan-Mentero, V., Laouer, H., Hajji, M., and Nasri, M. (2014). Fucans from a Tunisian brown seaweed *Cystoseira barbata*: structural characteristics and antioxidant activity. *International Journal of Biological Macromolecules* **66**, 281-288.

Senapati, S., Sayed, A., Moeez, S., Kumar, A., and Ahmad, A. (2012). Intracellular synthesis of gold nanoparticles using alga *Tetraselmis kochinensis*. *Material Letters* **79**, 116-118.

Senthilkumar, K., and Kim, S-K. (2014). Anticancer effects of fucoidan. Chapter seven. *Advances in Food and Nutrition Research* **72**, 195-213.

Sepeur, S. (2008). Nanotechnology-technical basics and applications. Hannover: vincentz, 1-13.

Shankar, S. S., Ahmad, A., and Sastry, M. (2003). Geranium leaf assisted biosynthesis of silver nanoparticles. *Biotechnol. Prg*. **19**, 1627-1631.

Shankar, S. S., Rai, A., Ahmad, A., and Sastry, M. (2004). Rapid synthesis of Au, Ag, and bimetallic Au core-Ag nanoparticles using Neem (*Azadirachta indica*) leaf broth. *Colloid Interface Sci*. **275**, 496- 502.

Sharma, N. C., Sahi, S. V., Nath, S., Parson, J. G., Gardea-Torrensdey, and Pal, T. (2007). Synthesis of plant-mediated gold nanoparticles and catalytic role of biomatrix-embedded nanomaterials. *Environ Sci Technol*. **41**, 5137-5142.

Shon, M-Y., Kim, T-H., and Sung, N-J. (2003). Antioxidant and free radical scavenging activity of *Phellinus baumii* (*Phellinus of Hymenochaetaceae*) extracts. *Food Chemistry* **82**, 593-597.

Sironmani, A., and Daniel, K. (2011). Silver nanoparticles- universal multifunctional particles for bio sensing, imaging for diagnostics and targeted drug delivery for therapeutic applications.

Drug discovery and development- present and future. Dr. Izet Kapetavonic (Ed.), ISBN: 978-953-307-615-7, InTech, available from: http//www.intechopen.com/books/drug-discovery-and-development-present-and-future/silver-nanoparticles-universal-multifunctional-nanoparticles-for-bio-sensing-imaging-for-diagnostics

Soisuwan, S., Warisnoichareen, W., Lirdpropamongkol, K., and Svast, J. (2010). Eco-friendly synthesis of fucoidan-stabilized gold nanoparticles. *American Journal of Applied Sciences* **7**, 1038-1042.

Solomon, S. D., Bahadory, M., Jeyarajasingam, A. V., Rutkowsky, S. A., and Boritz, C. (2007). Synthesis and study of silver nanoparticles. *Chemical Education* **84**, 322-325.

Song, J.Y., and Kim, B. S. (2009). Rapid biological synthesis of silver nanoparticles using leaf extracts. *Bioprocess Biosyst Eng*. **32**, 79-84.

Sousa, C., Botelho, C., and Oliveira, R. (2011). Nanotechnology applied to medical biofilms. 878-888.

Stegenga, H., Bolton, J. J., and Anderson, R. J. (1997). Seaweed of the South African west coast. Editor; Hall, A. V. ISBN 0-7992-1793-X. 203.

Sun, Q., Xiang, C., Jangwei, L., Zheng, M., Chen, Z., and Yu, C.-P. (2014). Green synthesis of silver nanoparticles using tea leaf extract and evaluation of their stability and antibacterial activity . *Colloid Surf. A: Phytochemic. Eng. Asp.* **444**, 226- 231.

Sun, Y., and Xia, Y. (2002). Shape-controlled synthesis of gold and silver nanoparticles. *Science* **298**, 2176-2179.

Supraja, S., Mohammed, A. S., Chakravarthy, N., Jayaprakash, P. A., Sagadev, E., Kasinathan, M. K., Sindhu, S., and Arumugam, P. (2013). Green synthesis of silver nanoparticles from *Cynodon dactylon* leaf extract. *International Journal of ChemTech Research* **5**, 271-277.

Takamatsu, S., Hodges, T. W., Rajbhadari, I., Gerwick, W. H., Hamann, M. T., and Nagle, D. G. (2003).Marine natural products as novel antioxidant prototypes. *Journal of Natural Products* **66**, 605-608.

Temime, L., Boëlle, P. Y., Courvalin, P., and Guillemot, D. (2003). Bacterial resistance to penicillin G by decreased affinity of penicillin-binding proteins: a mathematical model. *Emerging Infectious Diseases* **9**, 411-417.

Tengdelius, M., Gurav, D., Konradsson, P., Pahlsson, P., Griffith, M., and Oommen, O. P. (2015). Synthesis and anticancer properties of fucoidan-mimetic glycopolymer coated gold nanoparticles. *Chem. Commun*. **51**, 8532-8535.

Tobwala, S., Fan, W., Hines, C. J., Folk, W. R., and Ercal, N. (2014). Antioxidative potential of *Sutherlandia frutescenes* and its protective effects against oxidative stress in various cell cultures. *BMS Complementary and Alternative Medicine* **14**, 1-11.

Tripathy, R. M., Shrivastav, A., and Shrivastav, B. R. (2012). Biofabrication of gold nanoparticles using leaf of *Fucus bengghalensis* and their characterization. *International Journal of Pharma and Bio Sciences* **3**, 551-558.

Vaidyanathan, R., Kalishwaralal, K., Gpalram, S., and Gurunathan, T. (2009). Nanosilver- the burgeoning therapeutic molecule and its green synthesis. *Biotechnology Advances* **27**, 924-937.

Vithiya, K., and Sen, S. (2011). Biosynthesis of nanoparticles. *International Journal of Pharmaceutical Sciences and Research* **2**, 2781-2785.

Vivek, M., Kumar, P. S., Steffi, S., and Sudha, S. (2011). Biogenic silver nanoparticles by *Gelidiella aerosa* extract and their antifungal effects. *Avicenna Journal of Med Biotech*. **3**, 143-148.

Wang, Z. L. (2001). Characterization of nanophase materials. *Part. Part. Syst. Charact* **18**, 142-165.

World Health Organization. (2015). Media centre. Fact sheet: Antimicrobial resistance. www.who.int/mediacentre/factsheets/f5194/en/ Last updated on April 2015.

Wu, S., Yan, S., Qi, W., Huang, R., Cui, J., Su, R., and He, Z. (2015). Green synthesis of gold nanoparticles using apsertame and their catalytic activity for *p*-nitrophenol reduction. *Nanoscale Research Letters* **10**, 1-7.

Yang, M., Yang, Y., Liu, Y., Shen G., and Yu, R. (2006). Platinum nanoparticles-doped sol-gel/carbon nanotubes composite electrochemical sensors and biosensors. *Boisensors and Bioelectronics* **21**, 1125-1131.

Yu, J., Xu, D., Guan, H. N., Wang, C., Huang, L. K., and Chi, D. F. (2016). Facile one-step green synthesis of gold nanoparticles using *Citrus maxima* aqueous extracts and its catalytic activity. *Material letters* **166**, 110-112.

Zargar, M., Hamid, A. A., Barkar, F. A., Shamsudin, M. N., Shameli, K., Jahanshiri, F., and Farahani, F. (2011). Green synthesis and antibacterial effect of silver nanoparticles using *Vitex Negundo* L. *Molecules* **16**, 6667-6676.

7. APPENDIX A

CYTOTOXICITY ASSAY

a) **Tissue Culturing**

All the processes were performed inside the fume hood using aseptic technique. The cell lines used include MCF-7, MCF-12a, and HT-29.

PREPARATION OF MEDIA

Media that was used to grow cells in is Dulbecco's Modified Eagle's Media (DMEM) for MCF-7 and HT-29. Briefly, to 500 ml of DMEM media, 10% fetal bovine serum (FBS) and 1% of penstrep (penicillin-streptomycin) were added. MCF-12a grow in DMEM-F12 which required additional supplements such as hydrocortisone, EFG, and insulin.

TRANSFERRING CELLS FROM CRYO VIAL TO CELL CULTURING FLASK

Cells were removed from the freezer (-80 ºC) in 1 ml cryo vial. The cells were allowed to thaw at room temperature. After thawing, the cells were transferred to 15 ml centrifuge tube. Then, 5 ml of media (DMEM) was added to the cells. The mixture was then centrifuged at 3000 rpm for 5 minutes. From the centrifuged mixture, the supernatant was discarded and the pellet (which comprised cells) was resuspended in 5 ml of fresh media. The pipette was used to mix the cells and the media thoroughly. The cells were then ready to be transferred to tissue culturing flask (T25) as depicted on figure…. The flask containing cells was then incubated at 37 ºC, 5% CO2. The cells were viewed under the light microscope on a daily basis, with media being changed after every two days of incubation.

TRYPSINIZATION

Cells were trypsinized when they were confluent (70-90%). Briefly, the media was discarded from cell culture flask, and washed with dulbecco's phosphate buffer solution (DPBS) to ensure complete removal of media. After washing with PBS, 3 ml of 2 x trypsin was added. The mixture was then incubated for 5 minutes to allow for detachment for MCF-7, and MCF-12a. Incubation period for HT-29 was 10 minutes. To check cells for detachment, the cell culture flask was removed from the incubator to view under the light microscope (Nikon TMS, Leica EC3). When the cells are floating, then they had detached. The media was immediately added to cells in 2:1

ratio (media:Trypsin). Thus 6 ml of media was added to cells and the mixture was transferred to the 15 ml centrifuge tube. The mixture was then centrifuged at 3000 rpm for 5 minutes, 25 ºC (using Beckman coulter). The supernatant was discarded and the pellet was resuspended in 5 ml of fresh media.

CELL COUNT

For cell count, 10 µl of cells suspension was mixed with 10 µl of trypan blue stain. From this mixture, 10 µl was taken and added to the half-moon shaped chamber port on the Countess™ cell counting chamber slide. The slide was then inserted into the slide port on the instrument (Invitrogen™, Countess ™ automated cell counter). The number of live cells was used to calculate the volume of cells to be cultured in a 96 well plate. To each well, 100 µl of cells was added (1 x 10^5 live cells). The cells were incubated for 24 hours at 37 ºC and 5% CO2.

b) **CYTOTOXICITY STUDIES**

AgNPs were tested for cytotoxicity test. As a control, AuNP were also tested for cytotoxicity test. Cytotoxicity test is accomplished by employing MTT bio-assay. The whole process is outlined below.

TREATING WITH NANOPARTICLES

The media was discarded after 24 hours and the nanoparticles were added to the cells at varying concentrations in triplicate. The experiment was repeated one more time which amounted to two set of 96 well plates with same concentration of nanoparticles, and cells under the same conditions, but the experiments were performed on different days. The negative column consisted of cells and media only. One well did not have anything inside which serves as a blank. The 96 well plate was then incubated for 24 hours at 37 ºC, 5% CO2. The nanoparticles were removed from wells using multi-channel micropipette after 24 hours and the cells were washed with PBS to ensure complete removal of nanoparticles.

MTT ASSAY

From MTT stock solution (5 mg/ml) 1 ml was mixed with 10 ml of media. The solution was then added to each well in a volume of 100 µl. The 96 well plate was covered with foil after addition of MTT to protect MTT from light. MTT is sensitive to light. The sample, covered in foil, was

incubated for 4 hours at 37 ºC and 5% CO2. After incubation, MTT was then discarded before 100 µl of DMSO (>99.5%) was added to each well and incubated again for 15 minutes until the purple colour appears. The 96 well plate was taken to multi-plate reader (BMG Labtech). For cell viability, the absorbance was read at 570 nm.